Stability Analysis of Swarms

DISSERTATION

Presented in Partial Fulfillment of the Requirements for

the Degree Doctor of Phylosophy in the

Graduate School of The Ohio State University

By

Veysel Gazi, B.S.E.E., M.S.

* * * * *

The Ohio State University

2002

Ph.D. Examination Committee:

Professor Kevin M. Passino, Adviser

Professor José B. Cruz, Jr.

Professor Andrea Serrani

Approved by

Adviser

Electrical Engineering

ABSTRACT

Swarming, or aggregations of organisms in groups, can be found in nature in many organisms ranging from simple bacteria to mammals. Such behavior can result from several different mechanisms. For example, individuals may respond directly to local physical cues such as concentration of nutrients or distribution of some chemicals as seen in some bacteria and social insects, or they may respond directly to other individuals as seen in fish, birds, and herds of mammals. In this dissertation, we consider models for aggregating and social foraging swarms and perform rigorous stability analysis of emerging collective behavior. Moreover, we consider formation control of a general class of multi-agent systems in the framework of nonlinear output regulation problem with application on formation control of mobile robots. First, an individual-based continuous time model for swarm aggregation in an n-dimensional space is identified and its stability properties are analyzed. The motion of each individual is determined by two factors: (i) attraction to the other individuals on long distances and (ii) repulsion from the other individuals on short distances. It is shown that the individuals (autonomous agents or biological creatures) will form a cohesive swarm in a finite time. Moreover, explicit bounds on the swarm size and time of convergence are derived. Then, the results are generalized to a more general class of attraction/repulsion functions and extended to handle formation stabilization and uniform swarm density. After that, we consider social foraging swarms. We

assume that the swarm is moving in an environment with an "attractant/repellent" profile (i.e., a profile of nutrients or toxic substances) which also affects the motion of each individual by an attraction to the more favorable or nutrient rich regions (or repulsion from the unfavorable or toxic regions) of the profile. The stability properties of the collective behavior of the swarm for different profiles are studied and conditions for collective convergence to more favorable regions are provided. Then, we use the ideas for modeling and analyzing the behavior of honey bee clusters and in-transit swarms, a phenomena seen during the reproduction of the bees. After that, we consider one-dimensional asynchronous swarms with time delays. We prove that, despite the asynchronism and time delays in the motion of the individuals, the swarm will converge to a comfortable position with comfortable intermember spacing. Finally, we consider formation control of a multi-agent system with general nonlinear dynamics. It is assumed that the formation is required to follow a virtual leader whose dynamics are generated by an autonomous neutrally stable system. We develop a decentralized control strategy based on the nonlinear output regulation (servomechanism) theory. We illustrate the procedure with application to formation control of mobile robots.

Sevgili annem Hafize ve babam Hüseyin'e

ve

gelecek nesilin temsilcileri olan yeğenlerim

Fatma, Emine, Hüseyin, ve Okan'a

To my mother Hafize and my father Hüseyin

and

to my nieces Fatma and Emine and my nephews Hüseyin and Okan,

who are representatives of the next generation

ACKNOWLEDGMENTS

I would like to thank my adviser, Dr. Kevin M. Passino, for the patience, insight and guidance he offered me throughout the last six years. This dissertation would not be possible without his experience, encouragement, and support especially during the difficult moments of my studies. I would also like to thank Dr. José B. Cruz and Dr. Andrea Serrani for serving in my examination committee.

I'm grateful to The Scientific and Research Council of Türkiye for entrusting that I will be able to successfully complete a Ph.D. degree and giving me opportunity to study in the United States by financially supporting first nine months of my study here. I also would like to acknowledge the financial support from NIST, DAGSI, and the DARPA MICA program at different stages of my studies.

I would like to thank my family for always being there for me when I needed them, and always encouraging and supporting me in my studies, despite the financial difficulties they have always faced.

Finally, I want to thank my friends Manfredi Maggiore, Raúl Ordóñez, Mehmet Akar, Pierre-François Quet, Suat Gümüşsoy, and also other friends and colleagues in the Controls Group for their valuable discussions and suggestions, and in general creating a nice environment to be in and perform research.

VITA

July 29, 1973	Born - Kircali, Bulgaria
June, 1996	B.S. in Electrical and Electronics Engineering Middle East Technical University, Ankara, Türkiye
September 1996 - April 1997	Scholar of The Scientific and Research Council of Türkiye The Ohio State University, Columbus, Ohio
May 1997 - August 1998	Graduate Research Associate The Ohio State University, Columbus, Ohio
August, 1998	M.S. in Electrical Engineering The Ohio State University, Columbus, Ohio
September 1998 - August 2002	Graduate Research/Teaching Associate The Ohio State University, Columbus, Ohio

FIELDS OF STUDY

Major Field: Electrical Engineering

TABLE OF CONTENTS

Page

LIST OF FIGURES

Figure **Page**

CHAPTER 1

INTRODUCTION

Swarming, or aggregations of organisms in groups, can be found in nature in many organisms ranging from simple bacteria to mammals. Such behavior can result from several different mechanisms. For example, individuals may respond directly to local physical cues such as concentration of nutrients or distribution of some chemicals (which may be laid by other individuals). This process is called *chemotaxis* and is used by organisms such as bacteria or social insects (e.g., by ants in trail following or by honey bees in cluster formation). As another example, individuals may respond directly to other individuals (rather than the cues they leave about their activities) as seen in some higher organisms such as fish, birds, and herds of mammals.

Evolution of swarming behavior is driven by the advantages of such collective and coordinated behavior for avoiding predators and increasing the chance of finding food. This is because more individuals implies more sensors for detecting a predator or a food sources. Moreover, if a predator strikes, the probability of it catching any particular individual in the swarm is lower than compared to the case when that individual were alone. (Note that these are not the only advantages of swarming. For other issues and evolutionary tradeoffs in swarming see [82].) For example, in [45, 46] Grünbaum explains how social foragers as a group more successfully perform

chemotaxis over noisy gradients than individually. In other words, individuals do much better collectively compared to the case when they forage on their own, implying clear survival advantages due to the swarming behavior. Note that the evolutionary process can be viewed as an algorithmic design process which designs organisms and their behavior to be best (optimally) fit to their environment [27]. In other words, the evolutionary process is an optimization process that engineers the organisms and their behavior, and this process has been going on for millions of years. Therefore, by studying biological systems one may discover general principles which govern the operation of these systems, and which may be useful for developing similar engineering applications. In particular, operational principles from biological swarms can be used in engineering for developing distributed cooperative control, coordination, and learning strategies for autonomous multi-agent systems such as autonomous multi-robot applications, unmanned undersea, land, or air vehicles. The development of such highly automated systems is likely to benefit from biological principles including modeling of biological swarms, coordination strategy specification, and analysis to show that group dynamics achieve group goals.

In this dissertation we consider continuous time n-dimensional models for both swarm aggregations and social foraging and study the stability properties of the emergent behavior. Stability is defined as cohesiveness of the swarm. Then, we apply the ideas developed to modeling and stability analysis of honey bee clusters and in-transit swarms, which serves as a biological example. After that, we consider swarm aggregations in discrete time. In particular, we consider a discrete time asynchronous swarm model with time delays in one-dimensional space and study its stability properties using techniques developed in the parallel and distribution computation literature.

As a last topic in this dissertation we consider the formation control problem of a multi-agent system and develop a control strategy using techniques from nonlinear output regulation (servomechanism) literature.

1.1 Literature Overview

There are two fundamentally different approaches that researchers have been considering for analysis of swarm dynamics. These are *spatial* and *nonspatial* approaches. In the spatial approach the space (environment) is either explicitly or implicitly present in the model and the analysis. It can be divided into two distinct frameworks which are *individual-based* (or Lagrangian) framework and *continuum* (or Eulerian) framework [47]. In the individual-based models the basic description is the motion equation of each (separate) individual and therefore it is a natural approach for modeling and analysis of complex social interactions and aggregations. For example, a typical equation of motion considered for each individual within this framework is *Newton's motion equation*

$$m^i a^i = F^i,$$

where m^i is the *mass* of the individual, a^i is its *acceleration*, and F^i is the *total acting force* on the individual. The general understanding within this framework now is that the swarming behavior is a result of an interplay between a long range attraction and a short range repulsion between the individuals. For example, in fish attraction is based on vision and has a long range, whereas repulsion is based on pressure to the side (the lateral line) of the fish and has a short range (see for example [84] for detailed description as well as experimental results).

In the Eulerian framework, on the other hand, the swarm dynamics are described using a *continuum model* of the *flux*, namely *concentration* or *population density* (i.e., a model in which each member of the swarm is not considered as individual entity, but the swarm is a continuum described by its density in one, two, or three dimensional space) described by partial differential equations of the swarm density. The basic equation of the Euclidean models is an *advection-diffusion-reaction* equation of the form

$$\frac{\partial \rho}{\partial t} = \frac{\partial}{\partial x}\left(D(\rho)\frac{\partial \rho}{\partial x}\right) - \frac{\partial}{\partial x}\left(V(\rho)\rho\right) + B(\rho),$$

where the advection term $\frac{\partial}{\partial x}\left(V(\rho)\rho\right)$ and the diffusion term $\frac{\partial}{\partial x}\left(D(\rho)\frac{\partial \rho}{\partial x}\right)$ are the joint outcome of individual behavior and environmental influences, and the reaction term $B(\rho)$ is due to the population dynamics.

In the nonspatial approaches the population level swarming dynamics are described in a non-spatial way in terms of frequency distributions of groups of various size. They assume that groups of various sizes split or merge into other groups based on the inherent group dynamics, environmental conditions, and encounters with other groups. The drawback of the nonspatial approaches is that they need several "artificial" assumptions about fusion and fission of groups of various sizes in order to describe and analyze the population dynamics.

1.1.1 The Biological Literature

Biologists have been working on understanding and modeling of swarming behavior for a long time. See for example [9] and references therein (some of which date back to 1920's). The work by Breder [9] is one of the early efforts to "apply mathematical equations" to the grouping behavior in fish. He suggested a simple model composed

of attraction and repulsion components. He chose a constant attraction term and a repulsion term which is inversely proportional to the square of the distance between two members (or groups of members). His inspiration was from the Coulomb's law of electrostatic charges. He applied his model to four different species and compared the outcome with data from real fish schools. Using this method he determined the model parameters for the four different species he considered.

In [114] Warburton and Lazarus studied the affect on cohesion of a family of attraction/repulsion functions. They showed that all their models led to cohesion in simulations with different intermember distance. Among their models the convex attraction/repulsion function in which the maximum attraction is equal to the maximum repulsion was found best for cohesion. Analyzing the statistical properties of data they found that the group elongation (or shape) was positively correlated to the intermember (or interindividual) distance. Moreover, they showed that there is an equilibrium interindividual distance, where attraction balances repulsion, kept by members in a group and that the equilibrium distance decreases in large groups. Furthermore, in their model each member needed to monitor its distance to only few of its neighbors to prevent fragmentation of the group.

The article in [47] provides a good background and review of the swarm modeling concepts and literature such as spatial and nonspatial models, individual-based versus continuum models and so on. There the authors review the theoretical approaches for modeling animal aggregations caused by social interactions and describe both the *Hamiltonian* and the *Eulerian* frameworks in detail. This article is in a sense a complementary article to an earlier article in [80] that concentrated on dynamical aspects of animal aggregations.

In [30] Durrett and Levin compared four different approaches to modeling the dynamics of spatially distributed systems, which are *mean field approaches* (in which every individual is assumed to have equal probability of interacting with every other individual), *patch models* (that group discrete individuals into patches without additional spatial structure), *reaction-diffusion equations* (in which infinitesimal individuals are distributed in space, and *interacting particle systems* (in which individuals are discrete and the space is treated explicitly). They applied these four approaches to three different examples of species interactions in spatially distributed populations and compared the results. Each example had different realistic biological assumptions. They showed that the solutions of all the models did not always agree, and argued in favor of the discrete (individual based) models that treat the space explicitly.

In [48] the authors present a general continuous model for animal group size distribution (a nonspatial patch model). They consider a population with fixed size that is divided into groups of various dynamic sizes. They relate the group size distribution to the density-dependent rates of fusion and fission, that can be estimated from data and are related to the behavior of the individuals and the dynamics of the groups. For some of their prototype cases they find that the stationary distribution has a peak value (i.e., a most frequent group size), which emerges from the dynamics. They determine when such a peak emerges and show the existence and uniqueness of the stationary distribution. Stability of the stationary distribution is discussed and some progress on analysis is shown but not completed.

The article in [49] investigates the dynamic behavior of migrating herds by means of two dimensional discrete stochastic (or individual based) models. They use individual based approach to relate the collective behavior to individual decisions. In their

model the motion of each individual is a combined result of both density-independent and density-dependent decisions. They use a hierarchical decision scheme with short-range repulsion and long-range attraction. They analyze the dynamics of herds with members with both homogeneous and heterogeneous speeds. They explore the importance of a neutral zone (seen in some animals) where no attraction or repulsion is used.

Other work on model development for biological swarms by mathematical biologists include [44, 75, 71]. The work by Grindrod in [44] is an effort to generate a model for (spatial) aggregation and clustering of species and consider its stability (i.e., its ability to preserve the swarm density). He considered both single-species and multi-species communities and analyzed the effect of inter and intra community relations. His approach is important because the motion of the species in the model that he provided depends on the local density of the individuals and does not use intermediate attractants or repellents such as chemotactic materials. He assumed that every individual reacts directly to other individuals in its locality and moves to increase its likelihood for survival.

In [75] Mogilner and Edelstein-Keshet present a swarm model which is based on non-local interactions of the swarm members. Their model consists of integro-differential advection-diffusion equations with a convolution terms that describe attraction and repulsion. They show that if the density dependent repulsion is of higher order than the attraction, then their swarm model is realistic (i.e., it has constant interior density and sharp edges as observed in biological examples). They compare their model with some local models and argue that their model more accurately represents swarm behavior.

While [44, 75] consider a continuum (in space) model of a swarm, the article in [71] describes a spatially discrete model. The authors show that their model can describe the swarming behavior, i.e., the aggregation of individuals in dense populations.

Finally, the book by Parrish and Hamner [83] is a good reference on animal grouping (see also the references therein for other related work). Other general references are the books by Edelshtein-Keshet [31] and Murray [78]. Note also that for many organisms, swarming often occurs during *social foraging* and foraging theory is described in [102].

1.1.2 The Physics Literature

In parallel to the mathematical biologists there are a number of physicists who have done important work on swarming behavior. The general approach the physicists take is to model each individual as a particle, which they usually call a *self-driven* or *self-propelled particle*, and study the collective behavior due to their interaction. In particular, they analyze either the dynamic model of the density function or perform simulations based on a model for each individual particle (i.e., a distributed or Hamiltonian approach). Some articles consider the Newton's equation of motion. However, this is not the only type of model they consider. For example, many researchers consider a discrete time model that assumes that particles are moving with constant absolute velocity and at each time step each one travels in the average direction of motion of the particles in its neighborhood with some random perturbation. In other words, they consider a model of the form [110]

$$\begin{aligned} x^i(k+1) &= x^i(k) + v^i(k)\Delta t, \\ \theta^i(k+1) &= \frac{1}{1+N^i(k)}\left(\theta^i(k) + \sum_{j\in S^i(k)} \theta^j(k)\right) + \xi^i(k), \end{aligned}$$

where $x^i(k)$ is the position of individual i at time instant k, $\theta^i(k)$ is its orientation, $S^i(k)$ is the set of neighbors of individual i at time k and contains $N^i(k)$ individuals. The velocity of the swarm members is of constant magnitude $\|v^i(k)\| = v_0$ and Δt represents the time interval between two instants $(k+1)$ and k. The external variable $\xi^i(k)$ is assumed to be a random variable with uniform distribution in the interval $[-\frac{\eta}{2}, \frac{\eta}{2}]$. Using such a model they try to study the affect of the noise on the collective behavior and to validate their models through extensive simulations.

In [87] Rauch et al. explored a simplified set of swarm models, which were driven by the collective motion of social insects such as ants. In their model the swarm members move in an energy field that models the nutrient or chemotactic profile in biology. They show that some interesting phenomena such as formation of stable lines of traffic flow emerge.

In [107] Toner and Tu proposed a nonequilibrium continuum model for collective motion of large groups of biological organisms and later in [108] they develop a quantitative continuum theory of flocking. They show that their model predicts (models or represents) the existence of an *ordered phase* of flocks, in which all members of even an arbitrarily large flocks move together.

In [18] a simple self-driven lattice-gas model for collective biological motion is introduced. The authors show the existence of transition from individual random walks to collective migration. Similarly, Vicsek et al. introduce a simple simulation model for system of self-driven particles in [110]. They assume that particles are moving with constant absolute velocity and at each time step assume the average direction of motion of the particles in its neighborhood with some random perturbation (i.e., they consider the above mentioned model). They show that high noise (and/or low particle

density) leads to a no transport phase, where the average velocity is zero, whereas in low noise (and/or high particle density) the swarm is moving in a particular direction (that may depend on the initial conditions). They call this transition from a stationary state to a mobile state *kinetic phase transition*. Similarly, in [20] they present experimental results and mathematical model for forming bacterial colonies and collective motion of bacteria. The model is a simple self-propelled particle model that tries to capture the effect of nutrient diffusion, reproduction, extracellular slime deposition, chemoregulation, and inhomogeneous population. Other results in the same spirit include [21], where a nonequilibrium model was compared to some equilibrium XY model in ferromagnets, [19], where authors demonstrate similar results in one dimension, [111], where the effect of fluctuations on the collective motion of self-propelled particles is investigated, and [22], where the effect of noise and dimensionality on the scaling behavior of swarms of self-propelled particles is investigated.

Results of a similar nature by different authors can be found in [74, 100, 65]. In [74] the authors consider a dynamic model of swarms of self-propelled particles with attractive long-range interactions. They show that the system can be found in either coherent traveling state or incoherent oscillatory state and that the increase in noise intensity leads to a transition from a coherent to oscillatory state. Similarly, in [100] the authors propose a model that represents several kinds of cluster motion observed in nature including collective rotation, chaos, and wandering. The article in [65] describes a model that exhibits coherent localized solutions in one and two dimensions. The solution of the model is of finite extent and the density drops sharply to zero at the edges of the swarm as in biological swarms. Moreover, they develop continuum version of their discrete model and show that both models agree.

1.1.3 The Engineering Literature

In recent years, engineering applications such as formation control of multi-robot teams and autonomous air vehicles have emerged and this has increased the interest of engineers in swarms. Some examples include [43, 4]. In [43] the authors describe formation control strategies for autonomous air vehicles. They use optimization and graph theory approach to find the best set of communication channels that will keep the aircraft in the desired formation. Moreover, they describe reconfiguration strategies in case of faults or loss of aircraft. Results of a similar nature for ground multi-robot (multiple autonomous vehicle) teams can be found in [4], where the authors consider a strategy in which the formation behavior is integrated with other navigational behavior and present both simulation and implementation results for various types of formations and formation strategies.

In [88] Reif and Wang introduce the concept of *very large scale robotic* (VLSR) systems and consider a distributed control approach based on artificial force laws between individual robots and robot groups. The force laws are inverse-power or spring force laws incorporating both attraction and repulsion. The force laws can be distinct and to some degree they reflect the "social relations" among robots. Therefore, they call the method *social potential fields* method. Individual robot motion depends on the resultant artificial force imposed by the other robots and other components of the system such as obstacles. The approach is a distributed approach since each robot performs its own force and control calculations in a (possibly) asynchronous manner. It is an interesting and important work. However, it does not contain stability proof of the approach. Our model here can be viewed as a type of a social potential fields model (with different attraction/repulsion functions).

Another work on distributed formation control of robots is in [103], where the authors consider asynchronous distributed control and geometric pattern formation of multiple anonymous robots. The robots are anonymous in the sense that they all execute the same algorithm and they cannot be distinguished by their appearances. Moreover, the robots do not necessarily have a common coordinate system. The authors present an algorithm for moving the robots to a single point and also characterize the class of geometric patterns that the robots can form in terms of their initial configuration, and present some impossibility results. Gelenbe et al. provide a survey of autonomous search strategies by robots and animals in [42]. They first review the literature on coordination and search by robots, then summarize the research in the field of animal search.

Recently, formation control results that use control theory for controller development and stability analysis have begun to appear [28, 29, 32, 79, 64]. The article in [28, 29] proposes a method that uses only local information. They use the feedback linearization technique for controller design to exponentially stabilize the relative distances of the robots in the formation. Similar results are obtained also in [79], where the authors use formation constraints and control Lyapunov functions to develop the formation control strategy and prove stability of the formation (i.e., formation maintenance). Similarly, in [32] the same authors specify a model independent strategy for formation control of a multi-agent system. The results in [64], on the other hand, are based on using virtual leaders and artificial potentials for robot interactions in a group of agents for maintenance of the group geometry. They use the system kinetic energy and the artificial potential energy as a Lyapunov function to prove closed-loop

stability and employ a dissipative term to achieve asymptotic stability of the formation. The number of articles in this area with result in similar flavor is increasing fast. See for example [57]. Note however, not all types of formations may be possible. In other words, there may formations that may not be feasible given the system dynamics. The article in [106] describes a systematic framework for studying feasibility of formations for both undirected and directed type formations.

Note that several of the works described above [88, 64] (as well as a big portion of the work in this dissertation) are based on *artificial potential functions*. An example of another work that makes use of that concept is [86], where the authors consider cooperative control of multiple agents. In particular, they describe a cooperative search method for group of agents using artificial potentials and based on the concept of rivaling force. The concept of artificial potential functions is not new, and it has been used extensively for robot navigation and control [61, 90, 62].

One of the early works on generating distributed models of swarms is by Reynolds in [89]. He describes a distributed behavioral model for animated simulation of a flock of birds. The simulated flock is an elaboration of a particle system, with the simulated birds the particles. He implemented each bird as an independent actor that navigates according to its local perception of the dynamic environment.

Important work on swarm stability is given by Beni and coworkers in [56, 6]. In [56] they consider a synchronous distributed control method for discrete one and two dimensional swarm structures and prove stability in the presence of disturbances using Lyapunov methods. On the other hand, [6] is, to best of our knowledge, one of the first stability results for asynchronous methods. There they consider a *linear* swarm model and prove sufficient conditions for the asynchronous convergence of

the swarm to a synchronously achievable configuration. Although their method is asynchronous, they do not have time delays in the system. Therefore, their swarm members always have perfect information about the environment.

Swarm stability under *total asynchronism* (i.e., asynchronism with time delays) was first considered in [68, 67, 69]. In [68] a one dimensional discrete time totally asynchronous swam model is proposed and stability (swarm cohesion) is proved. The authors prove asymptotic convergence under total asynchronism conditions and finite time convergence under *partial asynchronism* conditions (i.e., total asynchronism with a bound on the maximum possible time delay). In [67], on the other hand, the authors consider a one dimensional discrete time partially asynchronous mobile swarm model and prove that cohesion will be preserved under certain conditions, expressed as bounds on the maximum possible time delay. In [68, 67, 69] the authors assume finite size of the swarm members (as opposed to point particles) to model real life vehicles (or species). Therefore, collision avoidance becomes an issue. They do not explicitly implement a collision avoidance algorithm such as in [35], for example; however, in [69] they design the control algorithm in a way that avoids collisions between the swarm members. Recently some results on the multidimensional case have been also obtained. For example, the work in [70] is focusing on extending the work in [68], [67] to the multidimensional case by imposing special constraints on the topology, the "leader" movements, and by using a specific communication topology.

Many of these works have been limited to either one or two dimensional space. Note that in one dimension, the problem of swarming is very similar to the problem of *platooning* of vehicles in *automated highway systems*, an area that has been studied extensively (see, for example, [5, 105, 104, 23] and references therein). Note also

that are ongong efforts to extend the *string stability* concepts in automated highway systems to two dimensional *mesh stability* (see for example [81]).

The recently popular "ant colony optimization" is an optimization method based on foraging in ant colonies and is discussed in [8]. There, the focus is on biomimicry for the solution of combinatorial optimization algorithms (e.g., shortest path algorithms) and swarming as we study it this dissertation is not considered. In [85] the author shows that chemotactic behavior of *E. coli* coupled with evolutionary and "elimination/dispersal events" provides for a non-gradient distributed and parallel optimization procedure that can be used for adaptive control and cooperative control problems. Also, the author there used a similar characterization of an "attractant-repellent profile" to ours, and also studied swarm behavior as a distributed optimization method. Member-member swarming mechanisms are different from here, and are only considered from an optimization perspective. Stability analysis was not considered in [8], or [85].

Developing models for swarming behavior is important in engineering not only because we can use them in developing swarms of autonomous agents, but also we can use these ideas in "controlling" natural flocks (herds, schools, swarms) of animals. An interesting example for this is the article in [109], where the authors develop a mobile robot that gathers a flock of ducks and maneuvers them safely to a specified goal position. They use a potential-field model of flocking behavior and using it investigate methods for generalized flock control (in simulation). Then they use the robot to control a real flock of ducks and show that the real world behavior of the ducks is similar to the expected one from simulations.

Finally, we would like to mention that models of multi-agent systems with interacting particles may represent not only biological or engineering swarms, but also other systems and can be used in different engineering applications. For example, in [17] the authors describe an optimization algorithm based on interaction of individuals in a population of particles, which is called *particle swarm optimization* (see also [58]). The book [58] discusses several different systems such as the operation of a brain that can be modeled as swarms of interacting agents. The aggregation behavior, which we are mostly concerned in this dissertation, in this case can represent the achievement of an agreement or a consensus between the interacting agents.

1.2 Dissertation Outline

In this dissertation we consider the problem of mathematically modeling and performing stability analysis of swarms (i.e., groups of agents). First, in Chapter 2 (see also [40]) we specify a continuous time n-dimensional swarm model based on artificial potential fields and perform stability analysis for stationary aggregating swarms, where stability is defined as cohesiveness of the swarm. The motion of the individuals in the swarm is based on long range attraction and short range repulsion with the other swarm members. We show that all the individuals converge to a small hyperball around the center of the swarm in a finite time and provide analytical bounds on the swarm size and time of convergence.

In Chapter 3 (see also [38]) we generalize the model considered in Chapter 2 for a class of attraction/repulsion functions. In particular, we allow for different types of attraction (e.g., linear or constant) and repulsion (e.g., bounded or unbounded). Then, we show that the model can easily extended to pair-dependent attraction/repulsion

functions and therefore can describe (guarantee) formation stabilization. Moreover, we show that by allowing the repulsion to be of "hardlimiting" type, we can achieve uniform swarm density (as in real biological swarms). Furthermore, we show that the model can easily be extended to the case in which the swarm members have point mass dynamics.

In Chapter 4 (see also [41, 39]) we consider social foraging swarms. In other words, we consider swarms which are moving in a profile of nutrients or toxic substances. The motion of the swarm members is assumed to be governed by two main factors: (i) a desire to stay close (but not too close) to the other individuals in the swarm, and (ii) a desire to find more food. We assume that the swarm members have the ability to sense (and move along) a gradient and represent the desire to find more food with a motion along the negative gradient of the profile. We consider and analyze the motion of the swarm in a plane, a quadratic, and multimodal Gaussian profiles and show convergence to more favorable (nutrient rich) regions and divergence from unfavorable (toxic) regions of the profile.

In Chapter 5 we use the ideas developed in Chapters 2, 3, and 4 for modeling and analysis of the aggregation and cohesiveness of honey bee clusters and in-transit swarms. The intention of this chapter is to provide a biological example for the work described in the previous chapters. We model the odor of the pheromones secreted by the queen bee and the other (worker) bees using profiles and assume that the bees move along the gradient of these profiles. Moreover, we incorporate unbounded repulsion on close distances between the bees. The analysis in this chapter is not very rigorous, since it is not easy to perform full scale rigorous analysis.

In Chapter 6 (see also [37]) we consider a discrete time one-dimensional asynchronous swarm model with time delays. We assume that one of the edge members of the swarm is stationary and analyze the stability (which is equivalent to the point stability in control theory) of the swarm. With the use of some results from parallel and distributed computation literature we show that despite asynchronism and time delays the swarm will converge to a constant "comfortable configuration." The extension of these results to higher dimensions is not straightforward and is not considered here.

In Chapter 7 we consider the formation control problem for a multi-agent system. First, we assume that the agents have have general nonlinear dynamics and show that the problem can be approached in the framework of decentralized nonlinear output regulation (servomechanism). After that, we focus on formation control of mobile robots and apply the controller developed for the general model. We develop both full information and error feedback controllers achieving the formation control objectives.

In Appendix A (see also [36]) we consider the decentralized output regulation problem for a class of nonlinear systems including a class of interconnected systems. This serves as a background for the results in Chapter 7, where we do not show the full derivation and the proof of the controller. Therefore, if one needs to see a proof of why an how the controller designed for the multi-agent system in Chapter 7 works, one may consult Appendix A (or [36]).

CHAPTER 2

AGGREGATING SWARMS

In this chapter we consider a model for stationary aggregating swarms, which operate based on long range attraction and short range repulsion between the swarm members. We analyze the stability properties of the emergent behavior, where stability is viewed as cohesiveness of the swarm. We show that cohesiveness is achieved in a finite time. Moreover, we derive explicit bounds on the swarm size and time of convergence.

2.1 The Swarm Model

Consider a swarm of M individuals (members) in an n-dimensional Euclidean space. We model the individuals as points and ignore their dimensions. The position of member i of the swarm is described by $x^i \in \mathbb{R}^n$. We assume synchronous motion and no time delays, i.e., all the members move simultaneously and know the exact (relative) position of all the other members. The motion dynamics evolve in continuous time. The equation of motion that we consider for individual i is given by

$$\dot{x}^i = \sum_{j=1, j\neq i}^{M} g(x^i - x^j), i = 1, \ldots, M, \tag{2.1}$$

where $g(\cdot)$ represents the function of attraction and repulsion between the members. In other words, the direction and magnitude of motion of each individual is determined

as a sum of the attraction and repulsion of all the other individuals on it. The attraction/repulsion function that we consider is

$$g(y) = -y\left[a - b\exp\left(-\frac{\|y\|^2}{c}\right)\right], \tag{2.2}$$

where a, b, and c are positive constants, $b > a$, and $\|y\| = \sqrt{y^\top y}$. For the $y \in \mathbb{R}^1$ case with $a = 1$, $b = 20$, and $c = 0.2$ this function is shown in Figure 2.1. In higher

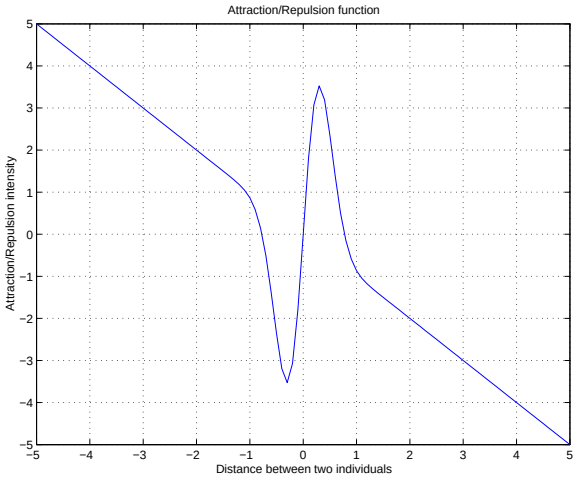

Figure 2.1: The attraction/repulsion function $g(\cdot)$.

dimensions (i.e., $y \in \mathbb{R}^n$), the function is exactly the same as in the one dimensional case, except that it acts on the line connecting the positions of the two members (i.e., the line on which the vector y lies).

Note that this function is attractive for large distances and repulsive for small distances. By equating $g(y) = 0$, one can easily find that $g(y)$ switches sign at the set of points defined as

$$\mathcal{Y} = \left\{ y = 0 \text{ or } \|y\| = \sqrt{c\ln\left(\frac{b}{a}\right)} = \delta \right\}.$$

Notice that we need $b > a$, since otherwise the expression will never switch sign except at zero and there will not be any repulsion between the members no matter how close they are to each other.

One drawback of the model here is that each individual needs to know the *relative* position of *all* the other individuals. This is not biologically very realistic (although in engineering it may be overcome with technology like the global positioning system). In biological swarms, often each individual can see (or sense) only the individuals in its neighborhood because the ranges of their senses are limited. Therefore, in nature the attraction or "desire to stick together" depends only on the individuals that it can sense. In order to have overcome this problem a model employing attraction only on nearest neighbors together with some concepts from graph theory can be used. However, this is a topic of further research.

Define the *center* of the swarm members as

$$\bar{x} = \frac{1}{M} \sum_{i=1}^{M} x^i. \tag{2.3}$$

Note that because of the symmetry of $g(\cdot)$ the center $\bar{x}$ is stationary for all t. In other words, since $g(\cdot)$ is symmetric with respect to the origin, member i moves toward every other member j exactly the same amount as j moves toward i. We express this more formally in the following lemma.

Lemma 1 *The center $\bar{x}$ of the swarm described by the model in Eq. (2.1) with an attraction/repulsion function $g(\cdot)$ as given in Eq. (2.2) is stationary for all t.*

Proof: Taking the derivative of $\bar{x}$ with respect to time we obtain

$$\dot{\bar{x}} = \frac{1}{M} \sum_{i=1}^{M} \dot{x}^i$$

$$
\begin{aligned}
&= -\frac{1}{M}\sum_{i=1}^{M}\sum_{j=1,j\neq i}^{M}(x^i - x^j)\left[a - b\exp\left(-\frac{\|x^i - x^j\|}{c}\right)\right] \\
&= -\frac{1}{M}\sum_{i=1}^{M}\sum_{j=1}^{M}(x^i - x^j)\left[a - b\exp\left(-\frac{\|x^i - x^j\|}{c}\right)\right] \\
&= -\frac{1}{M}\left[\sum_{i=1}^{M}x^i\sum_{j=1}^{M}\left[a - b\exp\left(-\frac{\|x^i - x^j\|}{c}\right)\right] - \sum_{j=1}^{M}x^j\sum_{i=1}^{M}\left[a - b\exp\left(-\frac{\|x^i - x^j\|}{c}\right)\right]\right] \\
&= 0,
\end{aligned}
$$

where we added $\left[a - b\exp\left(-\frac{\|x^i - x^j\|}{c}\right)\right](x^i - x^i) = 0$ to the summation in the second line to obtain the third, and interchanged the order of summation in the forth line.

■

Basically this lemma says that, on average, the swarm described by Eq. (2.1) with an attraction/repulsion function as given in Eq. (2.2) is not drifting. Note, however, that although it states that the center of the swarm is stationary, it does not say anything about the relative motions of the members with respect to it. It may be the case that the members diverge from the center while it stays stationary. Intuitively, however, we would expect the members to move toward the center for the given swarm model. In several of the results and discussions in this chapter we either implicitly or explicitly will use the fact that $\bar{x}$ is stationary.

2.2 Analysis of Swarm Cohesion

Our first result is about a swarm member which does not have any neighbors in its repulsion range. We call such a member a *free agent*.

Definition 1 *A swarm member i is called a* free agent *if*

$$\|x^i - x^j\| > \delta, \forall j \in S, j \neq i,$$

where $S = \{1, \ldots, M\}$ is the set of members of the swarm.

Note that since the distance from all the other members to a free agent is greater than δ, there will not be any repulsion force and the total force on this member will be a combined effect of all the attraction imposed by all the other members. We will show that this force is pointing toward the center $\bar{x}$ of the swarm, and therefore, the member is moving toward it. Before stating this result more rigorously, we define the error variable as

$$e^i = x^i - \bar{x},$$

for each individual $i = 1, \ldots, M$.

Lemma 2 *Assume that a member i of the swarm described by the model in Eq. (2.1) with an attraction/repulsion function $g(\cdot)$ as given in Eq. (2.2) is a free agent at time t and that its distance to the center $\bar{x}$ of the swarm is greater then δ, i.e.,*

$$\|e^i(t)\| = \|x^i(t) - \bar{x}\| > \delta.$$

Then, at time t its motion is in a direction of decrease of $\|e^i(t)\|$ (i.e., toward the center $\bar{x}$).

Proof: From the definition of the center $\bar{x}$ of the swarm we have $\sum_{j=1}^{M} x^j = M\bar{x}$. Subtracting Mx^i from both sides we obtain

$$\sum_{j=1}^{M}(x^i - x^j) = M(x^i - \bar{x}) = Me^i. \tag{2.4}$$

Then, the motion of member i can be represented as

$$\dot{x}^i = -\sum_{j=1, j\neq i}^{M} (x^i - x^j)\left[a + b\exp\left(-\frac{\|x^i - x^j\|^2}{c}\right)\right]$$

$$
\begin{aligned}
&= -a\sum_{j=1}^{M}(x^i - x^j) + b\sum_{j=1,j\neq i}^{M}\exp\left(-\frac{\|x^i - x^j\|^2}{c}\right)(x^i - x^j) \\
&= -aMe^i + b\sum_{j=1,j\neq i}^{M}\exp\left(-\frac{\|x^i - x^j\|^2}{c}\right)(x^i - x^j),
\end{aligned}
$$

where on the second line we added $a(x^i - x^i) = 0$, and substituted the value of $\sum_{j=1}^{M}(x^i - x^j)$ from Eq. (2.4) on the third.

Note that since $\dot{\bar{x}} = 0$, we have $\dot{e}^i = \dot{x}^i$. Choosing the Lyapunov function candidate for member i as

$$
V_i = \frac{1}{2}e^{i\top}e^i = \frac{1}{2}\|e^i\|^2
$$

and taking its derivative along the trajectory of the member we obtain

$$
\dot{V}_i = \dot{e}^{i\top}e^i = -aM\|e^i\|^2 + \sum_{j=1,j\neq i}^{M} b\exp\left(-\frac{\|x^i - x^j\|^2}{c}\right)(x^i - x^j)^\top e^i. \tag{2.5}
$$

Note that $b\exp\left(-\frac{\|x^i - x^j\|^2}{c}\right) > 0$ for all x^i and x^j. Therefore, $\dot{V}_i$ is bounded by

$$
\dot{V}_i \leq -aM\|e^i\|^2 + \sum_{j=1,j\neq i}^{M} b\exp\left(-\frac{\|x^i - x^j\|^2}{c}\right)\|x^i - x^j\|\|e^i\|. \tag{2.6}
$$

Since member i is a free agent, we have $\|x^i - x^j\| > \delta, \forall j \neq i$ and note that for that range the function $\exp\left(-\frac{\|x^i - x^j\|^2}{c}\right)\|x^i - x^j\|$ is a decreasing function of the distance with the maximum $\delta\exp\left(-\frac{\delta^2}{c}\right)$, which occurs at $\|x^i - x^j\| = \delta$. Using these facts, we have

$$
\begin{aligned}
\dot{V}_i &\leq -aM\|e^i\|^2 + b(M-1)\delta\exp\left(-\frac{\delta^2}{c}\right)\|e^i\| \\
&= -a\|e^i\|^2 - (M-1)\left[a\|e^i\| - b\delta\exp\left(-\frac{\delta^2}{c}\right)\right]\|e^i\|.
\end{aligned}
$$

For the second term to be negative semidefinite we need

$$
\|e^i\| \geq \frac{b\delta}{a}\exp\left(-\frac{\delta^2}{c}\right).
$$

Note, however, that $\frac{b}{a}\exp\left(-\frac{\delta^2}{c}\right) = 1$, which is obtained by substituting the value of δ and implies that we need $\|e^i\| \geq \delta$, which, on the other hand, holds by our hypothesis. Therefore, we have

$$\dot{V}_i \leq -a\|e^i\|^2 = -2aV_i,$$

which proves the assertion. ∎

Remark: From attraction/repulsion function $g(\cdot)$ in Eq. (2.2) one can see that one term in $g(\cdot)$ always gives attraction and the other repulsion and the resultant effect is their sum. This leads to similar terms in the derivative of the Lyapunov function in Eq. (2.5). If an individual is away from all the other individuals, the second term in the Lyapunov function is negligibly small compared to the first term and it moves toward the center. If it is close to the other individuals (i.e., in their repulsion range), then the second term becomes significant. ∎

Note that Lemma 2 does not imply that x^i will converge to $\bar{x}$ for all i. Intuitively, once a member gets to the vicinity of another member, then the repulsive force will be in effect and the conditions of Lemma 2 will not be satisfied anymore. However, it is important because it gives us an idea of the tendency of the individuals to move toward the center of the swarm. Therefore, it is normal to expect that the members will (potentially) aggregate and form a cluster around $\bar{x}$. To prove this we need to analyze the motion of the members which are not necessarily free agents and that is done in the next result.

Theorem 1 *Consider the swarm described by the model in Eq. (2.1) with an attraction/repulsion function $g(\cdot)$ as given in Eq. (2.2). As time progresses all the members*

of the swarm will converge to a hyperball

$$B_\epsilon(\bar{x}) = \{x : \|x - \bar{x}\| \leq \epsilon\},$$

where

$$\epsilon = \frac{b}{a}\sqrt{\frac{c}{2}} \exp\left(-\frac{1}{2}\right).$$

Moreover, the convergence will occur in a finite time bounded by

$$\bar{t} = \max_{i \in S} \left\{ -\frac{1}{2a} \ln\left(\frac{\epsilon^2}{2V_i(0)}\right) \right\}. \tag{2.7}$$

Proof: Choose any swarm member i. Let $V_i = \frac{1}{2}e^{i\top}e^i$ be the corresponding Lyapunov function. From the proof of Lemma 2 (see Eq. (2.5) we know that

$$\dot{V}_i = -aM\|e^i\|^2 + \sum_{j=1, j\neq i}^{M} b \exp\left(-\frac{\|x^i - x^j\|^2}{c}\right)(x^i - x^j)^\top e^i. \tag{2.8}$$

Therefore, if

$$\|e^i\| > \frac{b}{aM} \sum_{j=1, j\neq i}^{M} \exp\left(-\frac{\|x^i - x^j\|^2}{c}\right)\|x^i - x^j\|,$$

then we will have $\dot{V}_i < 0$. This bound is a function of the distance between the members. Note that each function in the sum on the right hand side is a bounded function and by using its maximum we can obtain a position independent bound. Solving for the maximum i.e., solving the equation

$$\frac{\partial}{\partial y}\left(y \exp\left(-\frac{y^2}{c}\right)\right) = \exp\left(-\frac{y^2}{c}\right) - \frac{2y^2}{c}\exp\left(-\frac{y^2}{c}\right) = 0,$$

we obtain that it occurs at $\|x^i - x^j\| = \sqrt{\frac{c}{2}}$, or in other words, the maximum occurs when the members are at a distance $\sqrt{\frac{c}{2}}$ from each other. Evaluating the maximum

we have $\sqrt{\frac{c}{2}}\exp\left(-\frac{\left(\sqrt{\frac{c}{2}}\right)^2}{c}\right) = \sqrt{\frac{c}{2}}\exp\left(-\frac{1}{2}\right)$. Substituting this in the above equation we obtain that $\dot{V}_i < 0$ as long as

$$\|e^i\| > \frac{b(M-1)}{aM}\sqrt{\frac{c}{2}}\exp\left(-\frac{1}{2}\right).$$

Define

$$\epsilon = \frac{b}{a}\sqrt{\frac{c}{2}}\exp\left(-\frac{1}{2}\right)$$

and note that $\epsilon > \frac{b(M-1)}{aM}\sqrt{\frac{c}{2}}\exp\left(-\frac{1}{2}\right)$. This implies that as $t \to \infty$, e^i converges within the ball around $\bar{x}$ defined by $\frac{b(M-1)}{aM}\sqrt{\frac{c}{2}}\exp\left(-\frac{1}{2}\right)$. Since $\epsilon > \frac{b(M-1)}{aM}\sqrt{\frac{c}{2}}\exp\left(-\frac{1}{2}\right)$ we have e^i converging to $B_\epsilon(\bar{x})$. Since member i was an arbitrary member, the result holds for all the members. To prove the finite time convergence note that the equation of $\dot{V}_i$ can be written as

$$\dot{V}_i \leq -a\|e^i\|^2 - a(M-1)\|e^i\|\left[\|e^i\| - \frac{b}{a(M-1)}\sum_{j=1,j\neq i}^{M}\exp\left(-\frac{\|x^i-x^j\|^2}{c}\right)\|x^i-x^j\|\right],$$

which implies that for $\|e^i\| \geq \epsilon$, we have

$$\dot{V}_i \leq -a\|e^i\|^2 = -2aV_i.$$

Therefore, the solution of V_i satisfies

$$V_i(t) \leq V_i(0)e^{-2at}.$$

For $\|e^i\| = \epsilon$ we have $V_i = \frac{1}{2}\epsilon^2$ and individual i enters the ϵ vicinity of $\bar{x}$ at time t_i when the right hand side of the above equation satisfies

$$V_i(0)e^{-2at_i} = \frac{1}{2}\epsilon^2.$$

Solving for t_i we obtain

$$t_i \leq -\frac{1}{2a}\ln\left(\frac{\epsilon^2}{2V_i(0)}\right).$$

Then, since S is a finite set, the maximum $\bar{t}$ of $t_i, i \in S$ exists and this proves the theorem. ∎

This result is important not only because it proves the cohesiveness of the swarm, but also it provides an explicit bound on the size of the swarm. Note that the bound ϵ makes intuitive sense. To see this note that increasing parameter a (i.e., increasing attraction) decreases the size of the bound ϵ. In contrast, increasing parameter b (i.e., increasing repulsion magnitude) or parameter c (increasing repulsion range) increases ϵ and these are intuitively expected results. For the $g(\cdot)$ function given in Figure 2.1 with parameters $a = 1$, $b = 20$, and $c = 0.2$, we have $\epsilon \approx 3.8$.

Note that the bound on the swarm size $\frac{b(M-1)}{aM}\sqrt{\frac{c}{2}}\exp\left(-\frac{1}{2}\right)$ depends on M. Therefore, for swarms with a small number of members the bound will differ significantly for different values of M. However, in biological swarms the number of the members M can be very large and as $M \to \infty$ we have $\frac{b(M-1)}{aM}\sqrt{\frac{c}{2}}\exp\left(-\frac{1}{2}\right) \to \epsilon$. In other words, ϵ is the maximum possible bound on the swarm size independent of the number of the swarm members. Therefore, for large values of M the size of the cohesive swarm is relatively independent of the number of the members. In other words, it is almost constant independent of the number of the individuals. This implies that as the number of the members increases the density of the swarm will also increase. This is inconsistent with some biological examples (where the density of the swarm remains relatively constant and the size of the swarm increases with the number of individuals) and is due to the particular attraction/repulsion function $g(\cdot)$ that we chose. In Chapter 3 we will see how this problem can be overcome.

Note also that even the bound $\frac{b(M-1)}{aM}\sqrt{\frac{c}{2}}\exp\left(-\frac{1}{2}\right)$ is conservative, because above we used $(x^i - x^j)^\top e^i \leq \|x^i - x^j\|\|e^i\|$ and also assumed that the functions $\exp\left(-\frac{\|x^i - x^j\|^2}{c}\right)\|x^i -$

$x^j\|$ are at their peak values for all i and j and these both are *never* the case. Therefore, the actual size of the swarm is, in general, smaller than ϵ.

2.3 Analysis of Swarm Member Behavior in a Cohesive Swarm

Theorem 1 shows only the region where the swarm members will converge and provides a bound on the size of the swarm and time of convergence. It does not, however, say anything about whether the swarm members will stop their motion or will start an oscillatory motion within the region and this issue needs to be investigated further. To this end, first, we define the state x of the system as the vector of the positions of the swarm members $x = [x^{1\top}, \ldots, x^{M\top}]^\top$. Let the invariant set of equilibrium points be

$$\Omega_e = \{x : \dot{x} = 0\}.$$

We will prove that as $t \to \infty$ the state $x(t)$ converges to Ω_e, i.e., the configuration of the swarm members converges to a constant arrangement.

Theorem 2 *Consider the swarm described by the model in Eq. (2.1) with an attraction/repulsion function $g(\cdot)$ as given in Eq. (2.2). As $t \to \infty$ we have $x(t) \to \Omega_e$.*

Proof: We choose the (generalized) Lyapunov function

$$J(x) = \frac{1}{2}\sum_{i=1}^{M-1}\sum_{j=i+1}^{M}\left[a\|x^i - x^j\|^2 + bc\exp\left(-\frac{\|x^i - x^j\|^2}{c}\right)\right].$$

Then, the gradient of $J(x)$ with respect to each x^i is given by

$$\nabla_{x^i} J(x) \;=\; \sum_{j=1, j\neq i}^{M}\left[a(x^i - x^j) - b(x^i - x^j)\exp\left(-\frac{\|x^i - x^j\|^2}{c}\right)\right]$$

$$
\begin{aligned}
&= \sum_{j=1, j\neq i}^{M} (x^i - x^j) \left[a - b \exp\left(-\frac{\|x^i - x^j\|^2}{c} \right) \right] \\
&= -\sum_{j=1, j\neq i}^{M} g(x^i - x^j) = -\dot{x}^i. \qquad (2.9)
\end{aligned}
$$

Now, taking the time derivative of the Lyapunov function along the motion of the system we obtain

$$
\dot{J}(x) = \left[\nabla_x J(x)\right]^\top \dot{x} = \sum_{i=1}^{M} \left[\nabla_{x^i} J(x)\right]^\top \dot{x}^i = \sum_{i=1}^{M} \left[-\dot{x}^i\right]^\top \dot{x}^i = -\sum_{i=1}^{M} \|\dot{x}^i\|^2 \leq 0, \quad (2.10)
$$

for all t. Then, using the LaSalle's Invariance Principle [59] we conclude that as $t \to \infty$ the state x converges to the largest invariant subset of the set defined as

$$
\Omega = \{x : \dot{J}(x) = 0\} = \{x : \dot{x} = 0\} = \Omega_e.
$$

Since each point in Ω_e is an equilibrium, Ω_e is an invariant set and this proves the result. ■

The proof of the above theorem shows the distributed aspect of the swarming behavior. In fact, it shows that the swarm members are performing *distributed optimization* (function minimization) of a common function (the generalized Lyapunov or cost function) using a *distributed gradient method*. In other words, each member computes its part of the gradient of the global function at its position (i.e., computes the gradient with respect to its motion variables) and moves along the negative direction of that gradient. The global function in this case is a function of the distances between the members. It may be possible to extend the idea to the more general case in which more general global cost function could be considered; however, this needs more research.

Another view on the distributed nature of the approach can be as follows. Define

$$J_i(x) = \frac{1}{2} \sum_{j=1, j\neq i}^{M} \left[a\|x^i - x^j\|^2 + bc \exp\left(\frac{\|x^i - x^j\|^2}{c} \right) \right].$$

Then, note that

$$\dot{x}^i = -\nabla_{x^i} J_i(x) = -\nabla_{x^i} J(x).$$

This can be interpreted as each member i performing an optimization of its private cost function $J_i(x)$, which results in minimizing of the combined cost function

$$J(x) = \frac{1}{2} \sum_{i=1}^{M} J_i(x)$$

to obtain the overall behavior of the swarm.

The combination of the above results (Theorems 1 and 2) prove that the swarm described by the model in Eq. (2.1) with an attraction/repulsion function $g(\cdot)$ as given in Eq. (2.2) will be cohesive and also that the members will converge to a constant position (or configuration). Note also that in any of the above analysis we did not use the dimension of the state space n. Therefore, the results obtained hold for any dimension n. Moreover, the results here are global. This is a consequence of the definition of the attraction/repulsion function $g(\cdot)$ in Eq. (2.2) over the entire domain.

2.4 Simulation Examples

In this section some simulation results will be presented in order to illustrate the theory presented in the previous sections. For ease of plotting we use only $n = 3$, however, qualitatively the results will be the same for higher dimensions. Figure 2.2 shows the paths of the members of a swarm in which there are $M = 51$ individuals. The initial positions of the swarm members are represented with circles and their

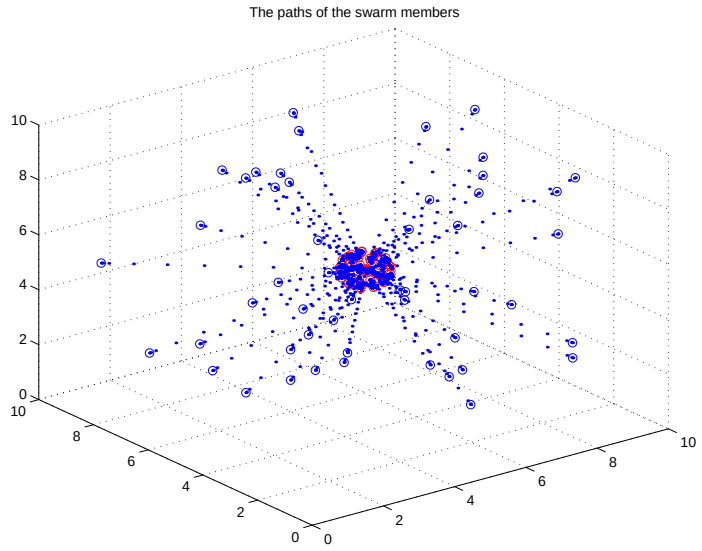

Figure 2.2: The paths of the swarm members.

paths with dots. Their positions after 10 seconds are also represented with circles. It is easily seen that, as expected, all the members move toward each other and form a cohesive swarm cluster. Figure 2.3 shows the positions of the swarm members after 10 seconds (shown as circles) and the center of the swarm (shown as a star). The center of the swarm is stationary for all time. In these simulations we used the $g(\cdot)$ function shown in Figure 2.1, i.e., the $g(\cdot)$ function given by Eq. (2.2) with $a = 1$, $b = 20$, and $c = 0.2$. For these values of the parameters, the swarm members are expected to converge to a ball with radius $\epsilon \approx 3.8$ around the center of the swarm. Note that the actual swarm size is much smaller than this since ϵ is a conservative bound, as discussed earlier.

Figure 2.4 shows the paths of the members of a swarm with $M = 60$ individuals and initial positions of the swarm members very close to each other. As expected, as the time progresses the swarm members move away from each other to a more

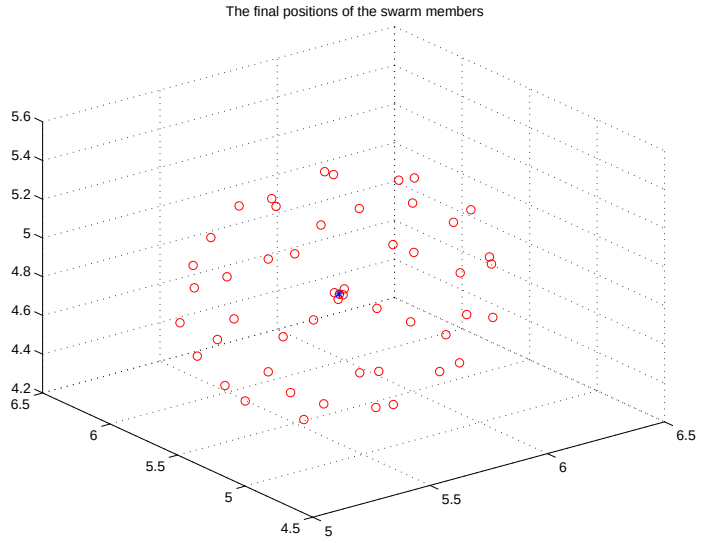

Figure 2.3: The swarm member positions after 10 seconds.

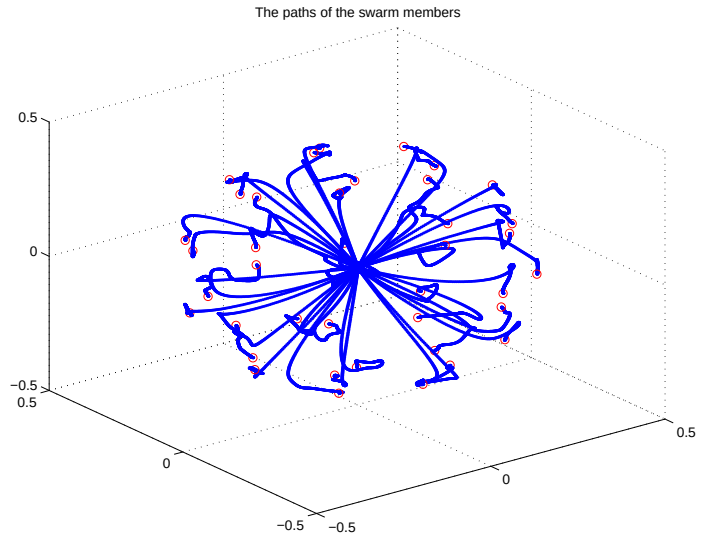

Figure 2.4: Paths of the individuals for very close initial positions.

comfortable distance. The trajectories shown illustrate their motion for 100 seconds. The plot of the positions of the swarm members after 100 seconds and the center

of the swarm for this case is comparable to the plot shown in Figure 2.3 and is not shown here. Moreover, the final positions of the swarm members are already clear from Figure 2.4. Note that once more the swarm size is much smaller (about 0.2 times) than the maximum swarm size determined by $\epsilon \approx 3.8$.

Note that the distance between the swarm members is less then the repulsion range δ of a member. This is expected since even though two members are on each others repulsion range δ, they cannot push each other because the other members are pulling them in a direction opposite of their repulsion. Then the equilibrium occurs when the attraction and repulsion balance and this balance occurs on intermember distances less then δ. (This is the case in biological swarms too.) Similar results are obtained when different parameters are used in $g(\cdot)$.

In this chapter, we identified a model for swarm aggregations and performed stability analysis of the emergent behavior. In the next chapter, we will generalize and extend these results to a more general class of attraction functions, uniform density swarms, and formation stabilization.

CHAPTER 3

A CLASS OF ATTRACTION/REPULSION FUNCTIONS FOR STABLE SWARM AGGREGATIONS

In this chapter we extend the results in Chapter 2 to a more general class of attraction/repulsion functions, which can include different types of attraction (e.g., linear or constant) and different types of repulsion (e.g., bounded or unbounded) for stable aggregation of stationary swarms. In addition to these, we also consider pair-dependent attraction/repulsion and show that for that case the model can be used stabilization of any needed formation. Furthermore, we show that with little modification of the model we can achieve uniform swarm density and also can add point mass dynamics.

3.1 The Class of Attraction/Repulsion Functions

We use the same swarm model as in Chapter 2. In other words, we consider motion dynamics that evolve in continuous time with the equation of motion of individual i given by

$$\dot{x}^i = \sum_{j=1, j\neq i}^{M} g(x^i - x^j), i = 1, \ldots, M, \tag{3.1}$$

where, $x^i \in \mathbb{R}^n$ is the position of individual i and $g : \mathbb{R}^n \to \mathbb{R}^n$ represents the function of attraction and repulsion between the individuals.

As a difference from Chapter 2 consider the attraction/repulsion functions $g(\cdot)$ of type

$$g(y) = -y\left[g_a(\|y\|) - g_r(\|y\|)\right], \tag{3.2}$$

where $g_a : \mathbb{R}^+ \to \mathbb{R}^+$ represents (the magnitude of) the attraction term and has a long range, whereas $g_r : \mathbb{R}^+ \to \mathbb{R}^+$ represents (the magnitude of) the repulsion term and has a short range, and $\|y\| = \sqrt{y^\top y}$ is the Euclidean norm. Let the constants l_a and l_r represent the ranges of attraction and repulsion, respectively. Then, from above, we have $l_a \geq l_r$. Moreover, we assume that on large distances attraction dominates, that on short distances repulsion dominates, and there is a unique constant distance δ on which attraction and repulsion balance. In other words, we assume that there exists δ such that $g_a(\delta) = g_r(\delta)$, and for $\|y\| > \delta$ we have $g_a(\|y\|) > g_r(\|y\|)$ and for $\|y\| < \delta$ we have $g_r(\|y\|) > g_a(\|y\|)$. One issue to note here is that for the attraction/repulsion functions $g(\cdot)$ defined as above we have $g(y) = -g(-y)$. In other words, the above $g(\cdot)$ functions are *odd* (and therefore symmetric with respect to the origin). This is an important feature of the functions and it leads to aggregation behavior. Note also that the combined term $-yg_a(\|y\|)$ represents the actual attraction, whereas the combined term $yg_r(\|y\|)$ represents the actual repulsion, and they both act on the line connecting the two interacting individuals, but in opposite directions. The vector y determines the alignment (i.e., it guarantees that the interaction vector is along the line on which y is located), the terms $g_a(\|y\|)$ and $g_r(\|y\|)$ affect only the magnitude, whereas their difference determines the direction (along vector y).

It has been observed in nature that there are attraction and repulsion forces (with attraction having longer range than repulsion) between individuals that lead to the swarming behavior [114, 47]. For example, for fish attraction is generally based on

vision and has a long range (provided the water is clear), whereas repulsion is based on the pressure on the side (the lateral line) of the fish and has a short range (but is stronger than attraction). Moreover, it has been observed that both attraction and repulsion are always "on" and the resulting behavior is due to the *interplay* between these two forces, and there is a distance (called "equilibrium distance" in biological literature) at which attraction and repulsion between two individuals balance. Note that our model is consistent (or captures) these observations.

The next assumption that we have about the attraction and repulsion functions is that there exist corresponding functions $J_a : \mathbb{R}^+ \to \mathbb{R}^+$ and $J_r : \mathbb{R}^+ \to \mathbb{R}^+$ such that

$$\nabla_y J_a(\|y\|) = y g_a(\|y\|) \quad \text{and} \quad \nabla_y J_r(\|y\|) = y g_r(\|y\|).$$

In other words, we choose $g_a(\|y\|)$ and $g_r(\|y\|)$ such that the above conditions are satisfied. Note that the functions $J_a(\|y\|)$ and $J_r(\|y\|)$ can be viewed as (potential) fields of attraction and repulsion, respectively, created around each individual. Moreover, the above assumption restricts the motion of the individuals toward each other along the gradient of these fields. For simplicity (and easy reference) we will denote with $\mathcal{G}$ the set of attraction/repulsion functions $g(\cdot)$ satisfying the assumptions stated so far.

An example of an attraction/repulsion function that satisfies the above conditions is the $g(\cdot)$ function in Eq. (2.2), that we considered in Chapter 2. In other words, the $g(\cdot)$ function in Eq. (2.2) is a special case of the class of functions in this chapter with $g_a(\|y\|) = a$ and $g_r(\|y\|) = b \exp\left(-\frac{\|y\|^2}{c}\right)$.

With the above in mind, note that the motion of each individual is given by

$$\begin{aligned} \dot{x}^i &= -\sum_{j=1, j\neq i}^{M} \left[g_a(\|x^i - x^j\|) - g_r(\|x^i - x^j\|) \right] (x^i - x^j) \\ &= -\sum_{j=1, j\neq i}^{M} \left[\nabla_{x^i} J_a(\|x^i - x^j\|) - \nabla_{x^i} J_r(\|x^i - x^j\|) \right], \end{aligned} \tag{3.3}$$

for all $i = 1, \ldots, M$. This implies that the minimum of $J_a(\|x^i - x^j\|)$ occurs on or around $\|x^i - x^j\| = 0$, whereas the minimum of $-J_r(\|x^i - x^j\|)$ (or the maximum of $J_r(\|x^i - x^j\|)$) occurs on or around $\|x^i - x^j\| \to \infty$, and the minimum of the combined $J_a(\|x^i - x^j\|) - J_r(\|x^i - x^j\|)$ occurs at $\|x^i - x^j\| = \delta$. Note that the first term in the motion equation of an individual is along the negative gradient of $J_a(\|x^i - x^j\|)$ and the second term is along the negative gradient of $-J_r(\|x^i - x^j\|)$. In other words, the first term tries to move x^i towards the minimum of $J_a(\|x^i - x^j\|)$ (which occurs on or around $\|x^i - x^j\| = 0$) and the second term tries to move x^i towards the minimum of $-J_r(\|x^i - x^j\|)$ or the maximum of $J_r(\|x^i - x^j\|)$ (which occurs on or around $\|x^i - x^j\| \to \infty$). The minimum of $J_a(\|x^i - x^j\|) - J_r(\|x^i - x^j\|)$, which occurs at $\|x^i - x^j\| = \delta$, is different from the minimums of both $J_a(\|x^i - x^j\|)$ and $-J_r(\|x^i - x^j\|)$ (as expected). In other words, at $\|x^i - x^j\| = \delta$ the attraction/repulsion profile between two individuals has a global minimum. Note, however, that the minimum of the combined profile when there are more than two individuals does not necessarily occur at $\|x^i - x^j\| = \delta$ for all $j \neq i$. If we view $J_a(\|x^i - x^j\|)$ and $-J_r(\|x^i - x^j\|)$ as potential energy profiles due to the relative positions of the individuals x^i and x^j, then their motions are along the negative gradient of the combined profile towards the minimum energy configuration.

Swarming in nature occurs in a distributed fashion. In other words, there is no leader (or boss) and each individual decides independently its direction of motion.

Our model captures this in its simplest form by having separate equations of motion of each individual (implying that it is a *Hamiltonian* model) that do not depend on an external variable (such as a command from a boss or another agent). In contrast, an individual's motion depends only on the position of the individual itself and its observation of the positions (or relative positions) of the other individuals. (Note that in the current model each individual knows the exact relative position of the other individuals. In other words, its observation is equal to the actual position without any error. Adding observation uncertainty is a topic of further research.)

As in Chapter 2 define the *center* of the swarm as $\bar{x} = \frac{1}{M}\sum_{i=1}^{M} x^i$. Note that since the functions $g(\cdot) \in \mathcal{G}$ are odd, and therefore symmetric with respect to the origin, given any $g(\cdot) \in \mathcal{G}$ it is possible to show that the result in Lemma 1 still holds, i.e., the center $\bar{x}$ of the swarm is stationary for all t as is stated formally in the following lemma.

Lemma 3 *The center $\bar{x}$ of the swarm described by the model in Eq. (3.1) with an attraction/repulsion function $g(\cdot) \in \mathcal{G}$ is stationary for all t.*

Proof: The proof of this lemma is very similar to the proof of Lemma 1. Let $g_{ar}(\|x^i - x^j\|) = g_a(\|x^i - x^j\|) - g_r(\|x^i - x^j\|)$. Then, the time derivative of center is given by

$$\begin{aligned}
\dot{\bar{x}} &= -\frac{1}{M}\sum_{i=1}^{M}\sum_{j=1,j\neq i}^{M} g_{ar}(\|x^i - x^j\|)(x^i - x^j) \\
&= -\frac{1}{M}\sum_{i=1}^{M-1}\sum_{j=i+1}^{M} \left[g_{ar}(\|x^i - x^j\|)(x^i - x^j) + g_{ar}(\|x^j - x^i\|)(x^j - x^i)\right] \\
&= 0.
\end{aligned}$$

■

Now, consider the state $x = [x^{1\top}, \ldots, x^{M\top}]^\top \in \mathbb{R}^{nM}$ of the system and the invariant set of equilibrium (or stationary) points $\Omega_e = \{x : \dot{x} = 0\}$. It can be shown that the result in Theorem 2 in Chapter 2 still holds, i.e., as $t \to \infty$ the state $x(t)$ converges to Ω_e, implying that the configuration of the swarm members converges to a constant arrangement.

Theorem 3 *Consider the swarm described by the model in Eq. (3.1) with an attraction/repulsion function $g(\cdot) \in \mathcal{G}$. For any $x(0) \in \mathbb{R}^{nM}$, as $t \to \infty$ we have $x(t) \to \Omega_e$.*

Proof: Similar to the proof of Theorem 2 we choose the (generalized) Lyapunov function $J : \mathbb{R}^{nM} \to \mathbb{R}$ defined as

$$J(x) = \sum_{i=1}^{M-1} \sum_{j=i+1}^{M} \left[J_a(\|x^i - x^j\|) - J_r(\|x^i - x^j\|) \right]. \tag{3.4}$$

Taking the gradient of $J(x)$ with respect to the position x^i of individual i one can show that

$$\nabla_{x^i} J(x) \;\; = \;\; -\dot{x}^i, \tag{3.5}$$

holds and the time derivative of the Lyapunov function along the motion of the system once more is given by

$$\dot{J}(x) = -\sum_{i=1}^{M} \|\dot{x}^i\|^2 \leq 0,$$

for all t implying decrease in $J(x)$ unless $\dot{x}^i = 0$ for all $i = 1, \ldots, M$. If the function $g(\cdot)$ is chosen such that the set defined as

$$\Omega_0 = \{x : J(x) \leq J(x(0))\}$$

is compact (which was the case with the $g(\cdot)$ function in Eq. (2.2) and therefore in the proof of Theorem 2), then using the LaSalle's Invariance Principle we can conclude that as $t \to \infty$ the state $x(t)$ converges to the largest invariant subset of the set defined as

$$\Omega_1 = \{x \in \Omega_0 : \dot{J}(x) = 0\} = \{x \in \Omega_0 : \dot{x} = 0\} \subset \Omega_e.$$

Note, however, that Ω_0 may not necessarily be compact for every $g(\cdot) \in \mathcal{G}$, which may happen if the corresponding $J(\cdot)$ is not radially unbounded. Therefore, the fact that $\dot{J}(x) \leq 0$ does not, in general, directly imply boundedness. This is because $J(x)$ is a summation of functions and even though given any i and j, $j \neq i$, we have the set

$$\{x^i, x^j : J_a(\|x^i - x^j\|) - J_r(\|x^i - x^j\|) \leq J_a(\|x^i(0) - x^j(0)\|) - J_r(\|x^i(0) - x^j(0)\|)\}$$

compact, the same is not implied for the summation (even though there always exists $\bar{c}$ such that the set $\Omega_{\bar{c}} = \{x : J(x) \leq \bar{c}\}$ is compact). In that case, in general, it may happen that some individuals diverge towards infinity contributing positively to $\dot{J}(x)$, whereas majority of the individuals move in a direction of decrease of $J(x)$ contributing negatively to $\dot{J}(x)$, and $\dot{J}(x)$ may be negative because the overall contribution of the diverging individuals may be smaller compared to the converging ones (which is possible because $J(x)$ is not radially unbounded). Note, however, that in our swarm for every individual i we have $\left[\nabla_{x^i} J(x)\right]^\top \dot{x}^i = -\|\dot{x}^i\|^2 \leq 0$, which implies that every individual moves in a direction of decrease of $J(x)$. Therefore, the set defined as

$$\Omega_x = \{x(t) : t \geq 0\} \subset \Omega_0$$

is compact and we still can apply LaSalle's Invariance Principle arriving at the conclusion that as $t \to \infty$ the state $x(t)$ converges to the largest invariant subset of the

set defined as

$$\Omega_2 = \{x \in \Omega_x : \dot{J}(x) = 0\} = \{x \in \Omega_x : \dot{x} = 0\} \subset \Omega_e.$$

Since in both of the above cases both Ω_1 and Ω_2 are invariant themselves and we have $\Omega_1 \subset \Omega_e$ and $\Omega_2 \subset \Omega_e$, we have $x(t) \to \Omega_e$ as $t \to \infty$ and this concludes the proof. ∎

Note that in some engineering swarm applications such as *uninhabited air vehicles* (UAV's) individuals never stop. Therefore, the results here may seem not to be applicable. However, note that these are results describing only aggregation. It is possible to extend these results to the mobile case by having a motion (or drift) term in the equation of motion together with the aggregation term described here (as we will see in Chapter 4). As a result, if all the individuals share exactly the same motion term (e.g., a predefined speed profile or trajectory of motion), then we will achieve a cohesive swarm moving collectively since the aggregating term would decay as they would arrange in the minimum energy configuration (relative arrangement) as the above result suggests. In other words, the results here will guarantee cohesiveness during motion.

Note that our approach is distributed in a sense that the individuals do not have to know the global Lyapunov or potential energy function $J(x)$ given in Eq. (3.4). Instead, it is sufficient if they know the local or their internal Lyapunov or potential energy function defined as

$$J_i(x) = \sum_{j=1, j\neq i}^{M} \left[J_a(\|x^i - x^j\|) - J_r(\|x^i - x^j\|) \right],$$

since

$$\dot{x}^i = -\nabla_{x^i} J_i(x) = -\nabla_{x^i} J(x),$$

where $J(x)$ can be written as $J(x) = \frac{1}{2}\sum_{i=1}^{M} J_i(x)$. Note also that for implementation each individual i may, instead of using actual position difference $(x^i - x^j)$ to the other individuals $j \neq i$, use some observation or estimate $\hat{e}^{ij} = (x^i - \hat{x}^j)$ of the position errors in determining its motion. However, the stability for this case needs to be investigated further.

The result in Theorem 3 is important. It proves that asymptotically the individuals will converge to a constant position. However, it does not say anything about where these positions will be. We conjecture that given the initial positions of the individuals $x^i(0), i = 1, \ldots, M$, the final configuration to which the individuals in the swarm will converge is unique. However, it is not easy to find a direct relation between $x(0)$ and the final position $x(\infty)$. This is an important problem, since it will solve the formation stabilization problem for autonomous agents obeying our model. Nevertheless, it can be shown that, with a little modification, the model can be generalized and applied to the formation control problem (as will be done later in this chapter).

One drawback of Theorem 3 is that it does not specify any bound on the resulting size of the swarm. Therefore, we need to investigate this issue further.

3.2 Swarm Cohesion Analysis

In this section, we will try to find bounds on the ultimate swarm size. To this end, consider again the error variable $e^i = x^i - \bar{x}$, for each individual $i = 1, \ldots, M$, and note that $\dot{e}^i = \dot{x}^i - \dot{\bar{x}} = \dot{x}^i$, since from Lemma 3 we have $\dot{\bar{x}} = 0$. Then, the derivative of the Lyapunov function $V_i = \frac{1}{2}\|e^i\|^2 = \frac{1}{2}e^{i\top}e^i$ is given by

$$\dot{V}_i = \dot{e}^{i\top}e^i = -\sum_{j=1, j\neq i}^{M} \left[g_a(\|x^i - x^j\|) - g_r(\|x^i - x^j\|)\right](x^i - x^j)^\top e^i. \qquad (3.6)$$

Below, we analyze the case in which we have a linear attraction and a constant or bounded repulsion.

3.2.1 Linear Attraction and Bounded Repulsion Case

In this section we consider the special case in which

$$g_a(\|y\|) = a$$

for some finite positive constant $a > 0$ and for all y (as is the one in Eq. (2.2)), which corresponds to linear attraction since the actual attraction is given by $yg_a(\|y\|) = ay$. Therefore, the analysis in this section is a direct generalization of the results in Chapter 2. Incorporating the value of $g_a(\|x^i - x^j\|)$ in Eq. (3.6) we obtain

$$\dot{V}_i = -a \sum_{j=1, j\neq i}^{M} (x^i - x^j)^\top e^i + \sum_{j=1, j\neq i}^{M} g_r(\|x^i - x^j\|)(x^i - x^j)^\top e^i.$$

Then, from Eq. (2.4, we know that $\sum_{j=1,j\neq i}^{M}(x^i - x^j) = Me^i$, substituting which in the $\dot{V}_i$ equation we obtain

$$\begin{aligned} \dot{V}_i &= -aM\|e^i\|^2 + \sum_{j=1, j\neq i}^{M} g_r(\|x^i - x^j\|)(x^i - x^j)^\top e^i \\ &\leq -aM\|e^i\| \left[\|e^i\| - \frac{1}{aM} \sum_{j=1, j\neq i}^{M} g_r(\|x^i - x^j\|)\|x^i - x^j\| \right], \end{aligned}$$

which implies that $\dot{V}_i < 0$ as long as $\|e^i\| > \frac{1}{aM}\sum_{j=1,j\neq i}^{M} g_r(\|x^i - x^j\|)\|x^i - x^j\|$. This, on the other hand, implies that as $t \to \infty$ asymptotically we have

$$\|e^i\| \leq \frac{1}{aM} \sum_{j=1, j\neq i}^{M} g_r(\|x^i - x^j\|)\|x^i - x^j\|.$$

Note that this equation holds for any type of repulsion, provided that the attraction is linear. Now, assume that the repulsion is bounded (as is the one in Eq. (2.2)), i.e., assume that

$$g_r(\|x^i - x^j\|)\|x^i - x^j\| \leq b,$$

for some finite positive constant b. Then, we conclude that asymptotically for this case we will have

$$\|e^i\| \leq \frac{b(M-1)}{aM} < \frac{b}{a} = \epsilon',$$

which provides a bound on the maximum ultimate swarm size. As in the case of Theorem 1, the convergence occurs in a finite time $\bar{t}$ as was given in Eq. (2.7) with ϵ replaced with ϵ'.

Remark: Note that if instead of having $g_a(\|y\|) = a$, we had $g(\cdot)$ such that

$$\sum_{j=1, j\neq i}^{M} g_a(\|x^i - x^j\|)(x^i - x^j)^\top e^i \geq \eta \|e^i\|^2,$$

for some $\eta > 0$ and for all $i = 1, \ldots, M$, then, with a similar analysis to above, we would be able to conclude that asymptotically we have

$$\|e^i\| \leq \frac{1}{\eta} \sum_{j=1, j\neq i}^{M} g_r(\|x^i - x^j\|)\|x^i - x^j\|.$$

■

The analysis in this section is a direct generalization of the results in Chapter 2. In the following sections, we will consider different cases which will allow for unbounded repulsion.

3.2.2 Linearly Bounded from Below Attraction and Unbounded Repulsion

By linearly bounded from below attraction we mean the case in which we have

$$g_a(\|x^i - x^j\|) \geq a,$$

for some finite positive constant a and for all $\|x^i - x^j\|$. For the repulsion functions, on the other hand, we will consider the unbounded functions satisfying

$$g_r(\|x^i - x^j\|) \leq \frac{b}{\|x^i - x^j\|^2}.$$

An example of attraction/repulsion function $g(\cdot)$ satisfying the above assumptions is shown in Figure 3.1.

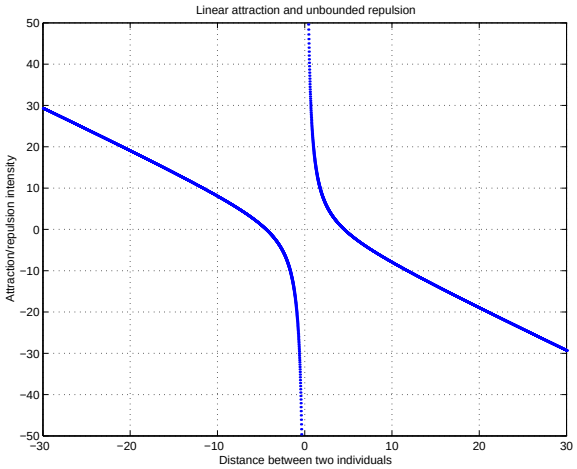

Figure 3.1: A $g(\cdot)$ function with linear attraction and unbounded repulsion.

First, we define the cumulative (or overall) Lyapunov function as $V = \sum_{i=1}^{M} V_i$ and note that since at equilibrium from Theorem 3 we know that $\dot{e}^i = \dot{x}^i = 0$, we also have $\dot{V}_i = 0$ for all i and therefore $\dot{V} = 0$. In other words, letting $g_{ar}(\|x^i - x^j\|) = g_a(\|x^i - x^j\|) - g_r(\|x^i - x^j\|)$ we have

$$\begin{aligned}
\dot{V} &= -\sum_{i=1}^{M} \sum_{j=1, j\neq i}^{M} g_{ar}(\|x^i - x^j\|)(x^i - x^j)^\top e^i \\
&= -\sum_{i=1}^{M-1} \sum_{j=i+1}^{M} \left[g_{ar}(\|x^i - x^j\|)(x^i - x^j)^\top e^i + g_{ar}(\|x^j - x^i\|)(x^j - x^i)^\top e^j \right] \\
&= -\sum_{i=1}^{M-1} \sum_{j=i+1}^{M} g_{ar}(\|x^i - x^j\|)\|x^i - x^j\|^2 \\
&= -\frac{1}{2} \sum_{i=1}^{M} \sum_{j=1, j\neq i}^{M} \left[g_a(\|x^i - x^j\|) - g_r(\|x^i - x^j\|) \right] \|x^i - x^j\|^2 = 0,
\end{aligned}$$

where to obtain the third line we used the fact that for any $\alpha \in \mathbb{R}$ we have

$$\alpha(x^i - x^j)^\top e^i + \alpha(x^j - x^i)^\top e^j = \alpha\|x^i - x^j\|^2, \tag{3.7}$$

which is true since $x^i - x^j = e^i - e^j$. From the above equation we obtain

$$\sum_{i=1}^{M} \sum_{j=1, j\neq i}^{M} g_a(\|x^i - x^j\|)\|x^i - x^j\|^2 = \sum_{i=1}^{M} \sum_{j=1, j\neq i}^{M} g_r(\|x^i - x^j\|)\|x^i - x^j\|^2. \tag{3.8}$$

This equation, in a sense, says that at equilibrium the (weighted by the distance) attraction and repulsion will balance.

Remark: Note that the cumulative Lyapunov function V is only one way to quantify the cohesion/dispersion of the swarm. In other words, instead of V, we could equally well choose

$$\bar{V} = \frac{1}{2} \sum_{i=1}^{M-1} \sum_{j=i+1}^{M} \|x^i - x^j\|^2,$$

which would quantify the interindividual distances instead of the distances to the center. In some applications, where the center is moving or the relative motion or positions to each other of the individuals is more important than their relative motion to a predefined point such as their center, it may be better to use a function like $\bar{V}$. In fact, we arrive at the same conclusion using $\bar{V}$ since it can be shown that

$$\dot{\bar{V}} = -\frac{M}{2} \sum_{i=1}^{M} \sum_{j=1, j\neq i}^{M} \left[g_a(\|x^i - x^j\|) - g_r(\|x^i - x^j\|)\right] \|x^i - x^j\|^2 = M\dot{V}.$$

■

One issue to notice here is that, if we had only attraction (i.e., if we had $g_r(\|x^i - x^j\|) \equiv 0$ for all i and j, $j \neq i$), then the above equation would imply that the swarm shrinks to a single point, which is the center $\bar{x}$. In contrast, if we had only repulsion (i.e., if we had $g_a(\|x^i - x^j\|) \equiv 0$ for all i and j, $j \neq i$), then the swarm

would disperse in all directions away from the center $\bar{x}$ towards infinity. Having the attraction dominating at large distances prevents the swarm from dispersing, whereas having the repulsion dominating on short distances prevents it from collapsing to a single point, and the equilibrium is established in between.

Note that since the actual attraction term is $yg_a(\|y\|)$, we have $g_a(\|x^i - x^j\|)\|x^i - x^j\| \geq a\|x^i - x^j\|$ for this case (and hence the name linearly bounded from below attraction). Then, we have

$$a\sum_{i=1}^{M}\sum_{j=1,j\neq i}^{M}\|x^i - x^j\|^2 \leq \sum_{i=1}^{M}\sum_{j=1,j\neq i}^{M} g_a(\|x^i - x^j\|)\|x^i - x^j\|^2.$$

Similarly, from the bound on $g_r(\|x^i - x^j\|)$ we know that $g_r(\|x^i - x^j\|)\|x^i - x^j\|^2 \leq b$ and obtain

$$\sum_{i=1}^{M}\sum_{j=1,j\neq i}^{M} g_r(\|x^i - x^j\|)\|x^i - x^j\|^2 \leq bM(M-1).$$

Now, note that from Eq. (2.4 we have $e^i = \frac{1}{M}\sum_{j=1}^{M}(x^i - x^j)$ and therefore for the sum of the squares of the error we obtain

$$\sum_{i=1}^{M}\|e^i\|^2 = \frac{1}{M}\sum_{i=1}^{M}\sum_{j=1,j\neq i}^{M}(x^i - x^j)^\top e^i = \frac{1}{M}\sum_{i=1}^{M-1}\sum_{j=i+1}^{M}\|x^i - x^j\|^2 = \frac{1}{2M}\sum_{i=1}^{M}\sum_{j=1,j\neq i}^{M}\|x^i - x^j\|^2,$$

where we again used the fact in Eq. (3.7) to obtain the second equality.

Combining these equations with Eq. (3.8) we obtain

$$2aM\sum_{i=1}^{M}\|e^i\|^2 \leq bM(M-1)$$

which implies that at equilibrium we have

$$\frac{1}{M-1}\sum_{i=1}^{M}\|e^i\|^2 \leq \frac{b}{2a}.$$

Then, for the *root mean square* of the error we have

$$e_{rms} = \sqrt{\frac{1}{M}\sum_{i=1}^{M}\|e^i\|^2} \leq \sqrt{\frac{b}{2a}} = \epsilon_{rms},$$

which establishes a bound on the swarm size.

3.2.3 Almost Constant Attraction and Unbounded Repulsion

In this section we consider the attraction functions that satisfy $g_a(\|x^i - x^j\|) \to 0$ as $\|x^i - x^j\| \to \infty$. However, we assume also that

$$g_a(\|x^i - x^j\|) \geq \frac{a}{\|x^i - x^j\|}.$$

For the repulsion function we use the same type of functions as in the previous section, i.e., functions satisfying

$$g_r(\|x^i - x^j\|) \leq \frac{b}{\|x^i - x^j\|^2}.$$

An example of attraction/repulsion function $g(\cdot)$ satisfying the above assumptions is shown in Figure 3.2.

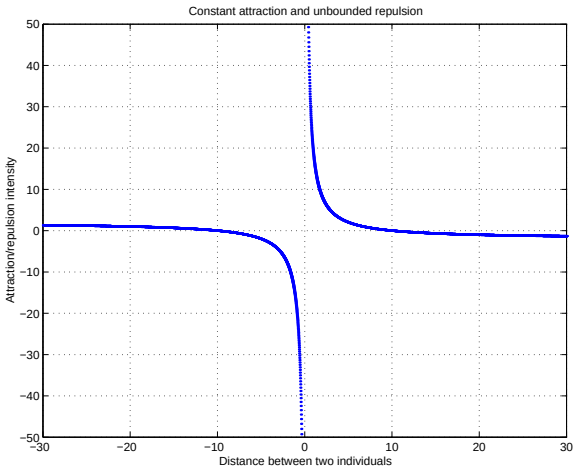

Figure 3.2: A $g(\cdot)$ function with constant attraction and unbounded repulsion.

For this case we have

$$a \sum_{i=1}^{M} \sum_{j=1, j\neq i}^{M} \|x^i - x^j\| \leq \sum_{i=1}^{M} \sum_{j=1, j\neq i}^{M} g_a(\|x^i - x^j\|)\|x^i - x^j\|^2.$$

Also, since

$$\|e^i\| = \frac{1}{M}\left\|\sum_{i=1}^{M}(x^i - x^j)\right\| \leq \frac{1}{M}\sum_{i=1}^{M}\|x^i - x^j\|$$

we obtain, in a similar manner to earlier,

$$aM\sum_{i=1}^{M}\|e^i\| \leq bM(M-1)$$

which implies that

$$\frac{1}{M-1}\sum_{i=1}^{M}\|e^i\| \leq \frac{b}{a}.$$

In other words, the *average* of the error will satisfy

$$e_{avg} = \frac{1}{M}\sum_{i=1}^{M}\|e^i\| \leq \frac{b}{a} = \epsilon_{avg},$$

at equilibrium, which constitutes a bound on the swarm size.

3.3 Other Extensions

3.3.1 Hardlimiting Repulsion for Uniform Swarm Density

During the analysis in Chapter 2 we realized that the bound on the swarm size is independent of the number of individuals M. This leads to the fact that as the number of individuals increases, the density of the swarm will increase which is not always consistent with swarms in nature. The same drawback is true for the results derived so far in this chapter including the case where we used unbounded repulsion. In this section we will see that a small modification of the model will prevent this from occurring.

Note that the unbounded repulsion functions we chose are such that

$$\lim_{\|x^i - x^j\| \to 0^+} g_r(\|x^i - x^j\|)\|x^i - x^j\| = \infty$$

Therefore, even though this will prevent the individuals from occupying the same space (or prevent collisions, in some sense), it does not guarantee the uniform density of the swarm. As the number of individuals in the swarm increases the total overall attraction on each individual increases and the individuals move closer and closer, even though they cannot occupy the same space. In order to avoid this, we can introduce a finite body size (or private area) of the individuals by using a "hardlimiting" repulsion function satisfying

$$\lim_{\|x^i - x^j\| \to \eta^+} g_r(\|x^i - x^j\|)\|x^i - x^j\| = \infty,$$

where η is a small positive parameter determining the finite body size (or private area) of the individuals.

However, we would like to emphasize that for this case the results (i.e., the derived bounds on the swarm size) in this chapter will not hold, which is exactly what we would like to achieve in this section. In fact, for this case we would expect the size of the swarm to depend on the number of the individuals and the density of the swarm to remain uniform recovering the characteristics of real biological swarms. This is because with the assumption that the initial positions of the individuals are such that $\|x^i(0) - x^j(0)\| > \eta$, we will have $\|x^i(t) - x^j(t)\| > \eta$ for all t and for all pairs (i, j). We will illustrate this with simulations at the end of this chapter.

3.3.2 Formation Stabilization

In this section we will show that with a simple modification our model can be applied to the problem of formation stabilization. First, note that in a given formation the distances between different pairs of individuals can be different. In other words, the equilibrium distance δ is dependent on the pairs (i, j) (therefore we will denote

the equilibrium distances with δ_{ij}). To accommodate this we consider the case in which the attraction/repulsion function $g(\cdot)$ are pair dependent. In other words, we have

$$\dot{x}^i = \sum_{j=1, j\neq i}^{M} g^{ij}(x^i - x^j), i = 1, \ldots, M, \tag{3.9}$$

where $g^{ij}(x^i - x^j) = -g^{ji}(x^j - x^i)$. However, $(x^i - x^j) = (x^k - x^l)$ does not necessarily imply $g^{ij}(x^i - x^j) = g^{kl}(x^k - x^l)$. This implies that the attraction and repulsion functions, and therefore the equilibrium distance δ_{ij} for different pairs (i, j), can be different. Then, given a desired formation with desired inter-agent distances d_{ij}, one can choose the attraction/repulsion functions $g^{ij}(\cdot)$ such that $\delta_{ij} = d_{ij}$ for every pair of individuals (i, j). This, in turn, results in the fact that the generalized Lyapunov function $J(x)$ has a unique minimum achieved at the desired formation. Then, in the light of Theorem 3 (which still holds) we know that asymptotically the desired formation will be achieved. Note that this is similar to the approach in [79] and is in contrast to the approach in [64], where the authors use virtual leaders in order to achieve formations. We would like also to emphasize that for this case Lemma 3 still holds, i.e., the center of the swarm is stationary. In other words, the model is for stabilizing stationary formations around their center $\bar{x}$.

Note that the results in preceding sections will still hold for the case in which the attraction/repulsion functions $g(\cdot)$ were pair dependent, as described in Eq. (3.9), as long as each of the attraction and repulsion functions $g^{ij}(\cdot) \in \mathcal{G}$. For that case, the bounds will be given in terms of the minimum attraction parameter $a_m = \min_{1\leq i,j\leq M}\{a_{ij}\}$ and the maximum repulsion parameter $b_m = \max_{1\leq i,j\leq M}\{b_{ij}\}$.

3.3.3 Adding Point-Mass Dynamics

In the swarm model that we described in the preceding sections we did not have mass in the equation of motion of the individuals. However, note that it is not difficult to extend the model in order to include such effects. One option is to consider point mass dynamics similar to the models for other animal aggregations such as in [80, 114, 47, 64]. In particular, it can be assumed that the equation of motion of each individual is given in Eq. (3.1) can be modified to be

$$\begin{aligned} \dot{x}^i &= v^i \\ \dot{v}^i &= \frac{1}{m_i}\left[\sum_{j=1,j\neq i}^{M} g(x^i - x^j) - \alpha_i\right], i = 1, \ldots, M, \end{aligned} \tag{3.10}$$

where m_i is the mass of the i^{th} individual and α_i is such that $v^{i\top}\alpha_i > 0$ if $v^i \neq 0$. (Note that similar model was considered recently in [64].) Then, as in [64] using the generalized Lyapunov function

$$J'(x) = \frac{1}{2}\sum_{i=1}^{M} m_i \|v^i\|^2 + J(x),$$

where $J(x)$ is as given in Eq. (3.4), one can show that results similar to the ones described so far follow. In particular, taking the time derivative of $J'(x)$ we obtain

$$\begin{aligned} \dot{J}'(x) &= \sum_{i=1}^{M} m_i \dot{v}^{i\top} v^i + \sum_{i=1}^{M} [\nabla_{x^i} J(x)]^\top \dot{x}^i \\ &= \sum_{i=1}^{M} \left[m_i \dot{v}^i + \nabla_{x^i} J(x)\right]^\top v^i \\ &= -\sum_{i=1}^{M} v^{i\top} \alpha_i, \end{aligned}$$

which obtained using the fact that $\nabla_{x^i} J(x) = -\dot{x}^i = -v^i$. Then, with the above choice of α_i we obtain $\dot{J}'(x) \leq 0$. In particular we can choose $\alpha_i = v^i$ we obtain

exactly the same as Eq. (2.10) implying that Theorem 3 also holds in this case. However, note that some of the other results (e.g., Theorem 1 and the other bounds) are not necessarily guaranteed to hold for this case and may need further analysis.

Note that this system can be viewed as a point mass control system with a control input u^i given by

$$u^i = -\nabla_{x^i} J(x) - \alpha_i = \sum_{j=1, j\neq i}^{M} g(x^i - x^j) - \alpha_i$$

which guarantees that as $t \to \infty$ we have $v^i \to 0$.

3.4 Simulation Examples

In this section we will provide some simulation examples in order to illustrate the operation of the swarm model. Once again we chose $n = 3$ for the simulations for easy visualization, however, note that the results hold for any n. We first choose the case of almost constant attraction and unbounded repulsion with $g_a(\|x^i - x^j\|) = \frac{a}{\|x^i - x^j\|}$, and $g_r(\|x^i - x^j\|) = \frac{b}{\|x^i - x^j\|^2}$ with parameters $a = b = 0.2$. We chose $M = 31$ members whose initial conditions are initialized randomly. The plot in Figure 3.3 shows the behavior of the swarm for about 15 seconds. As expected, the behavior of the swarm is similar to those in Chapter 2, i.e., the individuals form a cohesive cluster (around the center) as predicted by the theory. For this case we have the bound $\epsilon_{avg} = \frac{b}{a} = 1$ as the ultimate size of the swarm. The plot in Figure 3.4 shows the average e_{avg} of the distances of the individual positions to the swarm center. Note that the average converges to a value smaller than ϵ_{avg}, confirming the analytical derivations. The behavior of the swarm for the other two cases is similar.

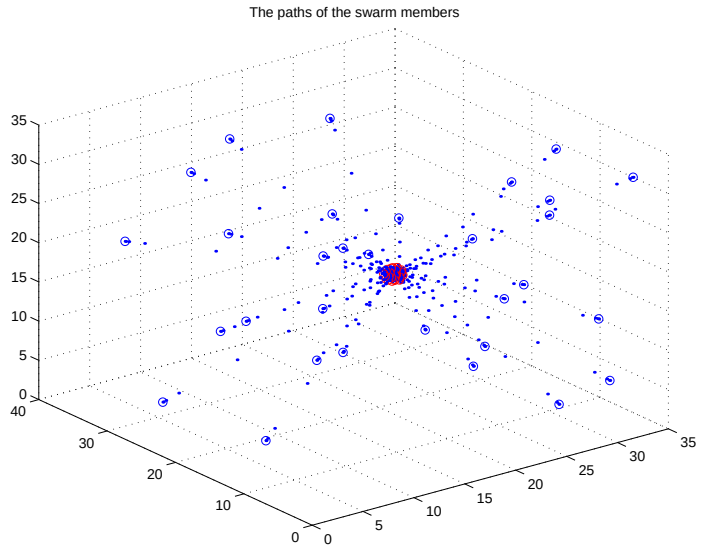

Figure 3.3: The motion of the swarm members.

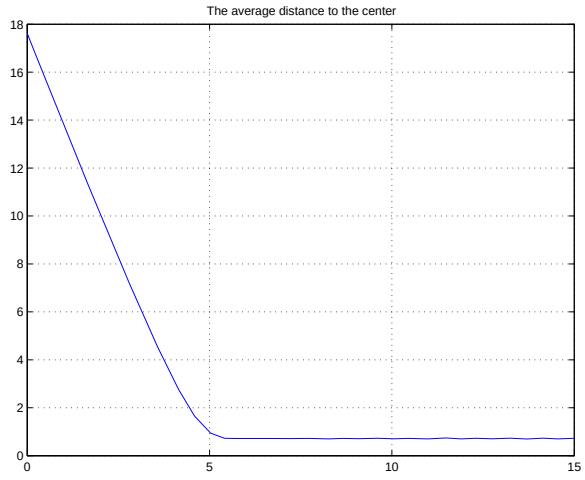

Figure 3.4: The average distance of the individuals to the center.

Now, we will illustrate the case in which swarm density is constant as in biological swarms. With this objective in mind consider the case of hardlimiting repulsion with

$$g_r(\|x^i - x^j\|) = \frac{b}{(\|x^i - x^j\| - c)^2}$$

with $c = 2$. In other words, we would like the individuals to keep a distance of at least $c = 2$ units apart from each other. The aggregating behavior of the swarm for this case with random initial positions satisfying $\|x^i(0) - x^j(0)\| > c$ for all pairs (i, j) is similar to the previous case shown in Figure 3.3. The difference, however, is that the minimum distance between any pair of individuals is always greater than $c = 2$ as desired (see the plot in Figure 3.5). Figure 3.6 shows the interindividual distances

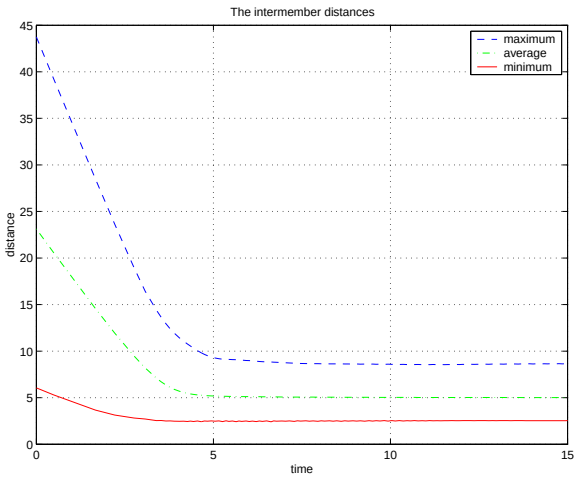

Figure 3.5: The interindividual distances for $M = 31$.

for the case in which we increased the number of individuals from $M = 31$ to $M = 61$. As one can see, while the minimum distance between pairs is still greater than $c = 2$, the maximum distance is larger, implying that the size of the swarm scaled with the number of individuals while the density of the swarm remained constant which, on the other hand, conforms our expectations. Having the swarm density constant is an important feature of the real biological swarms and this shows that our model with hardlimiting repulsion can describe that fact.

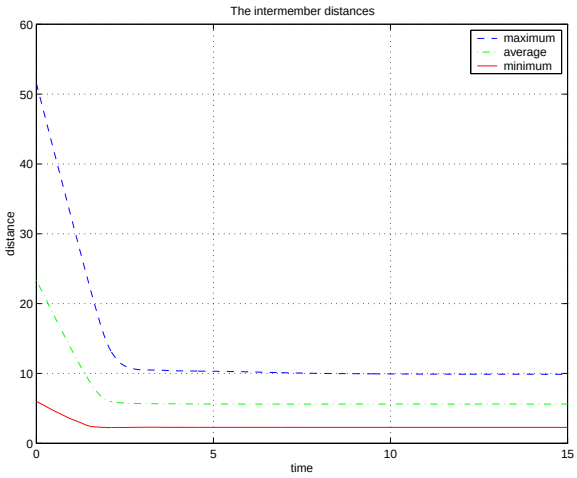

Figure 3.6: The interindividual distances for $M = 61$.

Now, consider the model with pair dependent attraction/repulsion functions, i.e., consider the model in Eq. (3.9). Assume that we have six agents which are required to form a formation of an equilateral triangle with three of the agents in the middle of each edge and distances between two neighboring agents equal to 1. For this case we design the attraction/repulsion functions for each pair of individuals such that the generalized Lyapunov function achieves a unique minimum at the desired formation. This is done by choosing $g^{ij}(\cdot)$'s such that the equilibrium distances are one of $\delta_{ij} = 1$, $\delta_{ij} = 2$, or $\delta_{ij} = \sqrt{3}$ for different pairs (i, j) of individuals depending on their relative location in the desired formation. Figure 3.7 shows the trajectories of the agents with initial positions chosen at random. As one can see the agents move and form the required formation while avoiding collisions in accordance with the expectations since we used unbounded repulsion.

In Chapter 2 and this chapter we considered stationary aggregating swarms. In other words, we considered swarms in which the center of mass is stationary and

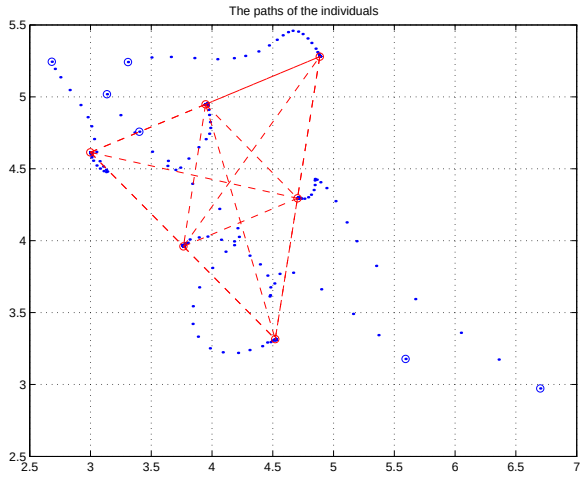

Figure 3.7: Equilateral triangle formation of 6 agents.

the motion of the individuals depends only on the relative position of the other individuals. In Chapter 4 we will consider social foraging swarms. In other words, we will consider a swarm model in which the motion of individuals is affected by an external profile of nutrients or toxic substances.

CHAPTER 4

SOCIAL FORAGING SWARMS

In this chapter we consider a model for social foraging swarms. In other words, we consider swarms that move in a profile of nutrients or toxic substances. We assume that the motion of each individual depends on the attraction and repulsion to the other individuals (as in aggregating swarms) as well as attraction to more favorable (nutrient rich) regions or repulsion from unfavorable (toxic) regions of the profile.

In order to describe the problem that we consider in intuitive level consider Figure 4.1 where simple bacterial chemotaxis is shown. In nature if we have a liquid

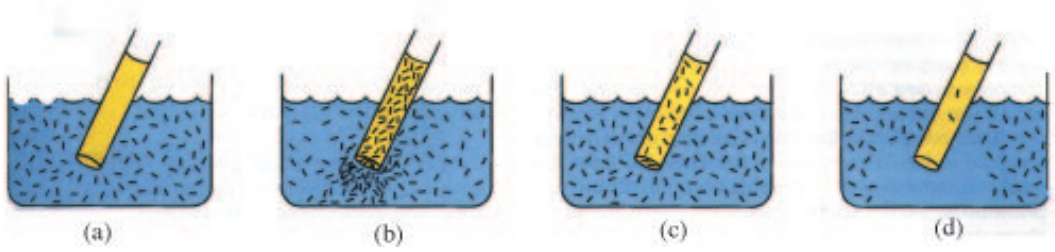

Figure 4.1: Bacterial *chemotaxis* (figure from [72]).

with homogeneous concentration of nutrients and with some bacteria in the liquid, as time progresses the density of the bacteria also becomes uniform in the container

as is shown in Figure 4.1(a). Then, if a tube with higher concentration of nutrients is inserted, it can be observed that bacteria swarm in the areas of higher nutrients as shown in Figure 4.1(b) and with time as they eat the food the density becomes again uniform (Figure 4.1(b)). However, if a toxic substances are inserted into the tube, then one can observe that bacteria swim away from the toxic substances as shown in Figure 4.1(d). This behavior of the bacteria is called *chemotaxis*. It is known that bacteria is able sense (approximate) gradients of the environment, which allows it to achieve such a behavior. Our objective in this chapter is to model and analyze this kind of behavior. We will represent the nutrients and toxic substances with a profile. However, in our model the profile will be constant, i.e., it will not dissipate as in the above example. Moreover, we will have also interindividual attractions in the model.

4.1 The Swarm Model

Consider again M individuals (members) in an n-dimensional Euclidean space with position vector of individual i denoted by $x^i \in \mathbb{R}^n$. Let $\sigma : \mathbb{R}^n \to \mathbb{R}$ represent the attractant/repellent profile or the "σ-profile" which can be a profile of nutrients or some attractant or repellent substances (e.g., food/nutrients, pheromones laid by other individual, or toxic chemicals). Assume that the areas that are minimum points are "favorable" to the individuals in the swarm. For example, assume that $\sigma(y) < 0$ represents attractant or nutrient rich, $\sigma(y) = 0$ represents a neutral, and $\sigma(y) > 0$ represents a noxious environment at y. (Note that $\sigma(\cdot)$ can be a combination of several attractant or repellent profiles.)

We consider the equation of motion of each individual i described by

$$\dot{x}^i = -\nabla_{x^i}\sigma(x^i) + \sum_{j=1, j\neq i}^{M} g(x^i - x^j),\ i = 1, \ldots, M, \tag{4.1}$$

where $g(\cdot)$ represents the function of mutual attraction and repulsion between the individuals and is an *odd* function of the form of Eq. (3.2)

$$g(y) = -y\left[g_a(\|y\|) - g_r(\|y\|)\right], \tag{4.2}$$

with all the assumptions in Chapter 3 satisfied, i.e., $g(\cdot) \in \mathcal{G}$.

The term $-\nabla_{x^i}\sigma(x^i)$ represents the motion of the individuals towards regions with higher nutrient concentration and away from regions with high concentration of toxic substances. Note that the implicit assumption that the individuals know the gradient of the profile at their position is not very restrictive since it is known that some organisms such as bacteria are able to construct local approximations to gradients [85].

Remark: We would like to emphasize that even though we get our inspiration from biological swarms, our model constitutes also a kinematic model for swarms of engineering multi-agent systems. In the context of multi-agent systems the profile $\sigma(\cdot)$ constitutes an *artificial potential field* that models the environment containing obstacles or threats to be avoided (analogous to toxic substances) and targets to be moved towards (analogous to food). In systems with real agents (with their specific dynamics) the trajectories generated by our model can be used as reference trajectories for the agents to follow. ■

The objective here is to analyze the qualitative properties of the collective behavior (motions in n-space) of the individuals. With this in mind, consider again the *center* of the swarm as $\bar{x} = \frac{1}{M}\sum_{i=1}^{M} x^i$. Then, one can show that the motion of the center is given by

$$\dot{\bar{x}} \;=\; \frac{1}{M}\sum_{i=1}^{M}\left[-\nabla_{x^i}\sigma(x^i) - \sum_{j=1, j\neq i}^{M}\left(a - b\exp\left(-\frac{\|x^i - x^j\|^2}{c}\right)\right)(x^i - x^j)\right]$$

$$
\begin{aligned}
&= -\frac{1}{M}\sum_{i=1}^{M}\nabla_{x^i}\sigma(x^i) - \frac{1}{M}\sum_{i=1}^{M}\sum_{j=1,j\neq i}^{M}\left(a - b\exp\left(-\frac{\|x^i - x^j\|^2}{c}\right)\right)(x^i - x^j) \\
&= -\frac{1}{M}\sum_{i=1}^{M}\nabla_{x^i}\sigma(x^i), \qquad (4.3)
\end{aligned}
$$

since

$$
\frac{1}{M}\sum_{i=1}^{M}\sum_{j=1,j\neq i}^{M}\left(a - b\exp\left(-\frac{\|x^i - x^j\|^2}{c}\right)\right)(x^i - x^j) = 0.
$$

Remark: Note that the collective behavior in Eq. (4.3) has a kind of averaging (filtering or smoothing) effect. This may be important if the σ-profile is a noisy function (or there is a measurement error or noise in the system as discussed in [45, 46]). In other words, if the σ-profile were a "noisy function" and the individuals were moving individually (without interindividual attraction/repulsion), then they could get stuck at a local minima, whereas if they swarm, since they are moving collectively, the other individuals will "pull" them out of such local minima. ■

One issue to note here is that as in [85] it is possible to view the foraging (and therefore social foraging) problem here as a *distributed optimization problem* (in which each individual is individually searching for the minimum) or an *optimal control problem*, where the objective is to find the "optimal" control policy or search strategy that will maximize, for instance, the energy intake per time spent foraging. Here, we are not concerned with this problem. We specify the search strategy, which is a type of distributed gradient search, and are concerned with stability or convergence properties of the strategy. Still, however, it is an optimization or distributed function minimization problem. Note that in nature there are many species with a variety of foraging or search strategies; some of these are most certainly not gradient-based and hence lie outside the scope of this work.

In this chapter we will consider attraction/repulsion functions which are continuous and have *linear attraction*, i.e., $g_a(\|x^i - x^j\|) = a$ for some $a > 0$ and all $\|x^i - x^j\|$, and *bounded repulsion*, i.e., $g_r(\|x^i - x^j\|)\|x^i - x^j\| \leq b$ for some $b > 0$ and all $\|x^i - x^j\|$. In other words, we consider the attraction/repulsion discussed in Section 3.2.1. The continuity assumption is needed in order to guarantee the existence and uniqueness of the solutions of the system. This assumption leads to the fact that $g(\cdot)$ vanishes at the origin and brings a concern about collisions between the individuals. However, by setting the magnitude of the repulsion high enough it is possible to avoid collisions at the expense of getting a larger swarm size. Another possibility is to choose unbounded repulsion, i.e., choose $g_r(\cdot)$ such that $g_r(\|x^i - x^j\|)\|x^i - x^j\| \to \infty$ as $\|x^i - x^j\| \to 0$ as in Chapter 3. However, incorporating unbounded repulsion in the context of social foraging swarms is a topic of further research. One function that satisfies these conditions is the function $g(\cdot)$ in Eq. (2.2) discussed in Chapter 2.

4.2 Cohesion Analysis

Note that for the error $e^i = x^i - \bar{x}$ we have

$$\dot{e}^i = -\nabla_{x^i}\sigma(x^i) - \sum_{j=1, j\neq i}^{M} [a - g_r(\|x^i - x^j\|)](x^i - x^j) + \frac{1}{M}\sum_{j=1}^{M} \nabla_{x^j}\sigma(x^j),$$

and for the Lyapunov function $V_i = \frac{1}{2}\|e^i\|^2 = \frac{1}{2}e^{i\top}e^i$ we obtain

$$\begin{aligned} \dot{V}_i &= -aM\|e^i\|^2 + \sum_{j=1, j\neq i}^{M} g_r(\|x^i - x^j\|)(x^i - x^j)^\top e^i \\ &\quad - \left[\nabla_{x^i}\sigma(x^i) - \frac{1}{M}\sum_{j=1}^{M} \nabla_{x^j}\sigma(x^j)\right]^\top e^i. \end{aligned} \tag{4.4}$$

Now, we have two assumptions.

Assumption 1 *There exists a constant $\bar{\sigma} > 0$ such that $\|\nabla_y \sigma(y)\| \leq \bar{\sigma}$ for all y.*

Assumption 2 *There exists a constant $A_\sigma > -aM$ such that*

$$\left[\nabla_{x^i}\sigma(x^i) - \frac{1}{M}\sum_{j=1}^{M}\nabla_{x^j}\sigma(x^j)\right]^\top e^i \geq A_\sigma\|e^i\|^2$$

for all x^i and x^j.

Note that Assumption 1 is a very reasonable assumption that is satisfied with almost any realistic profile (e.g., plane and Gaussian profiles). In contrast, Assumption 2 is a more restrictive assumption. Therefore, it may be satisfied only by few profiles (e.g., a quadratic profile). With this in mind we state the following result.

Lemma 4 *Consider the swarm described by the model in Eq. (4.1) with interindividual attraction/repulsion function $g(\cdot)$ as given in Eq. (4.2) with linear attraction (i.e., $g_a(\|x^i - x^j\|) = a$ for some $a > 0$ and all $\|x^i - x^j\|$) and bounded repulsion, (i.e., $g_r(\|x^i - x^j\|)\|x^i - x^j\| \leq b$ for some $b > 0$ and all $\|x^i - x^j\|$). Then, as $t \to \infty$ we have $x^i(t) \to B_\epsilon(\bar{x}(t))$, where*

$$B_\epsilon(\bar{x}(t)) = \{y(t) : \|y(t) - \bar{x}(t)\| \leq \epsilon\}$$

and

- *If Assumption 1 is satisfied, then*

$$\epsilon = \epsilon_1 = \frac{(M-1)}{aM}\left[b + \frac{2\bar{\sigma}}{M}\right],$$

- *If Assumption 2 is satisfied, then*

$$\epsilon = \epsilon_2 = \frac{b(M-1)}{aM + A_\sigma}.$$

Proof: **Case 1:** From Assumption 1 one can show that we have

$$\left\| \nabla_{x^i} \sigma(x^i) - \frac{1}{M} \sum_{j=1}^{M} \nabla_{x^j} \sigma(x^j) \right\| \leq \frac{2\bar{\sigma}(M-1)}{M}.$$

Using this bound and the bound on the repulsion to overbound $\dot{V}_i$ we obtain

$$\dot{V}_i \leq -aM\|e^i\| \left[\|e^i\| - \frac{b(M-1)}{aM} - \frac{2\bar{\sigma}(M-1)}{aM^2} \right],$$

which implies that as long as $\|e^i\| > \epsilon_1$ we have $\dot{V}_i < 0$.

Case 2: Using Assumption 2 one can show that $\dot{V}_i$ satisfies

$$\dot{V}_i \leq -(aM + A_\sigma)\|e^i\| \left[\|e^i\| - \frac{b(M-1)}{aM + A_\sigma} \right].$$

Therefore, we conclude that as long as $\|e^i\| > \epsilon_2$ we have $\dot{V}_i < 0$. ∎

This result is important because it proves the cohesiveness of the swarm and provides a bound on the swarm size, defined as the radius of the hyperball centered at $\bar{x}(t)$ and containing all the individuals. Therefore, since the center $\bar{x}(t)$ is not stationary, in order to analyze the collective behavior of the swarm we need to consider its motion.

In species that engage in social foraging it has been observed that the individuals in swarms desire to be close (but not too close) to other individuals. In the mean time, they want to find more food. The balance between these desires determines the size of the swarm (herd, flock or school). Our model captures this by having an interindividual attraction/repulsion term and also a term due to the environment (or the nutrient profile) affecting their motion. In the results above, the resulting swarm sizes depend on the interindividual attraction/repulsion parameters (a and b) and the parameters of the nutrient profile ($\bar{\sigma}$ and A_σ). Moreover, the dependence on these parameters makes intuitive sense. Larger attraction (larger a) leads to a smaller

swarm size, larger repulsion (larger b) leads to a larger swarm size, larger $\bar{\sigma}$ (fast changing landscape) leads to a larger swarm. These concepts are present in foraging theory in biology and model the balance of the desire of the individuals to "stick together" with the desire to "get more food" that was created by evolutionary forces. Note also the effect of A_σ on the bound ϵ_2. If $A_\sigma > 0$, then ϵ_2 decreases with increase in A_σ which is expected since there is an extra attractive force on the individuals. If, on the other hand, $A_\sigma < 0$, then ϵ_2 increases with increase in the magnitude of A_σ. The threshold $A_\sigma = -aM$ is the point at which the interindividual attraction is not anymore guaranteed to "hold the swarm together" since it is counterbalanced by the repulsion from the profile. In other words, beyond that threshold the repulsion is so intense that the "desire to keep away from the center of the profile" dominates (or is more plausible than) the "desire to stick together." This helps to quantify the inherent balance between the sometimes conflicting desires for swarm cohesiveness and for following cues from the environment to find food. Such behavior can be seen in, for example, fish schools when a predator attacks the school. In that case the fish move very fast in all directions away from the predator [84].

Note that the desire of the individuals to "stick together" depends on the interindividual attraction parameter a and the number of individuals M. This is consistent with *some* biological swarms, where it has been observed that individuals are attracted more to larger (or more crowded) swarms. In nature the values of these parameters have been tuned for millions of years by the evolutionary process.

The above result is an asymptotic result, i.e., $x^i(t) \to B_\epsilon(\bar{x}(t))$ as $t \to \infty$. Note, however, that for any $\epsilon^* > \epsilon$, $x^i(t)$ will enter $B_{\epsilon^*}(\bar{x}(t))$ in a finite time. In other words,

it can be shown that the swarm of any size a little larger than ϵ will be formed in a finite time.

4.3 Motion along a Plane Attractant/Repellent Profile

In this section we assume that the profile is described by a *plane* equation of the form

$$\sigma(y) = a_\sigma^\top y + b_\sigma, \tag{4.5}$$

where $a_\sigma \in \mathbb{R}^n$ and $b_\sigma \in \mathbb{R}$. One can see that $\nabla_y \sigma(y) = a_\sigma$ and Assumption 1 holds with $\bar{\sigma} = \|a_\sigma\|$. However, we also note that $\nabla_{x^i}\sigma(x^i) - \frac{1}{M}\sum_{j=1}^{M} \nabla_{x^j}\sigma(x^j) = 0$ for all i, implying that the last term in Eq. (4.4) vanishes. Therefore, for this profile we have

$$\epsilon = \epsilon_p = \frac{b(M-1)}{aM}$$

as the bound on the size of the swarm. Note that this is exactly the same bound obtained for aggregating swarms. This is because for this profile, when we consider the relative motions of the individuals with respect to the center, the effect of the profile cancel out. Note also that for this case we have

$$\dot{\bar{x}}(t) = -a_\sigma,$$

which implies that the center of the swarm will be moving with the constant velocity vector $-a_\sigma$ (and eventually will diverge towards infinity where the minimum of the profile occurs).

The motions in this section can be viewed as a model of a foraging herd that moves in a constant direction (while keeping its cohesiveness) with a constant speed such as the one considered in [49]. Another view of the system in this section could be as a model of a multi-agent system in which the autonomous agents move in a

formation with a constant speed. In fact, transforming the system to e^i coordinates we obtain

$$\dot{e}^i = \sum_{j=1, j\neq i}^{M} g(e^i - e^j), i = 1, \ldots, M,$$

which is exactly the model of an aggregating swarm considered in Chapter 2 and Chapter 3. Therefore, all the results obtained in these chapters apply for e^i. In particular, we have $\dot{e}^i(t) \to 0$ as $t \to \infty$. In other words, the swarm converges to a constant configuration or a formation (i.e., constant relative positions) that moves with a constant speed in the direction of $-a_\sigma$. Then, by choosing the attraction/repulsion functions to be pair dependent $g^{ij}(\cdot)$ as was discussed in Section 3.3.2, we can achieve any desired moving formation.

4.4 Quadratic Attractant/Repellent Profiles

In this section, we will consider

$$\sigma(y) = \frac{A_\sigma}{2}\|y - c_\sigma\|^2 + b_\sigma, \tag{4.6}$$

where $A_\sigma \in \mathbb{R}$, $b_\sigma \in \mathbb{R}$, and $c_\sigma \in \mathbb{R}^n$. Note that this profile has a global extremum (either a minimum or a maximum depending on the sign of A_σ) at $y = c_\sigma$. Its gradient at a point $y \in \mathbb{R}^n$ is given by

$$\nabla_y \sigma(y) = A_\sigma(y - c_\sigma).$$

Assume that $A_\sigma > -aM$. Then, with a simple manipulation one can show that for this profile Assumption 2 holds with strict equality. Therefore, the result of Lemma 4 holds with the bound

$$\epsilon_q = \epsilon_2 = \frac{b(M-1)}{aM + A_\sigma}.$$

Now, let us analyze the motion of the center $\bar{x}$. Substituting the gradient in the equation of motion of $\bar{x}$ given in Eq. (4.3) we obtain

$$\dot{\bar{x}} = -A_\sigma(\bar{x} - c_\sigma).$$

Defining the error between the center $\bar{x}$ and the extremum point c_σ as $e_\sigma = \bar{x} - c_\sigma$, we have

$$\dot{e}_\sigma = -A_\sigma e_\sigma,$$

which implies that as $t \to \infty$ we have $e_\sigma(t) \to 0$ if $A_\sigma > 0$ and that $e_\sigma(t) \to \infty$ if $A_\sigma < 0$ and $e_\sigma(0) \neq 0$. Therefore, we have the following result.

Lemma 5 *Consider the swarm described by the model in Eq. (4.1) with interindividual attraction/repulsion function $g(\cdot)$ as given in Eq. (4.2). Assume that the σ-profile of the environment is given by Eq. (4.6). As $t \to \infty$ we have*

- *If $A_\sigma > 0$, then $\bar{x}(t) \to c_\sigma$ (i.e., the center of the swarm converges to the global minimum c_σ of the profile), or*
- *If $A_\sigma < 0$ and $\bar{x}(0) \neq c_\sigma$, then $\bar{x}(t) \to \infty$ (i.e., the center of the swarm diverges from the global maximum c_σ of the profile).*

Note that this result holds for any A_σ, i.e., we do not need the assumption $A_\sigma > -aM$. (We need the assumption $A_\sigma > -aM$ to guarantee cohesiveness of the swarm, i.e., to guarantee the bound ϵ_q on the swarm size.) Note also that for the case with $A_\sigma > 0$ for any finite $\epsilon^* > 0$ (no matter how small) it can be shown that $\|\bar{x}(t) - c_\sigma\| < \epsilon^*$ is satisfied in a finite time. In other words, $\|\bar{x}\|$ enters any ϵ^* neighborhood of c_σ in a finite time. In contrast, for the case with $A_\sigma < 0$ and $\bar{x}(0) \neq c_\sigma$

for any $D > 0$ (no matter how large) it can be shown that $\|\bar{x}(t) - c_\sigma\| > D$ is satisfied in a finite time, implying that $\|\bar{x}\|$ leaves any bounded D-neighborhood of c_σ in a finite time. If $A_\sigma < 0$ and $\bar{x}(0) = c_\sigma$, on the other hand, then $\bar{x}(t) = c_\sigma$ for all t. In other words, for this case the swarm will be either "trapped" around the maximum point because of the interindividual attraction (i.e., desire of the individuals to be close to each other) or will disperse in all directions if the interindividual attraction is not strong enough (i.e., $A_\sigma < -aM$). Note, however, that even if they disperse, the center $\bar{x}$ will not move and stay at c_σ.

Here, we did not consider the $A_\sigma = 0$ case. This is because if $A_\sigma = 0$ then the profile is uniform everywhere and $\nabla_y \sigma(y) = 0$ for all $y \in \mathbb{R}^n$. Therefore, the existence of the profile does not affect the motion of the individuals and stability analysis is reduced to the case of nondrifting aggregating swarms considered in Chapter 2 and Chapter 3.

Combining the results of Lemmas 4 and 5 together with the above observations gives us the following result.

Theorem 4 *Consider the swarm described by the model in Eq. (4.1) with interindividual attraction/repulsion function $g(\cdot)$ as given in Eq. (4.2) with linear attraction and bounded repulsion. Assume that the σ-profile of the environment is given by Eq. (4.6) and that $A_\sigma > -aM$. Then, the following hold*

- *If $A_\sigma > 0$, then for any $\epsilon^* > \epsilon_2$ all individuals $i = 1, \ldots, M$, will enter $B_{\epsilon^*}(c_\sigma)$ in a finite time,*

- *If $A_\sigma < 0$ and $\bar{x}(0) \neq c_\sigma$, then for any $D < \infty$ all individuals $i = 1, \ldots, M$, will exit $B_D(c_\sigma)$ in a finite time.*

This result is important because it gives finite time convergence (divergence) of *all* the individuals to nutrient rich (from toxic) regions of the profile.

Quadratic profiles are rather simple profiles and the results in this section are intuitively expected. In the next section, we will consider a profile which is a sum of Gaussians and has multiple extremum points.

4.5 Multimodal Gaussian Attractant/Repellent Profiles

In this section, we will consider a profile which is a combination of *Gaussian* profiles,

$$\sigma(y) = -\sum_{i=1}^{N} \frac{A_\sigma^i}{2} \exp\left(-\frac{\|y - c_\sigma^i\|^2}{l_\sigma^i}\right) + b_\sigma, \tag{4.7}$$

where $c_\sigma^i \in \mathbb{R}^n$, $l_\sigma^i \in \mathbb{R}^+$, $A_\sigma^i \in \mathbb{R}$ for all $i = 1, \ldots, N$, and $b_\sigma \in \mathbb{R}$. Note that since the A_σ^i's can be positive or negative there can be both hills and valleys leading to a "more irregular" profile as in [85].

The gradient of the profile at a point y is given by

$$\nabla_y \sigma(y) = \sum_{i=1}^{N} \frac{A_\sigma^i}{l_\sigma^i}(y - c_\sigma^i) \exp\left(-\frac{\|y - c_\sigma^i\|^2}{l_\sigma^i}\right).$$

Note that for this profile Assumption 1 is satisfied with $\bar{\sigma} = \sum_{i=1}^{N} \frac{|A_\sigma^i|}{\sqrt{2l_\sigma^i}} \exp\left(-\frac{1}{2}\right)$. Therefore, from Lemma 4 we have

$$\epsilon_G = \epsilon_1 = \frac{(M-1)}{aM}\left[b + \frac{1}{M}\sum_{i=1}^{N} |A_\sigma^i| \sqrt{\frac{2}{l_\sigma^i}} \exp\left(-\frac{1}{2}\right)\right]$$

as the bound on the swarm size.

Using the profile gradient equation we can write the equation of motion of the swarm center $\bar{x}$ as

$$\dot{\bar{x}} = -\frac{1}{M}\sum_{j=1}^{N} \frac{A_\sigma^j}{l_\sigma^j} \sum_{i=1}^{M} (x^i - c_\sigma^j) \exp\left(-\frac{\|x^i - c_\sigma^j\|^2}{l_\sigma^j}\right).$$

As one can see, it is not obvious from this equation how the center $\bar{x}$ will move. Therefore, for this type of profile it is not easy to prove convergence of the individuals to minima of the profile for the general case. However, under some conditions it is possible to prove convergence to the vicinity of a particular c_σ^j (if c_σ^j is the center of a valley) or divergence from the neighborhood of a particular c_σ^j (if c_σ^j is the center of a hill).

Lemma 6 *Consider the swarm described by the model in Eq. (4.1) with interindividual attraction/repulsion function $g(\cdot)$ as given in Eq. (4.2). Assume that the σ-profile of the environment is given by Eq. (4.7). Moreover, assume that for some $k, 1 \leq k \leq N$, we have*

$$\|x^i(0) - c_\sigma^k\| \leq h_k \sqrt{l_\sigma^k}$$

for some h_k and for all $i = 1, \ldots, M$, and that for all $j = 1, \ldots, N, j \neq k$ we have

$$\|x^i(0) - c_\sigma^j\| \geq h_j \sqrt{l_\sigma^j}$$

for some $h_j, j = 1, \ldots, N, j \neq k$ and for all $i = 1, \ldots, M$. (This means that the swarm is sufficiently near c_σ^k and sufficiently far from other $c_\sigma^j, j \neq k$.) Moreover, assume that

$$\frac{A_\sigma^k}{\sqrt{l_\sigma^k}} h_k \exp\left(-h_k^2\right) > \frac{1}{\alpha} \sum_{j=1, j\neq k}^{N} \frac{|A_\sigma^j|}{\sqrt{l_\sigma^j}} h_j \exp\left(-h_j^2\right),$$

is satisfied for some $0 < \alpha < 1$. Then, for $e_\sigma^k = \bar{x} - c_\sigma^k$ as $t \to \infty$ we will have

- *If $A_\sigma^k > 0$, then $\|e_\sigma^k(t)\| \leq \epsilon_G + \alpha h_k \sqrt{l_\sigma^k}$*
- *If $A_\sigma^k < 0$ and $\|e_\sigma^k(0)\| \geq e_{max}(0) + \alpha h_k \sqrt{l_\sigma^k}$, then $\|e_\sigma^k(t)\| \geq \epsilon_G + \alpha h_k \sqrt{l_\sigma^k}$, where $e_{max} = \max_{i=1,\ldots,M}\{e^i\}$.*

Proof: Let $V_\sigma^k = \frac{1}{2} e_\sigma^{k\top} e_\sigma^k$ be the Lyapunov function.

Case 1: $A_\sigma^k > 0$**:** Taking the derivative of V_σ^k along the motion of the swarm we have

$$\begin{aligned}
\dot{V}_\sigma^k &= -\sum_{j=1}^{N} \frac{A_\sigma^j}{M l_\sigma^j} \sum_{i=1}^{M} \exp\left(-\frac{\|x^i - c_\sigma^j\|^2}{l_\sigma^j}\right) (x^i - c_\sigma^j)^\top e_\sigma^k \\
&= -\frac{A_\sigma^k}{M l_\sigma^k} \sum_{i=1}^{M} \exp\left(-\frac{\|x^i - c_\sigma^k\|^2}{l_\sigma^k}\right) \|e_\sigma^k\|^2 - \frac{A_\sigma^k}{M l_\sigma^k} \sum_{i=1}^{M} \exp\left(-\frac{\|x^i - c_\sigma^k\|^2}{l_\sigma^k}\right) e^{i\top} e_\sigma^k \\
&\quad - \sum_{j=1, j\neq k}^{N} \frac{A_\sigma^j}{M l_\sigma^j} \sum_{i=1}^{M} \exp\left(-\frac{\|x^i - c_\sigma^j\|^2}{l_\sigma^j}\right) (x^i - c_\sigma^j)^\top e_\sigma^k \\
&\leq -\frac{A_\sigma^k}{M l_\sigma^k} \sum_{i=1}^{M} \exp\left(-\frac{\|x^i - c_\sigma^k\|^2}{l_\sigma^k}\right) \|e_\sigma^k\|^2 + \frac{A_\sigma^k}{M l_\sigma^k} \sum_{i=1}^{M} \exp\left(-\frac{\|x^i - c_\sigma^k\|^2}{l_\sigma^k}\right) \|e^i\| \|e_\sigma^k\| \\
&\quad + \sum_{j=1, j\neq k}^{N} \frac{|A_\sigma^j|}{M l_\sigma^j} \sum_{i=1}^{M} \exp\left(-\frac{\|x^i - c_\sigma^j\|^2}{l_\sigma^j}\right) \|x^i - c_\sigma^j\| \|e_\sigma^k\| \\
&\leq -\frac{A_\sigma^k}{M l_\sigma^k} \sum_{i=1}^{M} \exp\left(-\frac{\|x^i - c_\sigma^k\|^2}{l_\sigma^k}\right) \|e_\sigma^k\| \times \\
&\quad \times \left[\|e_\sigma^k\| - e_{max} - \frac{\sum_{j=1, j\neq k}^{N} \frac{|A_\sigma^j|}{M l_\sigma^j} \sum_{i=1}^{M} \exp\left(-\frac{\|x^i - c_\sigma^j\|^2}{l_\sigma^j}\right) \|x^i - c_\sigma^j\|}{\frac{A_\sigma^k}{M l_\sigma^k} \sum_{i=1}^{M} \exp\left(-\frac{\|x^i - c_\sigma^k\|^2}{l_\sigma^k}\right)} \right],
\end{aligned}$$

which implies that we have $\dot{V}_\sigma^k < 0$ as long as $\|e_\sigma^k\| > e_{max} + \alpha h_k \sqrt{l_\sigma^k}$, and from Lemma 4 we know that as $t \to \infty$ we have $e_{max}(t) \leq \epsilon_G$.

Case 2: $A_\sigma^k < 0$**:** Similar to above, for this case it can be shown that

$$\dot{V}_\sigma^k \geq \frac{|A_\sigma^k|}{M l_\sigma^k} \sum_{i=1}^{M} \exp\left(-\frac{\|x^i - c_\sigma^k\|^2}{l_\sigma^k}\right) \|e_\sigma^k\| \left[\|e_\sigma^k\| - e_{max} - \alpha h_k \sqrt{l_\sigma^k} \right],$$

which implies that if $\|e_\sigma^k\| > e_{max} + \alpha h_k \sqrt{l_\sigma^k}$, we have $\dot{V}_\sigma > 0$. In other words, $\|e_\sigma^k\|$ will increase. From Lemma 4 we have that e_{max} is decreasing. Therefore, since by hypothesis $\|e_\sigma^k(0)\| > e_{max}(0) + \alpha h_k \sqrt{l_\sigma^k}$ we have that $\dot{V}_\sigma > 0$ holds at $t = 0$. Now, consider the boundary $\|e_\sigma^k\| = \epsilon_G + h_k \sqrt{l_\sigma^k}$. It can be shown that on the boundary we

have

$$\dot{V}_\sigma \geq \frac{|A_\sigma^k| h_k (1-\alpha) \left(\epsilon_G + h_k \sqrt{l_\sigma^k}\right) \exp\left(-h_k^2\right)}{\sqrt{l_\sigma^k}} > 0,$$

from which using (a corollary to) the Chetaev Theorem we conclude that $\|e_\sigma^k\|$ will exit the $\epsilon_G + h_k\sqrt{l_\sigma^k}$-neighborhood of c_σ^k. ∎

Now, combining the results of Lemmas 4 and 6 we can state the following result.

Theorem 5 *Consider the swarm described by the model in Eq. (4.1) with interindividual attraction/repulsion function $g(\cdot)$ as given in Eq. (4.2) with linear attraction and bounded repulsion. Assume that the σ-profile of the environment is given by Eq. (4.7). Assume that the conditions of Lemma 6 hold. Then, as $t \to \infty$ all individuals will*

- *Enter the hyperball $B_{\epsilon_5}(c_\sigma^k)$, where $\epsilon_5 = 2\epsilon_G + \alpha h_k \sqrt{l_\sigma^k}$, if $A_\sigma^k > 0$, or*
- *Leave the $h_k\sqrt{l_\sigma^k}$-neighborhood of c_σ^k, if $A_\sigma^k < 0$.*

The only drawback of the above result is that we need

$$2\epsilon_G + \alpha h_k \sqrt{l_\sigma^k} < h_k \sqrt{l_\sigma^k}$$

in order for the result to make sense. This implies that we need

$$\epsilon_G < \left(\frac{1-\alpha}{2}\right) h_k \sqrt{l_\sigma^k}$$

which sometimes may not be easy to satisfy. However, one issue to note is that ϵ_G is a very conservative bound. In reality, the actual size of the swarm is typically much smaller than the bound (e.g., one can derive a tighter bound on the *root-mean-square* of the error as was done in Chapter 3 for aggregating swarms.) Therefore, effectively,

ϵ_G can be replaced with $e_{max}(\infty) < \epsilon_G$ and it may be easier to satisfy the above condition.

Remark: If $N = 1$ we have a *Gaussian* profile (i.e., we have only a single valley or hill), which is a special case of the multimodal Gaussian profiles considered in this section. For this case, the conditions of Lemma 6 are automatically satisfied (i.e., the swarm members are automatically sufficiently close to the single center and sufficiently far from other centers). Then, as in the case of the quadratic profile, it can be shown that as $t \to \infty$ all the individuals converge to the neighborhood of the single minimum for $A_\sigma > 0$ or exit any bounded neighborhood of the single maximum for $A_\sigma < 0$. The results obtained, however, are weaker than the ones for the quadratic profile. For example, for the Gaussian profile we cannot show that the center $\bar{x}(t)$ converges to c_σ for $A_\sigma > 0$ (which was possible for the quadratic profile). ■

4.6 Analysis of Individual Behavior in a Cohesive Swarm

The results above do not provide information about the ultimate behavior of the individuals. In other words, they do not specify whether the individuals will eventually stop moving (as was the case in aggregating swarms) or will end up in oscillatory motions within the specified regions. In this section, we will investigate the ultimate behavior of the individuals. In particular, we will analyze the ultimate behavior of the individuals in a quadratic profile with $A_\sigma > 0$, and in a multimodal Gaussian profile with the conditions of Lemma 6 for the $A_\sigma^k > 0$ case satisfied. To this end, once again we consider the state $x = [x^{1\top}, \ldots, x^{M\top}]^\top$ of the system and the invariant set of equilibrium points be $\Omega_e = \{x : \dot{x} = 0\}$. We will prove that for the

above mentioned cases as $t \to \infty$ the state $x(t)$ converges to Ω_e, i.e., eventually all the individuals stop moving.

Theorem 6 *Consider the swarm described by the model in Eq. (4.1) with an attraction/repulsion function $g(\cdot)$ as given in Eq. (4.2) with linear attraction and bounded repulsion. Assume that the σ-profile is one of the following*

- *A quadratic profile in Eq. (4.6) with $A_\sigma > 0$, or*
- *A multimodal Gaussian profile in Eq. (4.7) with conditions of Lemma 6 for the $A_\sigma^k > 0$ case satisfied.*

Then, as $t \to \infty$ we have the state $x(t) \to \Omega_e$.

The proof of this result follows the lines in the proof of Theorem 3 in Chapter 3 and therefore is omitted.

One issue to note here is that for the cases excluded in the above theorem, i.e., for the plane profile, quadratic profile with $A_\sigma < 0$, and the multimodal Gaussian profile for the case with $A_\sigma^k < 0$ or with initial conditions not necessarily satisfying the conditions of Theorem 5, the sets defined as $\Omega_c = \{x : J(x) \leq J(x(0))\}$ may not be compact. Therefore, we cannot apply the LaSalle's Invariance Principle (on which the proof is based) for these cases. Moreover, since they are (possibly) diverging, intuitively we do not expect them to stop their motion. Furthermore, note that for the plane profile we have $\Omega_c = \emptyset$. In other words, there is no equilibrium for the swarm moving in a plane profile unless its slope is zero.

4.7 Simulation Examples

In this section we will provide some simulation examples to illustrate the theory in the preceding sections. We chose an $n = 2$ dimensional space for ease of visualization of the results and used the region $[0, 30] \times [0, 30]$ in the space. In all the simulations performed below we used $M = 11$ individuals. As parameters of the attraction/repulsion function $g(\cdot)$ in Eq. (2.2) we used $a = 0.01$, $b = 0.4$, and $c = 0.01$ for most of the simulations and $a = 0.1$ for some of them. We performed simulations for all the profiles discussed in this article.

The first plot shown in Figure 4.2 is for a plane profile with $a_\sigma = [0.1, 0.2]^\top$ for the plots on the left and $a_\sigma = [0.5, 1]^\top$ for those on the right. One easily can see

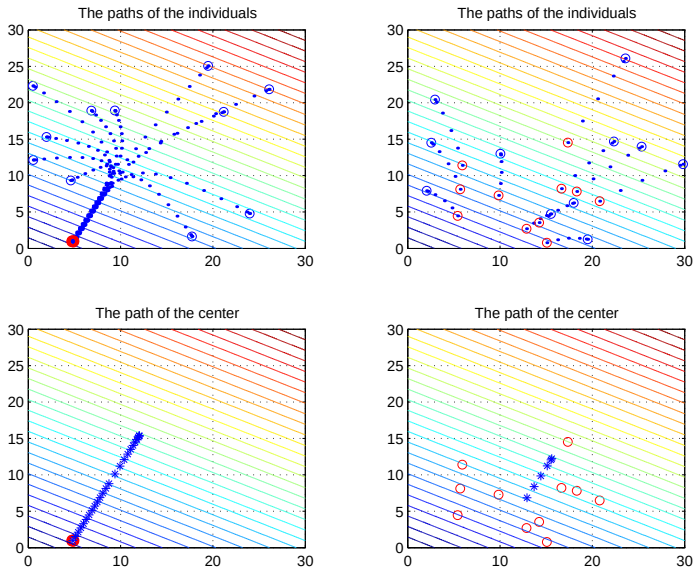

Figure 4.2: The response for a plane profile.

that in both of the cases, as expected, individuals move along the gradient a_σ exiting

the simulation region toward unboundedness. Note that for the case $a_\sigma = [0.1, 0.2]^\top$ initially some of the individuals move in a direction opposite to the negative gradient. This is because the interindividual attraction is much stronger than the intensity of the profile. In contrast, for the $a_\sigma = [0.5, 1]^\top$ case, the intensity of the profile is high enough to dominate the interindividual attraction. This, of course, does not mean that the swarm will not aggregate. As they move they will eventually aggregate as was shown in the preceding sections. We also show the plots of the centers. Note that the motion of the centers is similar for both of the cases (as expected).

The next result is for the quadratic profile as shown in Figure 4.3. We chose a

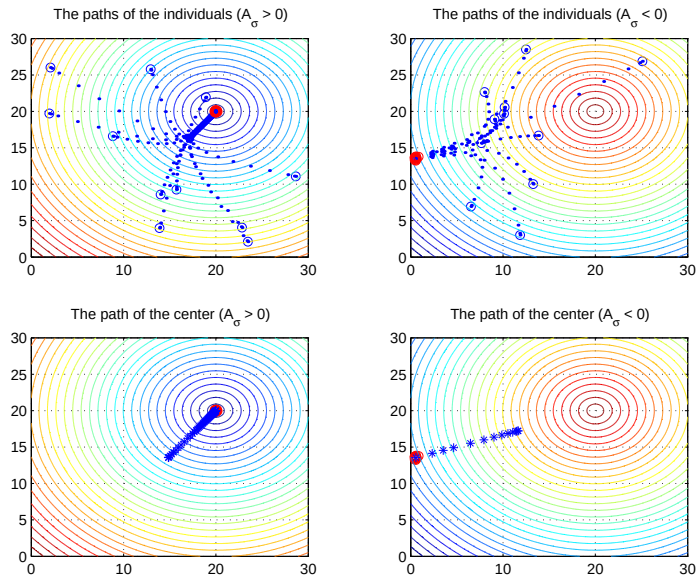

Figure 4.3: The response for a quadratic profile.

profile with extremum at $c_\sigma = [20, 20]^\top$ and magnitude $A_\sigma = \pm 0.02$. The two plots on the left of the figure show the paths of the individuals and the center of the swarm for the case $A_\sigma > 0$, whereas those on the right are for the $A_\sigma < 0$ case. Once more,

we observe that the results support the analysis of preceding sections. Note also that the center $\bar{x}$ of the swarm converges to the minimum of the profile c_σ for the $A_\sigma > 0$ case and diverges from the maximum for the $A_\sigma < 0$ case.

Results of a similar nature were obtained also for the Gaussian profile (i.e., a multimodal Gaussian profile with $N = 1$) as shown in Figure 4.4. Once more we

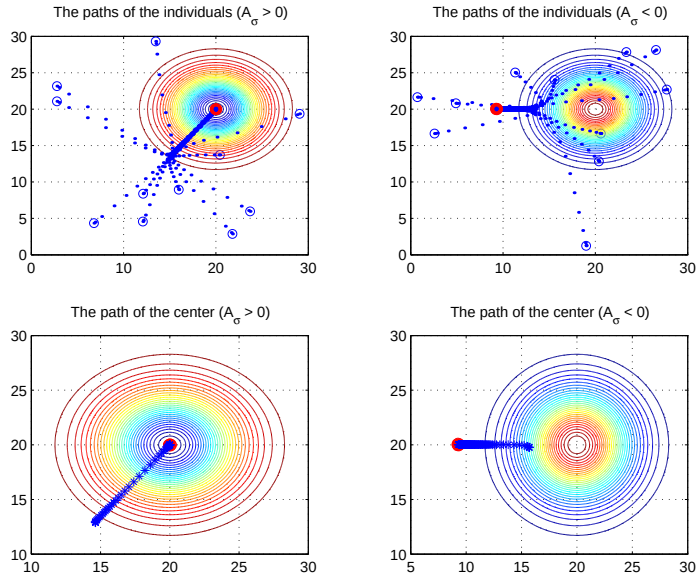

Figure 4.4: The response for a Gaussian profile.

chose $c_\sigma = [20, 20]^\top$ as the extremum of the profile. The other parameters of the profile were chosen to be $A_\sigma = \pm 2$ and $l_\sigma = 20$. Note that for the $A_\sigma > 0$ case, even though in theory it cannot be guaranteed that $\bar{x} \to c_\sigma$, in simulations we observe that this is apparently the case. This was happening systematically in all the simulations that we performed.

In the simulation examples for the multimodal Gaussian profile we used the profile shown in Figure 4.5, which has several minima and maxima. The global minimum is

located at $[15, 5]^\top$ with a magnitude of 4 and a spread of 10. The plot in Figure 4.6

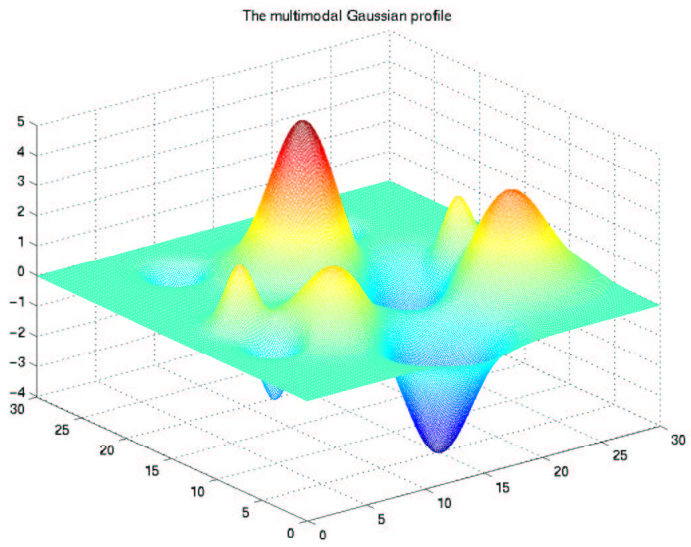

Figure 4.5: The multimodal Gaussian profile.

shows two example runs with initial member positions nearby a local minimum and show convergence of the entire swarm to that minimum. The attraction parameter a was chosen to be $a = 0.01$ for this case. Figure 4.7, on the other hand, illustrates the case in which we increased the attraction parameter to $a = 0.1$. You can see that the attraction is so strong that the individuals climb gradients to form a cohesive swarm. For this and similar cases, the manner in which the overall swarm will behave (where it will move) depends on the initial position of the center $\bar{x}$ of the swarm. For these two runs the center happened to be located on regions which caused the swarm to diverge. For some other simulation runs (not presented here) with different initial conditions the entire swarm converges to either a local or global minima. Figure 4.8 shows two runs for which we decreased the attraction parameter again to $a = 0.01$.

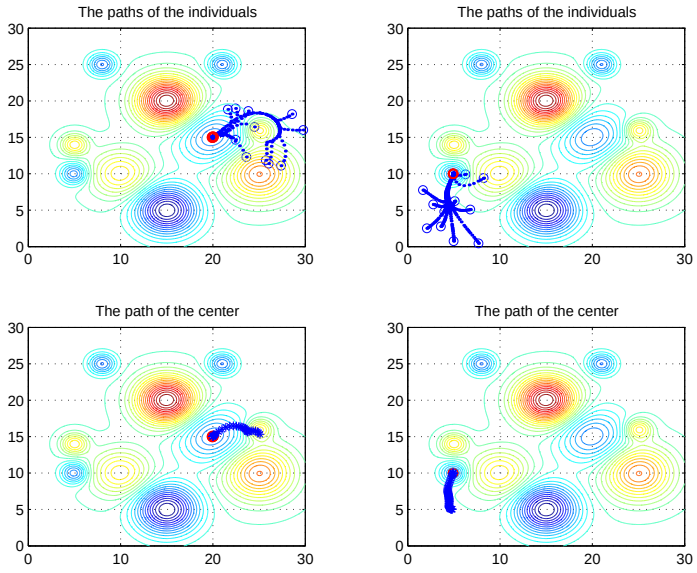

Figure 4.6: The response for a multimodal Gaussian profile (initial positions close to a minimum).

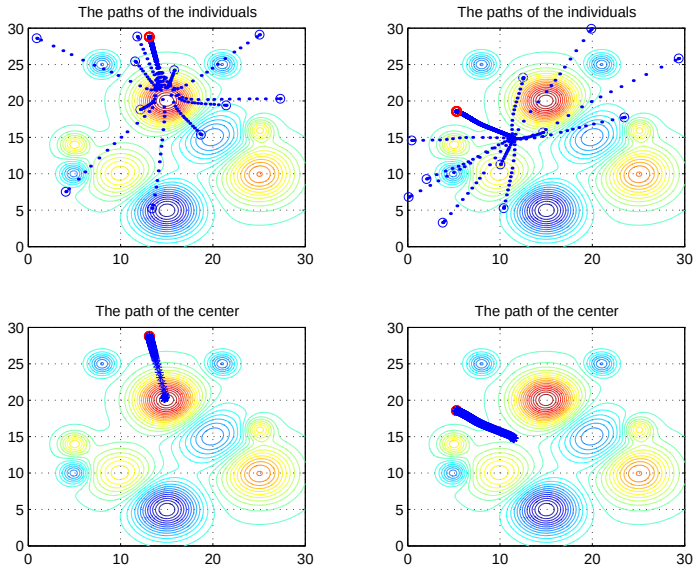

Figure 4.7: The response for a multimodal Gaussian profile.

For both of the simulations you can see that the swarm fails form a cohesive cluster

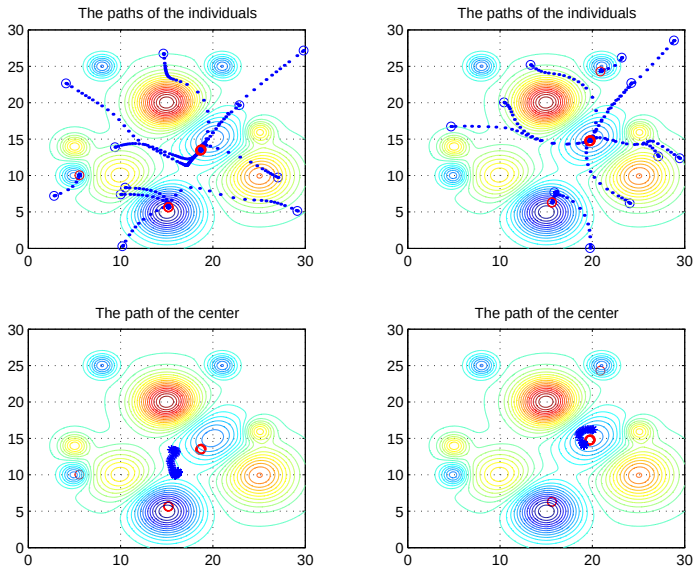

Figure 4.8: The response for a multimodal Gaussian profile.

since the initial positions of the individuals are such that they move to a nearby local minima and the attraction is not strong enough to "pull them out" of these valleys. This causes formation of several groups or clusters of individuals at different locations of the space. Note, however, that Lemma 4 still holds. The swarm does necessarily converge to a single minimum, because the size ϵ_G of the swarm is large and contains all the region in which all the individuals finally converge. For these reasons, the center $\bar{x}$ of the swarm does not converge to any minimum (as expected). Note also that during their motion to the groups, the individuals try to avoid climbing gradients and this results in motions resembling the motion of individuals in real biological swarms.

CHAPTER 5

MODELING AND ANALYSIS OF THE AGGREGATION AND COHESIVENESS OF HONEY BEE CLUSTERS AND IN-TRANSIT SWARMS

In this last chapter of of this dissertation, we consider swarming in honey bees as an example for real biological swarms. We use some of the ideas developed in Chapter 2, 3, and 4 for modeling and analysis of the aggregation and cohesiveness of honey bee clusters and in-transit swarms. The analysis in this chapter is not very rigorous. The reasons for that are that first it is difficult to perform a full scale rigorous analysis for the model that we consider, and second the intended audience are the researchers in biology, who are not very familiar with techniques like Lyapunov's stability theory. In the next section, we begin by providing some background on honey bees.

5.1 Introduction

A colony of honey bees achieves a high level of organization via dynamic division of labor, communications, and distributed decision making [93, 92, 116]. There is no "boss," yet the colony is very effective in foraging, comb construction, hive defense, thermoregulation, and other activities [93]. In nature a colony lives in, for example, the hollow of a tree. There is one queen, a few drones, and many workers. The queen's responsibility is reproduction since essentially it is the only bee that can lay

eggs. When a colony gets crowded the worker bees start rearing new queens and after some time the old queen leaves the hive with part of the workers and drones. Since she is the only bee that can lay eggs, her survival is of paramount importance for the survival of the colony. Therefore, the bees that leave the colony should not loose her. For that reason, once the queen leaves the hive the other bees cluster around her and they settle on a nearby location (e.g., a branch of a tree). The cluster stays at this location for a day or two while some of the bees, called scouts, search for a new suitable nest location. Once a new location is chosen, the cluster lifts, becomes airborne, and the swarm collectively moves to the new location. Some references on experimental work that study these activities are given in [101, 76, 10, 11, 77, 73, 3, 1, 95, 91]. During the process of choosing the new nest site, there is a distributed collective decision making process. However, here we will not consider this process. Instead, we are only interested in the swarming behavior of the bees, i.e., the clustering of the bees after they leave the original hive and the stable (cohesive) motion of the in-transit swarm while moving to the newly chosen nest site.

5.2 Clustering of the Honey Bees Around Their Queen

It is believed that clustering of the honey bees around their queen right after they leave their original hive is largely due to attraction of the bees to some of the pheromones laid by the queen. In particular, it is believed that the two pheromones *9-oxodecenoic acid* and *9-hydroxydecenoic acid* affect the cluster formation and stability in swarming honey bees [10, 11, 77, 73, 3] since the bees are attracted to these pheromones. Researchers believe that these two pheromones act together in a sense that 9-oxodecenoic acid attracts bees towards the queen from large distances, whereas

9-hydroxydecenoic acid "stabilizes" (or keeps cohesive) the cluster on short distances. Note, however, that these may not be the only substances or means in aiding in the cluster formation. For example, it has been observed that some bees expose their Nasonov glands (secreting Nasonov pheromone) to attract other bees and also communicate by other means such as buzz-running, waggle dancing, and a vibration signal [12, 94, 66]. In other words, the reasons for and mechanisms of swarming may be very complex and all the details are still not exactly known. However, it is not necessary to know all the details of the swarming mechanism in honey bees in order to describe the overall (or gross) behavior and as mentioned above it is known that the two most important aspects of swarming are the queen pheromones 9-oxodecenoic acid and 9-hydroxydecenoic acid. Here we will try to mathematically model the odor profile of the above acids and the motion of the bees along that profile.

5.2.1 Clustering with No Interindividual Attraction

Consider a $n = 3$ dimensional state space. (Note that for the below analysis this is not essential. In fact n can be of any order. We assume $n = 3$ in order to be consistent with real life swarms.) Assume that the queen is located at a position $x^q \in \mathbb{R}^n$ and that she is stationary. Denote with B the set of the rest of the bees (which left the original hive together with the queen). Assume that there are M (worker) bees in B and denote with x^i the position of the i^{th} worker bee. Below, first we will model the pheromone profile due to the queen secreted attractant pheromones and the "private area" of the bees. Then, we will specify the equation of motion of the bees along this profile and analyze the characteristics of the emergent behavior.

Modeling the Queen's Pheromone

It is natural to expect that the concentration of the odor released by the queen is high around her and is decreasing as the distance from her increases due to diffusion. (Here we do not distinguish between the odors of 9-oxodecenoic acid and 9-hydroxydecenoic acid. Instead, we consider their combined effect.) Therefore, we model the odor profile using a Gaussian type exponential function. In other words, we assume that the concentration or profile of the attractant odor released by the queen at a point $y \in \mathbb{R}^n$ is given by

$$J_a^q(y) = -\frac{b_q}{2} \exp\left(-\frac{\|y - x^q\|^2}{c_q}\right),$$

where $\frac{b_q}{2}$ is the "magnitude" and c_q is the "spread" of the profile. Such a profile is shown in the upper left plot of Figure 5.1 for the one dimensional case (i.e., $n = 1$) and parameters $b_q = 10$ and $c_q = 10$.

Note that the values of the profile at distances closer to the queen are smaller than those farther from her and the profile has a global minimum at $y = x^q$. We assume that lower values of the profile correspond to higher attractant concentration, similar to the nutrient profile in foraging swarms considered in Chapter 4. (Note that the sign of the values of the profile is not important for the below analysis. The above profile is negative; however, if it were required to be positive, we could simply add a constant and shift the entire profile up without affecting the subsequent analysis.) It is not clear to us whether in reality the decay in the odor is Gaussian. Moreover, for the analysis below it is not essential that the profile is of Gaussian type. In fact, it can be any regular function that has a global minimum at $y = x^q$. Here by a regular function we mean a function which is a decreasing function of the distance $\|x^i - x^q\|$.

For example, we could equally well choose

$$J_a^q(y) = -\frac{b_q}{\|y - x^q\|^2}$$

(assuming $y \neq x^q$) or any other similar function. We chose the Gaussian function because it represents a fast decaying profile and the decay in the queen odors might have such characteristics. Since honey bees are attracted to the odor, we would expect them to move to the point with higher odor concentration, i.e., toward the queen since the minimum of the profile occurs at the location of the queen. For this reason, it is natural to assume that the bees try to move along the (negative) gradient of the profile (i.e., for each bee i we have its position update be along $-\nabla_{x^i} J_a^q(x^i)$). Taking the gradient of the profile $J_a^q(y)$ at a point y we obtain

$$\nabla_y J_a^q(y) = \frac{b_q}{c_q}(y - x^q) \exp\left(-\frac{\|y - x^q\|^2}{c_q}\right).$$

One drawback of constraining the motion of the members (individual bees) on straight lines along $-\nabla_y J_a^q(y)$ (which are along $-(y - x^q)$), is that in order for them to encircle the queen we need them initially to be spread all around her. However, assuming this is not very restrictive.

Modeling the Body Size or Private Area of the Bees

In the above representation, the bees are modeled as point particles, i.e., the above model does not take into account the finite body size of the bees and the queen. Therefore, it will (probably) cause all the bees to move to a single point which is x^q, the position of the queen (since she does not move). To model the finite body size of the bees we introduce finite and very short range (about a body size range)

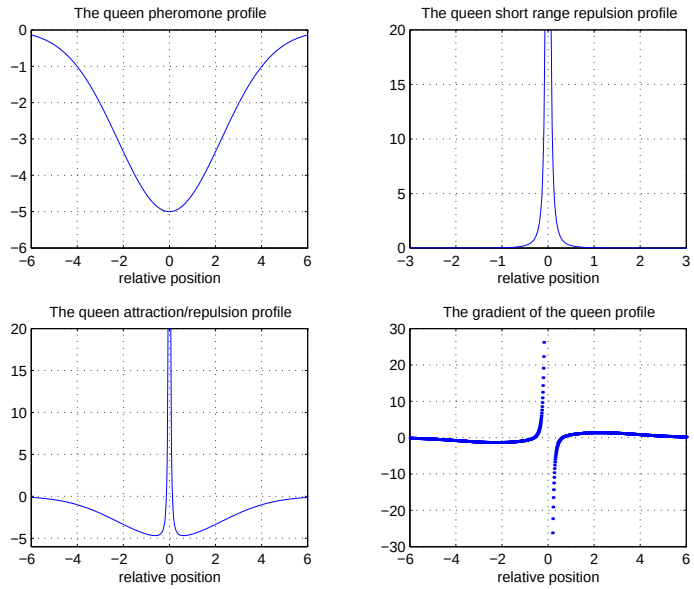

Figure 5.1: The queen profile and its gradient for $b_q = 10$, $c_q = 10$, $c_1^q = 0.1$, and $c_2^q = 0.1$.

unbounded repulsion in the form of

$$J_r^q(y) = \begin{cases} \left[\frac{c_1^q}{\|y-x^q\|^2} - \frac{c_2^q}{\|y-x^q\|}\right] + \frac{(c_2^q)^2}{4c_1^q}, & \text{if } \|y-x^q\| \le l_r^q = \frac{2c_1^q}{c_2^q}, y \neq x^q \\ 0, & \text{otherwise,} \end{cases}$$

where c_1^q and c_2^q are positive constants. An example of such a function is shown in the upper right plot in Figure 5.1 for the parameters $c_1^q = c_2^q = 0.1$. Note that the value of l_r^q is usually very small. The additive scalar $\frac{(c_2^q)^2}{4c_1^q}$ is used to scale the profile in order to avoid discontinuities. We would like to emphasize that having the repulsion as defined above is also not essential. In fact, any function with a gradient whose norm becomes unbounded on small distances (i.e., $\lim_{\|y-x^q\|\to 0^+} \|\nabla_y J_r^q(y)\| \to \infty$) and is nonzero only on a small range will suffice. If you would like to model the body size in a "hardlimiting" way, then you can choose a function satisfying

$\lim_{\|y-x^q\|\to\eta^+} \|\nabla_y J_r^q(y)\| \to \infty$ where η is a small positive constant representing the actual physical size of the queen bee, and assuming that initially $\|y - x^q\| > \eta$.

The gradient of $J_r^q(y)$ at a point y is given by

$$\nabla_y J_r^q(y) = \begin{cases} -(y - x^q)\left[\frac{2c_1^q}{\|y-x^q\|^4} - \frac{c_2^q}{\|y-x^q\|^3}\right], & \text{if } \|y - x^q\| \le l_r^q, y \neq x^q \\ 0, & \text{otherwise,} \end{cases}$$

which negated is along $(y - x^q)$ (i.e., in the opposite direction to the attraction to the pheromones). Note also that $\nabla_y J_r^q(l_r^q) = 0$ and there is no discontinuity in the gradient. We need continuity of $-\nabla_y J_r^q(y)$ for uniqueness of the solutions, because it will appear in the motion equation of the bees in the differential equation model that we specify below.

Combining these functions, the overall attraction/repulsion profile of the queen is given by

$$J^q(y) = J_a^q(y) + J_r^q(y).$$

Note that both $J_a^q(y)$ and $J_r^q(y)$ and therefore $J^q(y)$ are symmetric with respect to the position x^q of the queen bee and depend only on the distance to her (i.e., they depend only on $\|y - x^q\|$). This implies that we ignore the environmental effects such as the effect of the wind on the odor profile of the queen in the current model and analysis. The lower left plot in Figure 5.1 shows an example of such $J^q(y)$ profile, which is the summation of the upper two plots in the figure. The gradient of the profile is shown in the lower right plot. The gradient of the profile, which corresponds to the attraction/repulsion function $g(\cdot)$ in Eq. (3.2) in Chapter 3, is rather more important than the absolute value of the profile itself. In fact, in $\mathbb{R}^1$ if the gradient has the same sign as the relative position of an individual and the queen (the first and the third quadrant in the figure), then the individual is attracted to the queen

(which occurs on large distances), whereas if the gradient has the opposite sign to the relative position (the second and the forth quadrant in the figure), then the individual is repelled by the queen (which occurs on short distances). (In higher dimensions, the attractiveness/repulsiveness depends on the inner product of the gradient and the relative position vector.)

Similar to the queen bee, we can model the finite size of each individual (worker) bee i by the repulsion potential

$$J_r^i(y) = \begin{cases} \left[\frac{c_1^i}{\|y-x^i\|^2} - \frac{c_2^i}{\|y-x^i\|}\right] + \frac{(c_2^i)^2}{4c_1^i}, & \text{if } \|y-x^i\| \le l_r^i = \frac{2c_1^i}{c_2^i}, y \neq x^i \\ 0, & \text{otherwise,} \end{cases}$$

whose gradient is similar to the gradient of $J_r^q(y)$ above. Note that in this model so far we do not have attraction between the individual bees themselves. In other words, we ignore the effects of Nasonov pheromones secreted by (some) of the bees or any other type of interindividual attraction (by visually seeing the other bees, for example) as well as any communication between the bees. We will incorporate a simple type of interindividual attraction later. Incorporating dynamics based on some type of communication is a topic of further research.

Below, we will model the motion of the worker bees. Note that we do not specify an equation of motion for the queen since we assume that she is stationary. This is a reasonable assumption since we are concerned only with the clustering phenomena at this point. In experiments with real bees researchers sometimes confine the queen in a cage and fix the cage on a tree, on the ground, or in a hive away from the original swarm to observe whether the swarm members will move toward and form a cluster around her.

Modeling Bee Motion and Aggregation

The motion of each individual (worker) bee can be assumed to be along the direction of the gradient of the pheromone profile of the queen, while avoiding collisions with her and the other bees. In other words, the motion of each worker bee can be represented with

$$\begin{aligned}\dot{x}^i &= -\nabla_{x^i} J^q(x^i) - \sum_{j\in B, j\neq i} \nabla_{x^i} J_r^j(x^i) \\ &= -g_q(\|x^i - x^q\|)(x^i - x^q) + \sum_{j\in B, j\neq i} g_i(\|x^i - x^j\|)(x^i - x^j), \qquad (5.1)\end{aligned}$$

where

$$g_q(\|x^i - x^q\|) = \begin{cases} \frac{b_q}{c_q}\exp\left(-\frac{\|x^i-x^q\|^2}{c_q}\right) - \left[\frac{2c_1^q}{\|x^i-x^q\|^4} - \frac{c_2^q}{\|x^i-x^q\|^3}\right], & \text{if } \|x^i - x^q\| \le l_r^q, \\ \frac{b_q}{c_q}\exp\left(-\frac{\|x^i-x^q\|^2}{c_q}\right), & \text{otherwise,} \end{cases}$$

$$g_i(\|x^i - x^j\|) = \begin{cases} \left[\frac{2c_1^i}{\|x^i-x^j\|^4} - \frac{c_2^i}{\|x^i-x^j\|^3}\right], & \text{if } \|x^i - x^j\| \le l_r^i, \\ 0, & \text{otherwise,} \end{cases}$$

and B is the set of all bees excluding the queen with a total of M individuals (bees), as mentioned above. Note that there exists δ_q such that $g_q(\delta_q) = 0$ and

$$\begin{cases} g_q(\|x^i - x^q\|) < 0, & \text{if } \|x^i - x^q\| < \delta_q, \\ g_q(\|x^i - x^q\|) > 0, & \text{if } \|x^i - x^q\| > \delta_q. \end{cases}$$

Note also that we have

$$g_i(\|x^i - x^j\|) \ge 0,$$

for all i and for all j, where the equality holds for $\|x^i - x^j\| \ge l_r^i$. Now we make a simplification by assuming that the size and therefore the repulsion range and magnitude of all the worker bees is the same. In other words, we assume that $c_1^i = c_1$ and $c_2^i = c_2$ for all $i \in B$, which implies that $g_i(\|y\|) = g(\|y\|)$ for all $i \in B$.

One objection to the model in Eq. (5.1) could be the fact that in regions in which $\nabla_{x^i} J^q(x^i)$ is small, the motion of the i^{th} bee will also be slow. Note, however, that

we could choose $J^q(y)$ such that $\nabla_y J^q(y)$ is almost constant (e.g. $J^q(y) = b_q\|y - x^q\|$ with $\nabla_y J^q(y) = b_q \frac{(y-x^q)}{\|y-x^q\|}$). Even though such a $J^q(y)$ may not be a very realistic representation of the odor profile, it still may represent a good model. It may represent the case in which for the bee's motion it is not important what the underlying profile is, as long as it knows the direction of its gradient, and moves with constant speed along it.

Defining the distance between the position of the i^{th} bee and the queen as $e^i = x^i - x^q$ we obtain

$$\dot{e}^i = -g_q(\|e^i\|)e^i + \sum_{j\in B, j\neq i} g(\|x^i - x^j\|)(x^i - x^j),$$

since the queen is stationary (i.e., $\dot{x}^q = 0$). Now, let the *Lyapunov function* for the i^{th} bee be $V_i = \frac{1}{2}\|e^i\|^2 = \frac{1}{2}e^{i\top}e^i$. Taking its derivative along the motion of the bees we obtain

$$\dot{V}_i = -g_q(\|e^i\|)\|e^i\|^2 + \sum_{j\in B, j\neq i} g(\|x^i - x^j\|)(x^i - x^j)^\top e^i.$$

Note here that since the inner product $(x^i - x^j)^\top e^i$ can be both positive and negative, we cannot directly say anything about the sign of $\dot{V}_i$ and cannot directly draw conclusions about the motion of the bee. However, if the bee is far away (out of the repulsion range) of the queen and the other bees (i.e., if $\|e^i\| > \delta_q$ and $\|x^i - x^j\| > l_r$ for all $j \neq i$), then we can conclude that it moves towards the queen. To see this, note that if $\|x^i - x^j\| > l_r$ for all $j \neq i$, then we have $g(\|x^i - x^j\|) = 0$ for all $j \neq i$ implying that

$$\dot{V}_i = -g_q(\|e^i\|)\|e^i\|^2.$$

Moreover, since $\|e^i\| > \delta_q$ we have $g_q(\|e^i\|) > 0$ and therefore $\dot{V}_i < 0$ implying that V_i (and therefore $\|e^i\|$) decreases (i.e., the bee moves towards the queen).

Note that this is an expected result, which simply implies that if there are no other bees around the bee in question to hinder its motion, then its motion will depend only on the pheromone concentration (the attractant profile) and following its negative gradient (towards higher concentration since the smaller values represent higher concentration) will cause a motion towards the queen.

Note that since the bees only push each other on close distances, if we had a bee which has neighbors with $\|x^i - x^j\| < \delta$, but all these members were "behind" it with respect to its relative position to the queen, then we would have it also moving towards the queen. To see this, note that for all the bees who are "behind" it we have $(x^i - x^j)^\top e^i < 0$ implying $\dot{V}_i < 0$ and we arrive at the same conclusion as above. In contrast, if the i^{th} bee had neighbors with $\|x^i - x^j\| < \delta$, but some of them were in "front" of it, i.e., if $(x^i - x^j)^\top e^i > 0$ for some j, then we cannot directly derive any conclusion about the motion of the bee in question. Note, however, that intuitively, using an inductive procedure, it is possible to argue that the bees that are closest (in all directions) to the queen will first converge to her (based on the above observation). Then, they will be followed by the second inner circle of the bees and so on, until all the bees converge and form a cluster around the queen.

Stopping on the Cluster

Assume that $\dot{x}^q = 0$ and that $x^i(0) \neq x^q$ for all i and $x^i(0) \neq x^j(0)$ for all $j \neq i$. Now, note that the above model is very similar to the foraging swarm with a Gaussian nutrient profile. The only difference is that at the center of the profile there is an unbounded hump, and there is no interindividual attraction between the bees (i.e., there is only repulsion). Then, from the result in Theorem 3 we know that $x^i \to 0$ for all $i \in B$, i.e., all the bees will stop. However, since the bees may not be able to

stop in mid-air, some people may find the fact that they stop counter intuitive. Note, however, that so far we did not specify the final positions of the bees. Intuitively, it must be the case that they stop on a cluster around the queen.

Characteristics of Bee Cluster Packing

Since $\dot{x}^i \to 0$ we have also that $\dot{V}_i \to 0$. Equating $\dot{V}_i$ to zero (which corresponds to the final equilibrium) we have

$$\dot{V}_i = -g_q(\|e^i\|)\|e^i\|^2 + \sum_{j\in B, j\neq i} g(\|x^i - x^j\|)(x^i - x^j)^\top e^i = 0$$

from which we obtain

$$g_q(\|e^i\|)\|e^i\|^2 = \sum_{j\in B, j\neq i} g(\|x^i - x^j\|)(x^i - x^j)^\top e^i,$$

for all i. Now, note that $g_q(\|e^i\|)$ can be both positive and negative.

If $g_q(\|e^i\|) < 0$ (i.e., $\|e^i\| < \delta_q$), then the left hand side of the above equation is negative and right hand side has to be negative also. This implies that there exits at least one bee j such that $\|x^i - x^j\| < l_r$ (since for $\|x^i - x^j\| \geq l_r$ we have $g(\|x^i - x^j\|) = 0$) and $(x^i - x^j)^\top e^i < 0$. Since $(x^i - x^j) = (e^i - e^j)$ we have $(e^i - e^j)^\top e^i < 0$ or $\|e^i\|^2 < e^{j\top} e^i$ from where we obtain

$$\|e^i\| < \gamma_{i,j}\|e^j\| \leq \|e^j\|,$$

where $\gamma_{i,j}$ is the cosine of the angle between e^i and e^j. Note from the facts that $\gamma_{i,j}$ is the cosine and $\|x^i - x^j\| < l_r \leq \delta_q$ (here we assume that the queen's repulsion range or private area is equal to or larger than that of the worker bees), and $\|e^i\| > \delta_q$ and $\|e^j\| > \delta_q$ that $0.5 < \gamma_{i,j} \leq 1$ and as $\|e^i\|$ gets large $\gamma_{i,j} \approx 1$ even when individuals i and j are not necessarily aligned with the queen. From the cosine theorem we have

$$\|e^i\|^2 + \|e^j\|^2 - 2\gamma_{i,j}\|e^j\|\|e^i\| = \|x^i - x^j\|^2 < l_r^2.$$

Since $\gamma_{i,j} \leq 1$ we have

$$\|e^i\|^2 + \|e^j\|^2 - 2\|e^j\|\|e^i\| < l_r^2,$$

from where we obtain

$$\|e^j\| - \|e^i\| < l_r.$$

Combining this with the above inequality we have

$$\|e^i\| < \|e^j\| < \|e^i\| + l_r.$$

In other words, if bee i is within the queen's repulsion range during equilibrium, there must be at least one other bee j behind her which is blocking her motion away from the queen and pushing her towards the queen. Otherwise, we cannot have $\|e^i\| < \delta_q$ during equilibrium (as expected).

If $g_q(\|e^i\|) > 0$ (i.e., $\|e^i\| > \delta_q$), then the left hand side of the above equation is positive and the right hand side has to be positive also. By similar reasoning as above there must be at least one bee j such that $\|x^i - x^j\| < l_r$ and $(x^i - x^j)^\top e^i > 0$. Then, with analysis similar to above, we obtain

$$\|e^i\| > \gamma_{i,j}\|e^j\|.$$

Using the cosine theorem for e^j this time we have

$$\begin{aligned} \|e^j\|^2 &= \|e^i\|^2 + \|x^i - x^j\|^2 - 2(x^i - x^j)^\top e^i \\ &\geq (\|e^i\| - \|x^i - x^j\|)^2. \end{aligned}$$

Since $\|e^i\| > \delta_q$ and $\|x^i - x^j\| < l_r$ and with the assumption that $\delta_q \geq l_r$ we have $\|e^i\| > \|x^i - x^j\|$, and therefore we obtain

$$\|e^j\| \geq \|e^i\| - \|x^i - x^j\| > \|e^i\| - l_r.$$

Combining this with the previous inequality we obtain

$$\|e^i\| - l_r < \|e^j\| < \frac{1}{\gamma_{i,j}}\|e^i\|.$$

In other words, if bee i is far from the queen during equilibrium, then there must be at least one other bee j in front of her which is blocking her motion towards the queen.

Using the above two observations repeatedly for every individual and recalling the assumption that initially the bees are spread in all directions around the queen we see that they will cluster around her. Note, however, that the analysis so far do not depend on the assumption that the initial positions of the bees are spread in all directions around the queen. Therefore, they hold even if the initial positions of the bees do not satisfy that assumption. If they are spread all around, then they form a cluster around the queen with size depending on the number of bees in each direction relative to the queen. The largest swarm size (the worst case) occurs when all the bees are aligned (with each other and the queen) initially. In that case they form a line with a maximum possible size of $\delta_q + (M-1)l_r$ assuming that all of them are on the same side of the queen and $2\delta_q + (M-2)l_r$ if they are on both sides of the queen. Note that this is an expected result since our model assumes that the bees move only along the (negative) gradient of the queen pheromone profile combined with interindividual interactions and for the above special case the gradients along the motions of all the bees are aligned.

Consider the cumulative Lyapunov function $V = \sum_{i \in B} V_i$. As in Chapter 3 it can be shown that at equilibrium we have

$$\dot{V} = -\sum_{i \in B} g_q(\|e^i\|)\|e^i\|^2 + \frac{1}{2}\sum_{i \in B}\sum_{j \in B, j \neq i} g(\|x^i - x^j\|)\|x^i - x^j\|^2 = 0, \quad (5.2)$$

from which we obtain

$$\sum_{i\in B} g_q(\|e^i\|)\|e^i\|^2 = \frac{1}{2}\sum_{i\in B}\sum_{j\in B, j\neq i} g(\|x^i - x^j\|)\|x^i - x^j\|^2.$$

Therefore, we can say that during equilibrium on average we have

$$g_q(\|e^i\|)\|e^i\|^2 = \frac{1}{2}\sum_{j\in B, j\neq i} g(\|x^i - x^j\|)\|x^i - x^j\|^2,$$

from which we conclude that on average we have $\|e^i\| > \delta_q$ since right hand side is positive implying that the left hand side is also positive. Note that it is not possible to directly solve for the exact value of $\|e^i\|$ from the above equation since there are two possible solutions for a given value of the summation on the right.

Note that in the above model, the short range repulsion is only a kind of disturbance which does not allow the members to get close together, but does not change the overall stability properties of the system. To see this, consider the limiting case in which $\delta_q \to 0$ and $l_r \to 0$. Then, provided that the initial positions of the individuals are such that $x^i(0) \neq x^j(0)$ for all i and j, $j \neq i$, then we will asymptotically have $e^i \to 0$ for all i. Note, however, that we will never have $e^i = 0$ or $x^i = x^j$ for $j \neq i$. Having finite range repulsion does not change these properties. It only enlarges the region in which the bees converge.

Finally, we would like to note that, as in Section 3.3.1, one can use a hardlimiting repulsion to represent the real (or effective) body size of diameter η for each bee, i.e., one can choose $J_r^j(x^i)$ such that $\lim_{\|x^i - x^j\|\to\eta^+} \nabla_{x^i} J_r^j(x^i) = \infty$, in order to prevent the individuals i and j to move closer that the distance η to each other

5.2.2 Clustering with Interindividual Attraction

In the analysis so far we assumed that there was no interindividual attraction between the bees during the swarming process. However, we do not exactly know

whether this is the case in reality or not. In fact, the motion of the bees may be affected by the location of the other bees. In other words, they may be tending to go to the location with higher bee concentration based on, for example, visual information or some other cues such as Nasonov pheromone released by the other bees. In order to incorporate such an effect, we can add an interindividual attraction in the motion equation of the bees. In other words, for example, we could consider

$$g(\|x^i - x^j\|) = \left[\frac{c_1}{\|x^i - x^j\|^2} - \frac{c_2}{\|x^i - x^j\|}\right],$$

which corresponds to the attraction/repulsion potential

$$J_{ar}(\|x^i - x^j\|) = c_1 \ln(\|x^i - x^j\|) - c_2\|x^i - x^j\|.$$

Note that this corresponds to a constant attraction and unbounded repulsion. The equation of motion of the i^{th} worker be is still given by

$$\dot{x^i} \;\; = \;\; -g_q(\|e^i\|)e^i + \sum_{j\in B, j\neq i} g(\|x^i - x^j\|)(x^i - x^j).$$

However, we do not anymore have $g(\|x^i - x^j\|) \geq 0$. Instead, we have $g(l_r) = 0$ and

$$\begin{cases} g(\|x^i - x^j\|) > 0, & \text{if } \|x^i - x^j\| < l_r \text{ (repulsion)}, \\ g(\|x^i - x^j\|) > 0, & \text{if } \|x^i - x^j\| > l_r \text{ (attraction)}. \end{cases}$$

Note that the fact that as $t \to \infty$, $x^i \to 0$ for all i still holds with the attraction added. This implies that $\dot{V} = 0$ in Eq. (5.2) still holds. Assume for a moment that there is no attraction towards the queen. Then, the first term in the $\dot{V}$ equation is zero (see Eq. (5.2)) and we have

$$\frac{1}{2}\sum_{i\in B}\sum_{j\in B, j\neq i} g(\|x^i - x^j\|)\|x^i - x^j\|^2 = 0,$$

and by substituting the value of $g(\|x^i - x^j\|)$ we obtain

$$\sum_{i\in B}\sum_{j\in B, j\neq i} \left[c_1 - c_2\|x^i - x^j\|\right] = 0.$$

Rearranging the terms we obtain

$$\frac{1}{M(M-1)} \sum_{i \in B} \sum_{j \in B, j \neq i} \|x^i - x^j\| = \frac{c_1}{c_2} = l_r,$$

which implies that the average interindividual distance will be equal to $\frac{c_1}{c_2}$. In other words, the bees will be closely packed together. Therefore, for this case, $\frac{c_1}{c_2} = l_r$ cannot represent the physical size of a bee, but another parameter determining the interindividual distance between the bees in the cluster. If there is a need to represent the physical size of a bee, one needs to use a hardlimiting repulsion function.

Having found the compactness of the cluster formed by the bees with the assumption that there were no attraction towards the queen, we would expect that similar compactness is achieved in the cluster formed around the queen in the case when there is attraction to her. Note, however, that there may be a drawback in this model if the interindividual attraction dominates the attraction towards the queen. Specifically, if the parameters of the model are not properly set, then the bees may pass the queen, form a cluster somewhere else first, and then try to move collectively towards the queen. This behavior will not be biologically realistic for real life swarms. Therefore, the parameters of the queen pheromone profile should be set high enough and those of the interindividual attraction small enough so that the attraction to the queen is the dominating force.

5.2.3 Simulation of the Clustering of Honey Bees

Now, we present some simulation illustrating the clustering of the bees around their queen. The simulations that we present here are for the case in which there are no interindividual attractions between the worker bees. Figure 5.2 shows the paths of the worker bees during the clustering affect of them around the queen (we initialize

the queens initial position in between the other bees). As one can see, the bees are initially spread around, however, they move and form a cluster around the queen. Figure 5.3 shows the position of the bees after about 20 seconds (when the cluster is

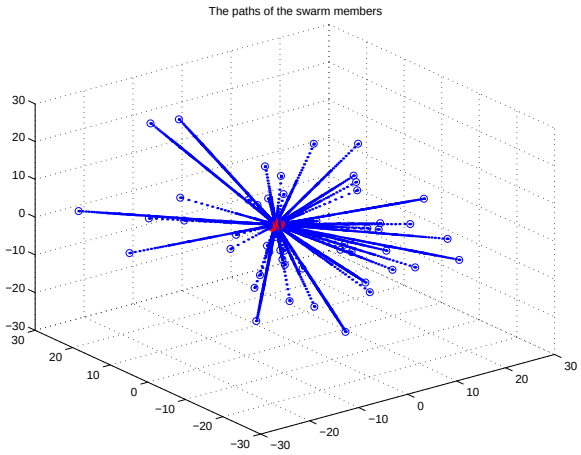

Figure 5.2: Clustering of the honey bees around the queen.

formed). As is seen from the figure, the bees (denoted by circles) are spread around the queen (denoted by a star) at a very close distance to her and to each other (as expected).

The first plot in Figure 5.4 shows the minimum interindividual distance and the minimum distance between the individuals and the queen (i.e., it shows $\min_{i\in S, j\in S, j\neq i} \|x^i - x^j\|$ and $\min_{i\in S} \|x^i - x^q\|$), whereas the second plot shows the maximum interindividual distance and the maximum distance between the individuals and the queen (i.e., it shows $\max_{i\in S, j\in S, j\neq i} \|x^i - x^j\|$ and $\max_{i\in S} \|x^i - x^q\|$). As you can see the minimum distance to the queen and the minimum interindividual distance both settle at values around 0.5, wheres the maximum distance to the queen settles at about 1 and the

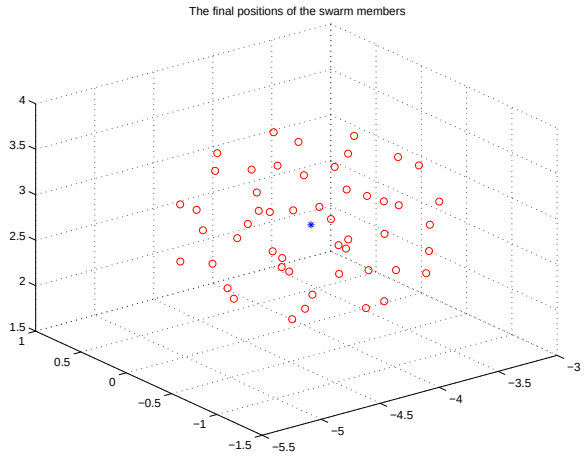

Figure 5.3: The position of the honey bees after 25 seconds (the cluster is formed).

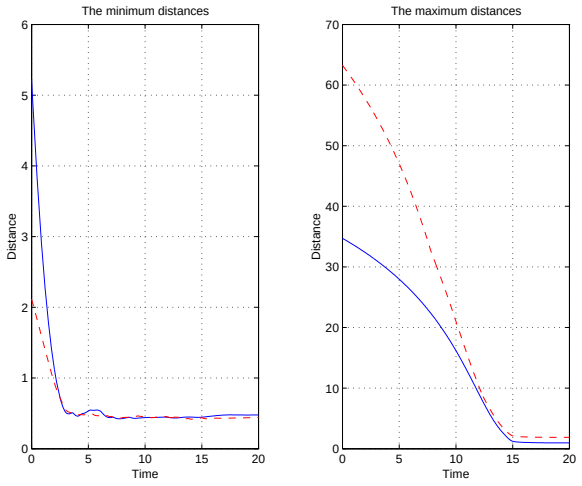

Figure 5.4: The minimum and the maximum distances between the queen and the individuals and interindividual distances.

maximum interindividual distance (which is the maximum size of the swarm) settles at a value around 2.

In the above simulations we used $M = 51$ individuals (excluding the queen), $c_1 = c_2 = 0.1$ for the parameters of the short range interindividual repulsion function

and $b_q = 10$, $c_q = 10$, and $c_1^q = c_2^q = 0.1$ for the parameters of the queen attraction and repulsion potentials, respectively. Note that for these parameters we have $l_r = \frac{2c_1}{c_2} = 2$. In other words, the final swarm size is as large as the repulsion range of a single bee. The above simulations seem to be consistent with the behavior of actual honey bees.

5.3 In-Transit Honey Bee Swarm

Although not exactly known, it has been observed that the motion of the honey bee swarms while moving to a new nest site is guided by the scouts who secret Nasonov pheromones to attract the other bees and also "fly through" the swarm. Moreover, the pheromones of the queen keep the bees in her close vicinity. To model all these aspects we divide the swarm of bees into three groups, which are the queen bee denoted by q, the scouts bees denoted by the set S, and the worker bees denoted by the set W. We assume that the sets of the scout bees and the worker bees are distinct, i.e., we assume that $S \cap W = \emptyset$. Moreover, note that for the set B defined in the previous section we have $B = S \cup W$.

5.3.1 Modeling the Scouts

We assume that the motion of the i^{th} scout bee (i.e., $i \in S$) can be described as

$$\dot{x}_s^i = -a_s(t)\frac{(x_s^i - x_f)}{\|x_s^i - x_f\|} - \sum_{j \in S, j \neq i} g_s(\|x_s^i - x_s^j\|)(x_s^i - x_s^j), x_s^i \neq x_f, \tag{5.3}$$

where x_s^i is the current position of the i^{th} scout bee $i \in S$ and x_f is the final nest position which the scout knows and we assumed that $x_s^i \neq x_f$. The parameter $a_s(t)$ is a speed profile parameter and is assumed to satisfy $a_1 \leq a_s(t) \leq a_2$ for some finite positive constants a_1 and a_2 (i.e., constants satisfying $0 < a_1 \leq a_2 < \infty$ for all $t \geq 0$).

In other words, we assume that the motion of the scout bees is determined only by its position, the position of the nest, and the relative position of the other scout bees (and is not affected by the position and the motion of the queen and the worker bees). For the case when $x_s^i = x_f$, we can choose

$$\dot{x}_s^i = 0, x_s^i = x_f,$$

implying that once a scout reaches the nest, it will stop and the pheromones of the other scouts will not affect it anymore. Another option for the scout motion once the nest is reached could be

$$\dot{x}_s^i = -\sum_{j \in S, j \neq i} g_s(\|x_s^i - x_s^j\|)(x_s^i - x_s^j), x_s^i = x_f.$$

In other words, in this case only the relative position of the other scouts will govern the motion of the scout in question (so they will be able to push it a little bit away from x_f). Note that no more than one scout can occupy x_f simultaneously.

According to the above model while the scouts move, they do not even try to avoid collisions with the other bees (it is the job of the other bees to do so). It is not known how biologically realistic this is. Above, the second term given by $g_s(\|x_s^i - x_s^j\|)(x_s^i - x_s^j)$ corresponds to the gradient of the function $J_s(\|x_s^i - x_s^j\|)$ (i.e., $g_s(\|x_s^i - x_s^j\|)(x_s^i - x_s^j) = \nabla_{x_s^i} J_s(\|x_s^i - x_s^j\|)$), where $J_s(\|x_s^i - x_s^j\|)$ is a "potential" function of type of $J^q(\cdot)$ discussed in the previous section, and has an attraction term to model the effect of the Nasonov pheromone profile laid by the scouts and a short range repulsion term to model the distance keeping (preventing collisions) of the bees during their flight. We assume that all the scouts lay the same amount of Nasonov pheromone and therefore use the same function $J_s(\cdot)$ for all of them. Note also that this can be considered as a motion in the direction along the negative gradient of the

attraction profile of the nest defined by

$$J_f(x) = a_s(t)\|x - x_f\|.$$

In other words, the above model basically assumes that the scouts move on straight lines toward the nest location (while also trying to keep an appropriate distance from each other but not necessarily from the other bees) with a variable speed determined by $a_s(t)$. It has been observed that the swarm starts motion with a slow speed then accelerates up to 11 kilometers per hour and when it is close to the nest it slows down [95]. We will use this parameter to adjust a realistic speed profile for the swarm.

5.3.2 Modeling the Queen and the Workers

We assume that the queen is attracted only by the scouts (due to the Nasonov pheromone secreted by them) and tries to follow them, which can be represented as

$$\dot{x}^q = -\sum_{j \in S} g_s(\|x^q - x_s^j\|)(x^q - x_s^j). \tag{5.4}$$

Note that above we used the same $g_s(\cdot)$ in the motion equation of the queen as that of the scouts. This is due to the assumption that all the bees (the queen, the scouts and the workers) observe the Nasonov pheromone profile in the same manner, for simplicity. Therefore, we will have the same $J_s(\cdot)$ and for that reason the same $g_s(\cdot)$ in the motion equation of all the bees.

We assume that the motion of the worker bees is given by a combination of a desire to stay near the queen (due to the queen secreted pheromones) and a desire to follow the scouts (due to the Nasonov pheromone secreted by them and perhaps other reasons such as following their "streaking" motion). Therefore, the motion of

the i^{th} worker bee $i \in W$ is given by

$$\dot{x}^i = -g_q(\|x^i - x^q\|)(x^i - x^q) - \sum_{j \in S} g_s(\|x^i - x_s^j\|)(x^i - x_s^j) + \sum_{j \in W} g(\|x^i - x^j\|)(x^i - x^j), \tag{5.5}$$

where, the term $-g_q(\|x^i - x^q\|)(x^i - x^q)$ represents the attraction to the queen (as before), the terms $-g_s(\|x^i - x_s^j\|)(x^i - x_s^j)$ are for their attraction to the scouts, and the terms $g(\|x^i - x^j\|)$ is a short range repulsion to model their distance keeping (avoiding collisions) among each other and is as was defined in the previous section. (Note, however, that even though the function type is similar to the one defined before, the parameters of the function may be different since the bees keep larger distances while in-transit compared to those in the cluster. This is true also for the profiles $J^q(\cdot)$ and $J_s(\cdot)$.)

Another component that could be added to the above motion equations is a long range attraction of the members to each other (as in the previous section). Since it is not known whether the bees are attracted to each other, here we will not do that. Note that the above set up is in a sense (or a special case of) the *social potential fields method* discussed in [88]. Note also that here we did not model the "fly through" of the scouts to guide the flying swarm. To incorporate these dynamics in the model and in the simulation will require a careful consideration and additional research.

5.3.3 Scout Motion

Now, let us analyze the qualitative behavior of the motion of the scouts. To this end, define the center of the scouts as

$$\bar{x}_s = \frac{1}{M_s} \sum_{i \in S} x_s^i,$$

where $M_s = |S|$ is the cardinality (the number of members) of the set S. Then, it can be shown that

$$\dot{\bar{x}}_s = -\frac{a_s(t)}{M_s} \sum_{i \in S} \frac{(x_s^i - x_f)}{\|x_s^i - x_f\|}. \tag{5.6}$$

Note that the result in Eq. (5.6) was obtained by assuming that $x_s^i \neq x_f$ for all $i \in S$, and this is a reasonable assumption assuming that the swarm is far away from the nest. Once they move very close to the nest it may happen that for some (and only one) $i \in S$ we have $x_s^i = x_f$ and Eq. (5.6) may not hold; however, since in that case we have already achieved convergence to the nest we do not need to analyze this case.

Defining the distance between the center $\bar{x}_s$ of the scouts and the new nest location x_f as $e_s = \bar{x}_s - x_f$ and letting the corresponding Lyapunov function be $V_s = \frac{1}{2}\|e_s\|^2$ we obtain

$$\dot{V}_s \leq -\frac{a_s(t)}{M_s} \sum_{i \in S} \frac{\|e_s\|}{\|x_s^i - x_f\|} \left[\|e_s\| - \frac{\sum_{i \in S} \frac{\|x_s^i - \bar{x}_s\|}{\|x_s^i - x_f\|}}{\sum_{i \in S} \frac{1}{\|x_s^i - x_f\|}} \right],$$

which implies that as long as

$$\|e_s\| > \frac{\sum_{i \in S} \frac{\|x_s^i - \bar{x}_s\|}{\|x_s^i - x_f\|}}{\sum_{i \in S} \frac{1}{\|x_s^i - x_f\|}}$$

we will have $\dot{V}_s < 0$. Let $x_{sM} = \max_{i \in S} \|x_s^i - \bar{x}_s\|$. Then, $\|e_s\| > x_{sM}$ guarantees that $\dot{V}_s < 0$, which, on the other hand, implies that as $t \to \infty$ we will have $\|e_s\| \leq x_{sM}$. Therefore, as $t \to \infty$ we will have that the nest is in between (or surrounded by) the scout bees.

Now, to analyze the ultimate behavior of the scouts consider the generalized Lyapunov function (or the "potential energy" function)

$$J_1(x_s) = a_s(t) \sum_{i \in S} \|x_s^i - x_f\| + \frac{1}{2} \sum_{i \in S} \sum_{j \in S, j \neq i} J_s(\|x_s^i - x_s^j\|),$$

where $x_s = [x_s^{1\top}, \ldots, x_s^{M_s\top}]^\top$ is the state of the scouts subsystem. Taking the gradient of $J_1(x_s)$ with respect to x_s^i we obtain

$$\nabla_{x_s^i} J_1(x_s) = a_s(t)\frac{(x_s^i - x_f)}{\|x_s^i - x_f\|} + \sum_{j\in S, j\neq i} g_s(\|x_s^i - x_s^j\|)(x_s^i - x_s^j) = -\dot{x}_s^i.$$

Then, the time derivative of $J_1(x_s)$ is given by

$$\dot{J}_1(x_s) = -\sum_{i\in S} \|\dot{x}_s^i\|^2 + \frac{da_s(t)}{dt}\sum_{i\in S} \|x_s^i - x_f\|.$$

From real life swarms we know that the bee swarm speeds up (increases its speed) after takeoff for some time (implying $\frac{da_s(t)}{dt} > 0$) and slows down (decreases its speed) while approaching the nest (implying $\frac{da_s(t)}{dt} < 0$). In other words, there are time instances t_1 and t_2 such that for $t \leq t_1$ we have $\frac{da_s(t)}{dt} > 0$, whereas for $t \geq t_2$ we have $\frac{da_s(t)}{dt} < 0$. Note that for $\frac{da_s(t)}{dt} > 0$ we cannot guarantee that $\dot{J}_1(x_s) < 0$, whereas, for the $\frac{da_s(t)}{dt} < 0$ we can say that this is the case. Note also that since we have $a_s(t) \geq a_1$ for all time t, it cannot be the case that $\frac{da_s(t)}{dt} < 0$ for all $t \geq t_2$. Therefore, we will require that $\frac{da_s(t)}{dt} \to 0$, or even further, we will assume that there is a time $t_3 > t_2$ such that for all $t \geq t_3$ we will have $\frac{da_s(t)}{dt} = 0$. This guarantees that for $t \geq t_3$ we have $\dot{J}_1(x_s) = -\sum_{i\in S} \|\dot{x}_s^i\|^2$ implying that $\dot{x}_s^i \to 0$ for all $i \in S$. In other words, all the scout bees will eventually stop (surrounding the new hive). With a similar analysis to the clustering case (discussed in the previous section) one can find the possible maximum distance of the scouts to the new hive once they stop (which will occur if all the scouts are aligned with the hive location).

5.3.4 Queen and Worker Motion

Note that the above analysis is not the full picture. Now we have to make sure that the queen and the worker bees follow the scouts during their journey to their

new home. To this end, define $e_q = x^q - x_f$ and the corresponding Lyapunov function as $V_q = \frac{1}{2}\|e_q\|^2$. Then, we have

$$\dot{V}_q \;\leq\; -\sum_{i\in S} g_s(\|x^q - x_s^i\|)\|e_q\| \left[\|e_q\| - \frac{\sum_{i\in S} g_s(\|x^q - x_s^i\|)\|x_s^i - x_f\|}{\sum_{i\in S} g_s(\|x^q - x_s^i\|)}\right],$$

which is obtained assuming that there is no scout in the vicinity of the queen (i.e., that $g_s(\|x^q - x_s^i\|) > 0$ for all $i \in S$). Note that this is a reasonable assumption once we assume that the scouts are in front of the swarm, while the queen is in the middle of the swarm. From there we see that if

$$\|e_q\| > \frac{\sum_{i\in S} g_s(\|x^q - x_s^i\|)\|x_s^i - x_f\|}{\sum_{i\in S} g_s(\|x^q - x_s^i\|)}$$

then we have $\dot{V}_q < 0$, which is guaranteed to be satisfied whenever $\|e_q\| > \max_{i\in S} \|x_s^i - x_f\|$ or the queen is "behind" the scout bees and there is no scout bee in her vicinity (i.e., repulsion range). Therefore, we will assume that the scouts initially (and therefore always) are "in front" of the queen (i.e., between the queen and the nest).

Now, let us look at the "potential energy" or the generalized Lyapunov function that the queen is trying to minimize with its motion. Let

$$J_2(x^q, x_s) = \sum_{i\in S} J_s(\|x^q - x_s^i\|),$$

and note that

$$\nabla_{x^q} J_2(x^q, x_s) = \sum_{i\in S} g_s(\|x^q - x_s^i\|)(x^q - x_s^i) = -\dot{x}^q$$

and

$$\nabla_{x_s^i} J_2(x^q, x_s) = -g_s(\|x^q - x_s^i\|)(x^q - x_s^i).$$

Then, we have

$$\dot{J}_2(x^q, x_s) \;=\; \nabla_{x^q} J_2^\top(x^q, x_s)\dot{x}^q + \sum_{i\in S} \nabla_{x_s^i} J_2^\top(x^q, x_s)\dot{x}_s^i$$

$$
\begin{aligned}
&= -\|\dot{x}^q\|^2 + \sum_{i\in S} \nabla_{x_s^i} J_2^\top(x^q, x_s)\dot{x}_s^i \\
&= \sum_{i\in S} g_s(\|x^q - x_s^i\|)(x^q - x_s^i)^\top(\dot{x}^q - \dot{x}_s^i),
\end{aligned}
$$

from which we can see that the motion of the queen is such that it tries to minimize $J_2(x^q, x_s)$ (which follows from the $-\|\dot{x}^q\|^2$ term), whereas, the motions of the scouts may not necessarily be in that direction. Now, in order to make sure that the queen is not falling behind, we need $\dot{J}_2(x^q, x_s) \leq 0$ during the motion. The equality $\dot{J}_2(x^q, x_s) = 0$ would imply that the queen is keeping a constant average distance to the scouts, whereas the strict inequality $\dot{J}_2(x^q, x_s) < 0$ would imply that she is getting closer to them. From the last equality we see that (assuming that there is enough distance between the queen and the scouts) we need $(x^q - x_s^i)^\top(\dot{x}^q - \dot{x}_s^i) \leq 0$ in order to have $\dot{J}_2(x^q, x_s) \leq 0$, which implies (assuming that the queen and the scout i were aligned) that if $(x^q - x_s^i) > l_r^s > 0$, where l_r^s is the repulsion range for the scouts (say, the queen is behind the scout), then we need $(\dot{x}^q - \dot{x}_s^i) \leq 0$ (or the queen moving at least as fast as the scout, i.e., $\|\dot{x}^q(t)\| \geq a_s(t)$) in order to contribute nonpositively to $\dot{J}_2(x^q, x_s)$. If they are not aligned, we will need the cosine of the angle between $(x^q - x_s^i)$ and $(\dot{x}^q - \dot{x}_s^i)$ to be nonpositive (or the angle be between 90^o and 270^o) in order to have the product $(x^q - x_s^i)^\top(\dot{x}^q - \dot{x}_s^i) \leq 0$. Note that from the second equality above we obtain

$$
\dot{J}_2(x^q, x_s) \leq -\|\dot{x}^q\|^2 + a_s(t) \sum_{i\in S} \nabla_{x_s^i} \|J_2^\top(x^q, x_s)\|,
$$

which can be guaranteed to be negative semidefinite if

$$
a_2 \leq \frac{\left\|\sum_{i\in S} g_s(\|x^q - x_s^i\|)(x^q - x_s^i)\right\|^2}{\sum_{i\in S} g_s(\|x^q - x_s^i\|)\|x^q - x_s^i\|}
$$

is satisfied. Then, given a_2 and the function $g_s(\cdot)$, there is always a set of initial conditions such that $l_r^s \leq \|x^q(0) - x_s^i(0)\| \leq \beta$ for all $i \in S$ and for some β such that the

above equation is satisfied for all t. In other words, if the queen is initially sufficiently close to the scouts (depending on the profile function $g_s(\cdot)$ and the maximum speed a_2), then she will follow them to the nest.

Note also that since once they reach the nest $\dot{x}_s^i \to 0$ for all $i \in S$, as shown before, we have $\dot{J}_2(x^q, x_s) \to -\|\dot{x}^q\|^2 < 0$, which implies that $\dot{x}^q \to 0$ as $t \to \infty$. Then, from the queen motion equation in Eq. (5.4) we see that she will stop no further than δ_s distance (the distance at which $g_s(\cdot) = 0$ or switches sign) from at least one scout.

Now, consider worker bee $i \in W$. Define its distance to the nest to be $e^i = x^i - x_f$ and the corresponding Lyapunov function $V_i = \frac{1}{2}\|e^i\|^2$. Then, we have

$$\dot{V}_i = -g_q(\|x^i - x^q\|)(x^i - x^q)^\top e^i - \sum_{j \in S} g_s(\|x^i - x_s^j\|)(x^i - x_s^j)^\top e^i + \sum_{j \in W, j \neq i} g(\|x^i - x^j\|)(x^i - x^j)^\top e^i.$$

Now, note that if that bee kept enough distance to all the other bees (including the scouts and the queen) during its motion, then we would have $g(\|x^i - x^j\|) = 0$ for all $j \in W, j \neq i$, $g_s(\|x^i - x_s^j\|) > 0$ for all $j \in S$, and $g_q(\|x^i - x^q\|) > 0$. Moreover, if the bee were located "behind" the queen and the scouts, then we would have $(x^i - x^q)^\top e^i > 0$ and $(x^i - x_s^j)^\top e^i > 0$ for all $j \in S$, implying that $\dot{V}_i < 0$. In other words, if the above conditions are satisfied, then the bee will move towards the nest. If, in contrast, the bee is located between the queen and the scouts, then the motion of the bee will be determined from the relative attraction from the scouts and the queen. Therefore, we can say that the attraction to the bees in the "rear" of the moving swarm will be in one direction only (forward). The bees located in the area between the queen and the scouts, on the other hand, will be attracted forward by the scouts and backward by the queen. However, since there is only one queen and many scouts, the direction of the overall cumulative attraction will be forward (assuming that the scouts are close enough). Moreover, since the attraction on the queen is only by the scouts in forward direction, she should be tending to move faster than

the workers in front of her. Similarly, the bees behind her should be tending to move faster then her, because they are attracted by her as well as the scouts. Therefore, we will have a swarm in which the speed will tend to "increase" as you move from front to the rear and this will keep the swarm cohesive (as long as the scouts are slow enough so that the rest can keep up with them).

By choosing the potential energy for the worker bees as

$$J_3(x) = \sum_{i \in W} J^q(\|x^i - x^q\|) + \sum_{i \in W} \sum_{j \in S} J_s(\|x^i - x_s^j\|) + \sum_{i \in W} \sum_{j \in W, j \neq i} J_r(\|x^i - x^j\|)$$

and using analogous arguments to those for the queen and the scouts, one can argue that for the worker bees also we will have $\dot{x}^i \to 0$ for all $i \in W$. Then, using the motion equation in Eq. (5.5) one can argue that each worker will have at least one close neighbor who is preventing it to move towards the queen and the scouts at equilibrium implying that they have reached close vicinity of the new hive.

5.3.5 Simulation of an In-Transit Swarm

Now we will present some simulation examples to illustrate the behavior of the in-transit honey bee swarm model. Figure 5.5 shows the plot of the trajectory of a honey bee swarm during motion from an initial position at $[0, 0, 0]^\top$ to the newly chosen nest position at $[50, 50, 50]^\top$. For the simulations in this section we used the parameters $c_1 = c_2 = c_1^q = c_2^q = c_1^s = c_2^s = 0.1$, $b_q = c_q = 30$, and $b_s = c_s = 20$, where the parameters c_1^s and c_2^s are the repulsion and b_s and c_s are the attraction parameters of the scouts, respectively. The other parameters are as defined in the earlier sections. As expected the swarm is preserving its cohesiveness during the entire motion.

Figure 5.6 shows the swarm after its arrival at the nest. The worker bees are represented by circles, the queen by a star, the scouts (we choose two scouts only)

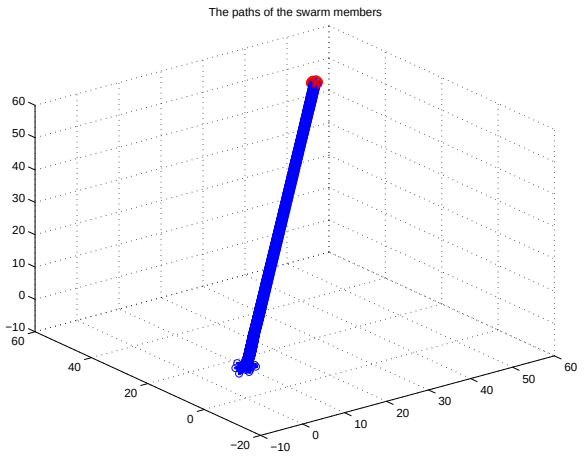

Figure 5.5: The trajectory of the motion of the honey bee swarm toward the new nest.

by squares and the nest location by a diamond. Note that the position of the scouts are on two different sides of the nest (as expected from the analysis in the preceding sections). Moreover, all the other bees including the queen are in the vicinity of the nest. The queen's position is also close to the center of the swarm. However, this is not necessarily always the case in every simulation run. Her final position depends on her initial position.

Figure 5.7 shows the speed profile of the swarm. We obtained this figure by averaging the velocities of the members on each interval of 5 meters and plot it with respect to the distance from the initial position. Recall that we could adjust the speed of the scouts, which affects the speed of the entire swarm. In this particular simulation we used a piecewise constant speed parameter $a_s(t)$, whose value was dependent on the average distance of the swarm to the nest. Note the similarity of this velocity profile plot with the plots in the literature (see for example [95]). Here we have the speed in kilometers per hour, implying that the swarm flew with a maximum speed

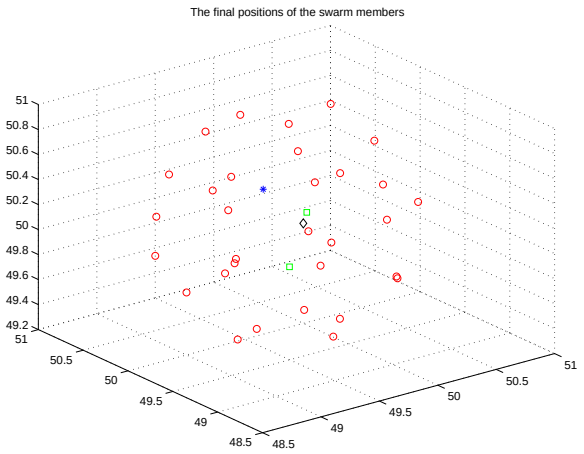

Figure 5.6: The honey bee swarm after it has arrived at the nest.

of about 8 kilometers per hour. Note that by adjusting $a_s(t)$ we can have any desired speed profile for the swarm. Here we chose $a_s(t)$ such that the swarm starts its motion slowly, then speeds up, and finally slows down as approaches the nest, as noted in the literature.

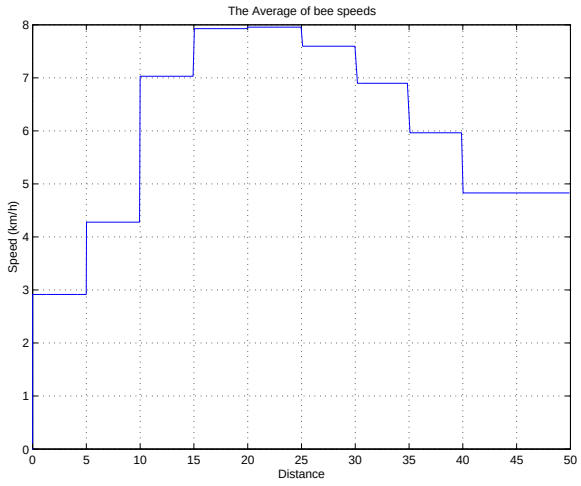

Figure 5.7: The average of the speeds of the bees in a honey bee swarm.

5.4 Discussion

The clustering in honey bees and in-transit honey bee swarms are spectacular phenomena that have been studied experimentally by biologists during the past several decades. However, many aspects of these phenomena are still not well understood. Moreover, to best of our knowledge, there has not been any mathematical model proposed so far. In this chapter we tried to use the ideas from the preceding chapters to develop a simple mathematical models for both aggregation of bees in clusters and in-transit swarms. The model consists of simple ordinary differential equations describing the motion of each individual bee. The equations incorporate terms for attraction towards the queen (or the scouts) due to the pheromones laid by her (or them) and an unbounded repulsion to incorporate a finite "private area" for each bee (in order to move beyond point particle models and incorporate their finite size, to some extent).

The pheromones are represented by a decaying function, a "profile," centered at their source (the queen or the scout bees) and the individuals try to move along the negative gradient of that profile towards higher pheromone concentration. We did not incorporate environmental disturbances such as the effect of the wind on the pheromone profile or the motion of the bees. Incorporating such dynamics is a topic of further research. Our model is simple and in some cases biologically not very realistic. For example, for the clustering case, in order for the model to describe real life clustering, we have to assume that initially the bees surround the queen (although this probably is usually the case). Otherwise, the group that they form around the queen will not be a real cluster. Moreover, the model (for clustering) lets us to perform a global analysis, whereas in real life bee swarms it is impossible to

have global convergence since the range of senses of the bees is limited. Similarly, in the in-transit swarm we assume that all the scouts are in front of the queen (and the other bees) and leading towards the nest, and this is apparently not always the case in real life bee swarms. Moreover, since the motion of the bees depends on the gradient of the overall (combined) profile, in regions where this gradient is small (i.e., the regions which are far away from the sources creating the profile) the bee will move slowly. Some may consider this unrealistic. However, it is possible to argue that the equation of motion that we used here does not represent the actual motion of a bee, but it represents its effective average motion. Therefore, in the regions where there is no distinguishable change in the pheromone concentration (i.e., the gradient is small) it "wanders around" in search for better concentration and on average slowly moves towards higher concentration regions. Despite all these drawbacks, provided the parameters of the model and the initial positions of the bees are set properly, the emergent behavior from the model is in general agreement with the behavior of real life bee swarms.

In our initial model we did not incorporate mass and therefore the related extra dynamics into the motion of the bees. However, such dynamics can easily be added as was shown for aggregating swarms in Chapter 3. One important conclusion which can be derived from the behavior of the model described is that it is not absolutely necessary to have higher intelligence in order to achieve swarming behavior. Instead, simple chemotaxis abilities and moving in a direction are sufficient. Even though such ability may not be all the components affecting the swarming behavior in honey bees, they seem to be important ingredients as is understood in the honey bee literature.

In order to better understand and model the clustering and swarming behavior in honey bees, there is a need for more experimental studies. For example, in order to model the effect of the pheromones, there is a need for studying how the pheromones diffuse and how their effects can best be modeled (here we did not use partial differential equation models to ensure some analytical tractability). Once the pheromone profile is sensed, how do the bees decide which direction to move? Can they sense the gradient (the change in concentration) and do they move along it (as we modeled here). It is known that even some simple bacteria such as *E. coli* can construct local approximation of a gradient and follow it [85] and it is natural to expect that the bees can do the same. However, this requires more study. Other aspects to study are the positions of the queen and the scouts in the airborne in-transit swarm. Is it really the case that the queen is somewhere in the middle? Are there any (relative) positions that the scouts choose to be in the swarm, or can they be anywhere just like the other worker bees? Why do the bees follow the scouts? Are they attracted to the Nasonov pheromone laid by them or are there other reasons such as the "streaking" phenomenon? They probably sense the presence of the queen during motion. Are they also attracted to her vicinity? If she escapes will they continue following the scouts (at least for some time) or will they follow her?

The analysis here makes intuitive sense. However, it is not always very rigorous. The main obstacle for performing a rigorous analysis is the fact that here we do not have (linear) interindividual attraction between the bees and the repulsion is unbounded. Nevertheless, our work is apparently the first directed towards developing a more realistic and rigorous mathematical model of the honey bee swarming behavior.

CHAPTER 6

ONE-DIMENSIONAL DISCRETE-TIME ASYNCHRONOUS SWARMS

In this chapter we consider one-dimensional discrete time asynchronous swarms with time delays. In other words, we consider a swarm model in which the member positions are scalars (i.e., they are on the real line), the individuals can move asynchronously, and there are time delays in sensing the positions of the neighbors. The motion of each individual is based on the relative location of its nearest neighbors on its both sides. We analyze the stability properties of the model and prove that the individuals will converge to a constant relative arrangement, that we call the *comfortable position* (with *comfortable intermember distance*). Our stability analysis employs some results on contractive mappings from the parallel and distributed computation literature.

6.1 The Swarm Model

In this section we introduce the swarm model that we consider in this chapter. First, we describe the model of a single swarm member. Then, we present the one-dimensional swarm model (i.e., when many swarm members are arranged next to each other on a line).

6.1.1 Single Swarm Member Model

The single swarm model described in this section is taken from [68, 67]. We present it here for convenience. The single swarm member model that we consider is shown in Figure 6.1. As seen in the figure, it has a *driving device* for performing the

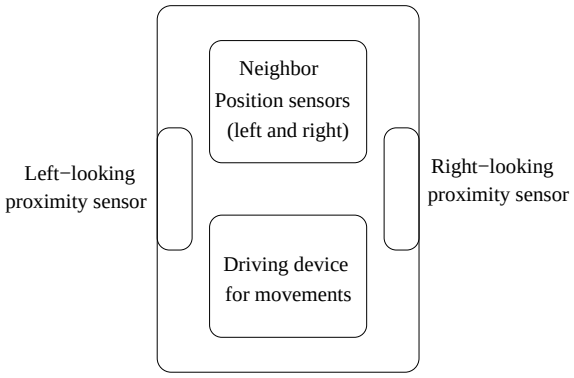

Figure 6.1: Single swarm member.

movements and a *neighbor position sensors* for sensing the position of the adjacent (left and right) neighbors. It is assumed that there is no restriction on the range on these sensors. In other words, we assume that they can provide the accurate position of the neighbor even if the neighbor is far away. Each swarm member also has two proximity sensors on both sides (left and right). These sensors have sensing range of $\epsilon > 0$ and can sense *instantaneously* in this proximity. Therefore, if another swarm member reaches an ϵ distance from it, then this will be *instantaneously* known by both of the members. However, if the neighbors of the swarm member are out of the range of the proximity sensor, then it will return an infinite value (i.e., $-\infty$ for the left sensor and $+\infty$ for the right sensor) or some large number that will be ignored

by the swarm member. The use of this sensor is to avoid collisions with the other members in the swarm.

In the next section we describe the model of a swarm (collection) of members described in this section arranged on a line.

6.1.2 One-Dimensional Swarm Model

Consider a discrete time one-dimensional swarm described by the model

$$\begin{aligned} x_1(k+1) &= x_1(k), \forall k \\ x_i(k+1) &= \max\Big\{x_{i-1}(k)+\epsilon, \min\Big\{x_i(k) - g\Big(x_i(k) \\ &\quad -\frac{x_{i-1}(\tau_{i-1}^i(k)) + x_{i+1}(\tau_{i+1}^i(k))}{2}\Big), \\ &\quad x_{i+1}(k)-\epsilon\Big\}\Big\}, \forall k \in \mathcal{K}^i, i = 2, \ldots, N-1 \qquad (6.1) \\ x_N(k+1) &= \max\{x_{N-1}(k)+\epsilon, x_N(k) - g(x_N(k) \\ &\quad -x_{N-1}(\tau_{N-1}^N(k)) - d)\}, \forall k \in \mathcal{K}^N, \end{aligned}$$

where $x_i(k), i = 1, \ldots, N$, represents the position of individual (member) i at time k and $\mathcal{K}^i \subseteq \mathcal{K} = \{1, 2, \ldots\}$ is the set of time instants at which member i updates its position. At the other time instants member i is stationary. In other words, we have

$$x_i(k+1) = x_i(k), \forall k \notin \mathcal{K}^i \text{ and } i = 2, \ldots, N. \qquad (6.2)$$

Note that the first member of the swarm is always stationary at position $x_1(0)$. The other members (except member N), on the other hand, try to move to the position which their current information tells them is the middle of their adjacent neighbors. In other words, they try to move to the position $c_i(k)$ defined as

$$c_i(k) = \frac{x_{i-1}(\tau_{i-1}^i(k)) + x_{i+1}(\tau_{i+1}^i(k))}{2}, i = 2, \ldots, N-1,$$

where $\tau_j^i, j = i-1, i+1$, is used to represent the time index at which member i obtained position information of its neighbor j. Of course due to the delays $c_i(k)$ may not be the midpoint between members $i-1$ and $i+1$ at time k. The last member (member N), on the other hand, tries to move to

$$c_N(k) = x_{N-1}(\tau_{N-1}^N(k)) + d,$$

what it perceives to be a distance d from its left neighbor. The constant d represents the *comfortable intermember distance*. Note that, in contrast to the work in [68, 67], only the N^{th} member of the swarm knows (or decides) the value of d. It is assumed that $d \gg \epsilon$.

The elements of $\mathcal{K}$ (and therefore of $\mathcal{K}^i$) should be viewed as indices of the sequence of physical times at which the updates occur (similar to the times of events in discrete event systems), not as actual times. In other words, they are integers that can be mapped to actual times. The sets $\mathcal{K}^i$ are independent from each other for different i. However, it is possible to have $\mathcal{K}^i \cap \mathcal{K}^j \neq \emptyset$ for $i \neq j$ (i.e., two or more members move simultaneously). Note that $\tau_j^i(k)$ satisfies $0 \leq \tau_j^i(k) \leq k$ for $k \in \mathcal{K}^i$, where $\tau_j^i(k) = 0$ means that member i did not obtain any position information about member j so far (it still has the initial position information), whereas $\tau_j^i(k) = k$ means that it has the current position information of member j. The constant ϵ is the range of the proximity sensors as discussed in the preceding section.

The function $g(\cdot)$ describes the attractive and repelling relationships between a swarm member and its adjacent neighbors. It determines the step size that a member will take toward the middle of its neighbors (if it is not already there). We assume

that

$$\underline{\alpha} y(t) \leq g(y(t)) \leq \bar{\alpha} y(t), \text{ if } y(t) \geq 0$$
$$\bar{\alpha} y(t) \leq g(y(t)) \leq \underline{\alpha} y(t), \text{ if } y(t) < 0, \tag{6.3}$$

where $\underline{\alpha}$ and $\bar{\alpha}$ are two constants satisfying

$$0 < \underline{\alpha} < \bar{\alpha} < 1.$$

Figure 6.2 shows the plot of one such $g(\cdot)$. In the figure we also plotted $\underline{\alpha} y(t)$ and $\bar{\alpha} y(t)$ for $\underline{\alpha} = 0.1$ and $\bar{\alpha} = 0.9$. Note that even though this $g(\cdot)$ function looks

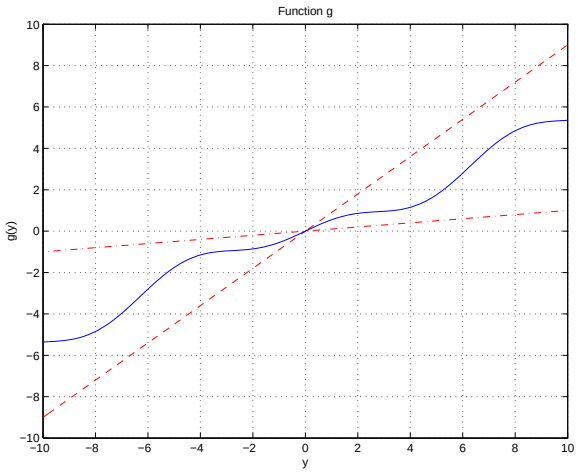

Figure 6.2: Example $g(\cdot)$ function.

different than the attraction/repulsion functions considered in the preceding chapters (see for example Eq. (3.2)), in reality it is not. To see this, assume that the argument for $g(\cdot)$ were not $x_i(k) - c_i(k)$, but were $x_i(k) - x_{i-1}(k) - d$, i.e., consider $g(x_i(k) - x_{i-1}(k) - d)$. Then, (assuming $x_i(k) - x_{i-1}(k) > 0$ for all k) we have $g(x_i(k) - x_{i-1}(k) - d) > 0$, i.e., the function is attractive, for $x_i(k) - x_{i-1}(k) > d$, and $g(x_i(k) -$

$x_{i-1}(k) - d) < 0$, i.e., the function is repulsive, for $x_i(k) - x_{i-1}(k) < d$. In other words, the attraction/repulsion functions considered here leads effectively to the same behavior as the attraction/repulsion functions considered in the preceding chapters for continuous time swarms. The difference in the shape of the function arises essentially from the different arguments it uses.

Notice that the model in Eq. (6.2) is in a sense a discrete event model which does not allow for collisions between the swarm members. This is because if during movement member i suddenly finds itself within an ϵ range of one (or both) of its neighbors, it will restrain its movement by that neighbor according to Eq. (6.2).

We will at times use the notation $x(k) = [x_1(k), \ldots, x_N(k)]^\top$ to represent the position at time k of all the members of the swarm. Define the swarm comfortable position as

$$x^c = [x_1(0), x_1(0) + d, \ldots, x_1(0) + (N-1)d]^\top.$$

In this chapter we consider the stability of this position by considering the motions of the swarm members when they are initialized at positions different from x^c. We will consider two cases: synchronous operation with no delays and totally asynchronous operation. These are described in the following two assumptions.

Assumption 3 (Synchronism, No Delays) *The sets $\mathcal{K}^i$ and the times $\tau_j^i(k)$ satisfy $\mathcal{K}^i = \mathcal{K}$ for all i and $\tau_j^i(k) = k$ for all i and $j = i-1, i+1$.*

This assumption says that all the swarm members will move at the same time instants. Moreover, every member will always have the current position information of its adjacent neighbors.

The next assumption, on the other hand, says that the members can move at totally independent time instants and that the "delay" between two measurements

performed by a member can become arbitrarily large. However, there always will be next time when the member will perform a measurement.

Assumption 4 (Total Asynchronism) *The sets $\mathcal{K}^i$ are infinite, and if $\{k_\ell\}$ is a sequence of elements of $\mathcal{K}^i$ that tends to infinity, then $\lim_{\ell\to\infty}\tau_j^i(k_\ell)=\infty$ for every j.*

Now we have the following preliminary result. We state it here, because it will be used in the next section.

Lemma 7 *For the swarm described in Eq. (6.2) given any $x(0)$, there exists a constant $\bar{b}=\bar{b}(x(0))$ such that $x_i(k)\leq\bar{b}$, for all k and all $i, 1\leq i\leq N$.*

Proof: We prove this via contradiction. Assume that $x_i(k)\to\infty$ for some $i, 1\leq i\leq N$. This implies that $x_j(k)\to\infty$ for all $j\geq i$. We will show that it must be the case that $x_{i-1}(k)\to\infty$. Assume the contrary. Then we have $x_i(k)-x_{i-1}(k)\to\infty$, whereas $x_{i-1}(k)-x_{i-2}(k)<b$ for some b. However, there is always a time $k^{i-1}\in\mathcal{K}^{i-1}$ at which member $i-1$ performs position sensing of its neighbors and since at some time $x_i(k)-x_{i-1}(k)\gg x_{i-1}(k)-x_{i-2}(k)$, it moves to the right. Repeating the argument for each time instant, we obtain $x_{i-1}(k)\to\infty$. Continuing this way it can be shown that $x_i(k)\to\infty$ for all $i\neq 1$. Moreover, since x_1 is constant and $x_2(k)-x_1(k)\to\infty$ we have all $x_i(k)-x_{i-1}(k)\to\infty, i=2,\ldots,N$. To see this assume that $x_2(k)-x_1(k)\to\infty$, whereas $x_3(k)-x_2(k)<b$ for some b. Then, there exists always a time $k^2\in\mathcal{K}^2$ at which member 2 performs a position sensing of its neighbors and it moves to the left. Therefore, it must be the case that $x_3(k)-x_2(k)\to\infty$. Repeating the argument for the other members we arrive at the conclusion that it should hold for all i. This leads to a contradiction since there is always a time

$k^N \in \mathcal{K}^N$ at which member N performs position sensing of its left neighbor. From the definition of the model if $x_N(k) - x_{N-1}(k) > d$ the N^{th} member will move to the left. In other words, $x_N(k) - x_{N-1}(k)$ cannot diverge. Then, there is always a time $k^{N-1} \in \mathcal{K}^N, k^{N-1} > k^N$ at which member $N-1$ performs position sensing of the neighbors, and since $x_{N-1}(k) - x_{N-2}(k) > x_N(k) - x_{N-1}(k)$ it moves to left. Therefore, $x_{N-1}(k) - x_{N-2}(k)$ also cannot diverge. Continuing with similar reasoning one can show that all $x_i(k) - x_{i-1}(k)$ are bounded implying the result. ■

This result is important, because it basically says that for the given swarm model unboundedness of the swarm member positions and intermember distances (the dissolution of the swarm) will not occur. Therefore, the main question to be answered is whether the swarm member positions $x(k)$ will have periodic solutions or will converge to some constant. In the next section we will analyze the system in the case of synchronism with no delays. This will be used later in the proof of our main result.

6.2 The System Under Total Synchronism

In this section we will assume that Assumption 3 holds (i.e., all the members move at the same time and they always have the current position information of the neighbors) and analyze the stability properties of the system.

Now we have the following preliminary result.

Lemma 8 *For the system in Eq. (6.2) assume that Assumption 3 holds (i.e., we have synchronism with no delays). If $x(k) \to \bar{x}$ as $k \to \infty$, where $\bar{x}$ is a constant vector, then $\bar{x} = x^c$.*

Proof: First of all, note that the intermember distances on all the states that the system can converge to are such that $\bar{x}_i - \bar{x}_{i-1} > \epsilon$ for all i (i.e., it is impossible for

the states to converge to positions that are very close to each other). To prove this, we assume that $\bar{x}_i - \bar{x}_{i-1} = \epsilon$ for some i and $\bar{x}_j - \bar{x}_{j-1} > \epsilon$ for all $j \neq i$ and seek to show a contradiction. In that case,

$$\bar{x}_{i+1} - \bar{x}_i > \epsilon$$

so

$$\bar{x}_i - \frac{\bar{x}_{i-1} + \bar{x}_{i+1}}{2} < 0$$

and we have from model constraints in Eq. (6.2) that

$$\bar{x}_{i-1} + \epsilon < \bar{x}_i - g\left(\bar{x}_i - \frac{\bar{x}_{i-1} + \bar{x}_{i+1}}{2}\right) < \bar{x}_{i+1} - \epsilon.$$

From Eq. (6.2) this implies that at the next time instant $k^i \in \mathcal{K}^i$ member i will move to the right toward member $i+1$. Therefore, it must be the case that $\bar{x}_{i+1} - \bar{x}_i = \epsilon$ since otherwise $\bar{x}_i - \bar{x}_{i-1} = \epsilon$ also cannot hold. Continuing this way one can prove that all intermember distances must be equal to ϵ. However, in that case, since $d \gg \epsilon$, from last equality in Eq. (6.2) we have

$$\bar{x}_N - g(\epsilon - d) > \bar{x}_{N-1} + \epsilon$$

and this implies that on the next time instant $k^N \in \mathcal{K}^N$ member N will move to the right. Therefore, no intermember distance can converge to ϵ. For this reason, to find $\bar{x}$ we can drop the min and max and consider only the middle terms in Eq. (6.2).

Since $x(k) \to \bar{x}$ as $t \to \infty$ it should be the case that ultimately

$$\begin{aligned}
\bar{x}_1 &= \bar{x}_1 \\
\bar{x}_i &= \bar{x}_i - g\left(\bar{x}_i - \frac{\bar{x}_{i-1} + \bar{x}_{i+1}}{2}\right), i = 1, \ldots, N-1 \\
\bar{x}_N &= \bar{x}_N - g(\bar{x}_N - \bar{x}_{N-1} - d),
\end{aligned}$$

from which we obtain

$$\begin{aligned} \bar{x}_1 &= x_1^c \\ 2\bar{x}_i &= \bar{x}_{i-1} + \bar{x}_{i+1}, i = 1, \ldots, N-1 \\ \bar{x}_N &= \bar{x}_{N-1} + d. \end{aligned} \tag{6.4}$$

Solving the second equation for $\bar{x}_{N-1}$ we have

$$2\bar{x}_{N-1} = \bar{x}_{N-2} + \bar{x}_N$$

from which we obtain

$$\bar{x}_{N-1} = \bar{x}_{N-2} + d.$$

Continuing this way, we obtain

$$\bar{x}_i = \bar{x}_{i-1} + d, \forall i = 1, \ldots, N-1.$$

Then since the first member is stationary we have $\bar{x}_1 = x_1(t) = x_1(0) = x_1^c$ and this proves the result. ■

This lemma basically says that x^c is the unique *fixed point* or *equilibrium point* of the system described by Eq. (6.2). In this chapter we analyze the stability of this fixed point which corresponds to the arrangement with comfortable intermember distance.

Lemma 9 *Assume that $x_i(0) - x_{i-1}(0) > \epsilon$ for all $i = 2, \ldots, N$. Moreover, assume that Assumption 3 holds (i.e., we have synchronism with no delays). Then, $x_i(k) - x_{i-1}(k) > \epsilon$ for all $i = 2, \ldots, N$, and for all k.*

Proof: We will prove this by induction. By assumption for $k = 0$ we have $x_i(0) - x_{i-1}(0) > \epsilon$ for all $i = 2, \ldots, N$. Assume that for some k we have $x_i(k) - x_{i-1}(k) > \epsilon$

for all $i = 2, \ldots, N$. Then we have

$$\frac{x_{i-1}(t) + x_{i-2}(t)}{2} < \frac{x_i(t) + x_{i-1}(t)}{2} - \epsilon. \tag{6.5}$$

On the other hand, from Eq. (6.4) we have

$$\begin{aligned} x_i(k+1) &= x_i(k) - \alpha_i \left(x_i(k) - \frac{x_{i-1}(k) + x_{i-2}(k)}{2} \right) \\ &= (1 - \alpha_i) x_i(k) + \alpha_i \left(\frac{x_{i-1}(k) + x_{i-2}(t)}{2} \right), \end{aligned}$$

where $\underline{\alpha} < \alpha_i < \bar{\alpha}$. Therefore, as shown in Figure 6.3, we have

$$\text{if } x_i(k) < \tfrac{x_{i-1}(k)+x_{i-2}(k)}{2}, \text{ then } x_i(k) < x_i(k+1) < \tfrac{x_{i-1}(k)+x_{i-2}(k)}{2},$$

and

$$\text{if } x_i(k) > \tfrac{x_{i-1}(k)+x_{i-2}(k)}{2}, \text{ then } x_i(k) > x_i(k+1) > \tfrac{x_{i-1}(k)+x_{i-2}(k)}{2}.$$

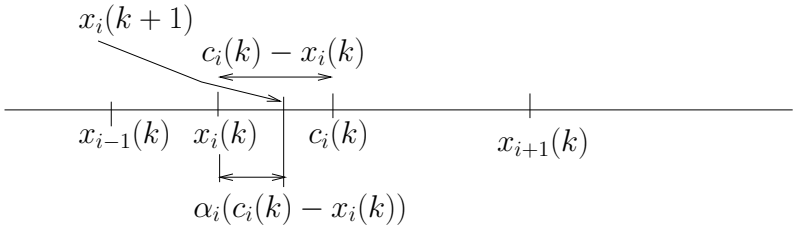

Figure 6.3: Step of a swarm member.

Then, Eq. (6.5) implies that $x_i(k+1) - x_{i-1}(k+1) > \epsilon$ and this completes the proof.

■

This lemma implies that for the synchronous case with no delays, provided that initially the members are sufficiently apart from each other, the proximity sensors

will not be used and that we can drop the min and max operations in Eq. (6.2) and the system can be represented as

$$\begin{aligned} x_1(k+1) &= x_1(k) \\ x_i(k+1) &= x_i(k) - g\left(x_i(k) - \frac{x_{i-1}(k) + x_{i+1}(k)}{2}\right), \\ x_N(k+1) &= x_N(k) + g\left(x_N(k) - x_{N-1}(k) - d\right). \end{aligned}$$

Define the following change of coordinates

$$\begin{aligned} e_1(k) &= x_1(k) - x_1^c \\ e_i(k) &= x_i(k) - (x_{i-1}(k) + d), i = 1, \ldots, N. \end{aligned}$$

Then, one obtains the following representation of the system

$$\begin{aligned} e_1(k+1) &= e_1(k) = 0, \\ e_2(k+1) &= e_2(k) - g\left(\frac{e_2(k) - e_3(k)}{2}\right), \\ e_i(k+1) &= e_i(k) - g\left(\frac{e_i(k) - e_{i+1}(k)}{2}\right) \\ &\quad + g\left(\frac{e_{i-1}(k) - e_i(k)}{2}\right), i = 3, \ldots, N-1, \\ e_N(k+1) &= e_N(k) - g(e_N(k)) + g\left(\frac{e_{N-1}(k) - e_N(k)}{2}\right). \end{aligned}$$

Noting that it is possible to write the $g(\cdot)$ function as

$$g(y(k)) = \alpha(k)y(k),$$

where

$$0 < \underline{\alpha} \leq \alpha(k) \leq \bar{\alpha} < 1,$$

we can represent the system with

$$e_2(k+1) = \left(1 - \frac{\alpha_2(k)}{2}\right) e_2(k) + \frac{\alpha_2(k)}{2} e_3(t),$$

$$
\begin{aligned}
e_i(k+1) &= \left(1 - \frac{\alpha_i(k)}{2} - \frac{\alpha_{i-1}(k)}{2}\right) e_i(k) \\
&\quad + \frac{\alpha_{i-1}(k)}{2} e_{i-1}(k) \\
&\quad + \frac{\alpha_i(k)}{2} e_{i+1}(k), i = 3, \ldots, N-1, \\
e_N(k+1) &= \left(1 - \alpha_N(k) - \frac{\alpha_{N-1}(k)}{2}\right) e_N(k) \\
&\quad + \frac{\alpha_{N-1}(k)}{2} e_{N-1}(k),
\end{aligned}
$$

where we dropped $e_1(k)$ since it is zero for all k. In other words, our system is, in a sense, a linear time varying system of the form

$$e(k+1) = A(k)e(k),$$

where $e(k) = [e_2(k), \ldots, e_N(k)]^\top$ and

$$
A(k) = \begin{bmatrix}
(1 - \frac{\alpha_2(k)}{2}) & \frac{\alpha_2(k)}{2} & 0 & \ldots & 0 \\
\frac{\alpha_2(k)}{2} & (1 - \frac{\alpha_3(k)}{2} - \frac{\alpha_2(k)}{2}) & \frac{\alpha_3(k)}{2} & & \vdots \\
0 & \frac{\alpha_3(k)}{2} & \ddots & \ddots & \vdots \\
\vdots & \ddots & \ddots & \frac{\alpha_{N-2}(k)}{2} & 0 \\
\vdots & \ddots & \frac{\alpha_{N-2}(k)}{2} & (1 - \frac{\alpha_{N-1}(k)}{2} - \frac{\alpha_{N-2}(k)}{2}) & \frac{\alpha_{N-1}(k)}{2} \\
0 & \ldots & 0 & \frac{\alpha_{N-1}(k)}{2} & (1 - \alpha_N(k) - \frac{\alpha_{N-1}(k)}{2})
\end{bmatrix}.
$$

Now we present the following lemma that will be used later.

Lemma 10 *The spectrum of the matrix $A(k)$, $\rho(A(k))$ satisfies*

$$\rho(A(k)) \leq 1$$

for all k.

Proof: Note that for the given $A(k)$ we have

$$\|A(k)\|_1 = \|A(k)\|_\infty = 1$$

for all k. On the other hand, for any given matrix $A(k)$ it is well known that the two norm satisfies

$$\|A(k)\|_2 \leq \|A(k)\|_1 \|A(k)\|_\infty.$$

Hence, since we have

$$\rho(A(k)) = \|A(k)\|_2,$$

we obtain

$$\rho(A(k)) \leq 1$$

for all k, which completes the proof. ∎

This lemma basically says that the eigenvalues of $A(k)$ (which are all real numbers since $A(k)$ is symmetric) lie on the unit disk for each k. However, this result is not satisfactory and we need to prove that all of the eigenvalues of $A(k)$ lie within the unit circle for each k. This is done with the help of the next lemma.

Lemma 11 *Let $\underline{\alpha} \leq \alpha_i(k) = \alpha_i \leq \bar{\alpha}$ for all k and $i = 2, \ldots, N$ (i.e., the α_i's in the matrix A are all constants). Then,*

$$\rho(A(k)) = \rho(A) < 1,$$

and we have $e(k) \to 0$ as $k \to \infty$.

Proof: To prove the assertion, note that $A(k)$ is a symmetric matrix. Therefore, there exists a unitary transformation P (i.e., $P^{-1} = P^\top$) such that $\bar{A} = PAP^\top$, where $\bar{A} = diag\{\bar{a}_2, \ldots, \bar{a}_N\}$. For the sake of contradiction assume that $\rho(A) = 1$. Then, it must be the case that $\bar{a}_i = 1$ for some $i, 2 \leq i \leq N$. Define the transformation $\bar{e} = Pe$. Then the system can be described as

$$\bar{e}(k+1) = \bar{A}\bar{e}(k).$$

Since $\bar{A}$ is diagonal and $\bar{a}_i = 1$ we have $\bar{e}_i(k) = \bar{e}_i(0)$ for all k, whereas $\bar{e}_j(k) \to 0$ as $k \to \infty$ for all $j \neq i$. This, on the other hand, implies that $e(k) \to P_i\bar{e}_i(0) = e^c$ as

$k \to \infty$, where P_i is the i^{th} column of P. Depending on the value of $\bar{e}_i(0)$, the value of e^c can be any number. However, this contradicts the result of Lemma 8. Therefore, $\bar{a}_i < 1$ for all $i = 2, \ldots, N$, and this implies that $\rho(A) < 1$. ∎

Since in the above lemma $\alpha = [\alpha_2, \ldots, \alpha_N]^\top$ was chosen arbitrary, the result holds for all α such that $\underline{\alpha} \leq \alpha_i \leq \bar{\alpha}$. Hence, we have

$$\rho(A(k)) < 1$$

for each k. Before proceeding define

$$\bar{\rho} = \sup_{\underline{\alpha} \leq \alpha_i \leq \bar{\alpha}, i=2\ldots N} \{\rho(A)\}.$$

Then, from the above result we have

$$\bar{\rho} < 1.$$

6.3 The System Under Total Asynchronism

In this section we return to the totally asynchronous case. In other words, we assume that Assumption 4 holds. To prove its stability we will use the result from the synchronous case and a result from [7]. For convenience we present this result here.

Consider the function $f : X \to X$, where $X = X_1 \times \ldots, \times X_n$, and $x = [x_1, \ldots, x_n]^\top$ with $x_i \in X_i$. The function f is composed of functions $f_i : X \to X_i$ in the form $f = [f_1, \ldots, f_n]^\top$ for all $x \in X$. Consider the problem of finding the point x^* such that

$$x^* = f(x^*)$$

using an asynchronous algorithm. In other words, use an algorithm in which

$$x_i(k+1) = f_i(x_1(\tau_1^i(k)), \ldots, x_n(\tau_n^i(k))), \forall t \in \mathcal{K}^i,$$

where $\tau_j^i(k)$ are times satisfying

$$0 \leq \tau_j^i(k) \leq k, \forall k \in \mathcal{K}.$$

For all the other times $k \notin \mathcal{K}^i$, x_i is left unchanged. In other words, we have

$$x_i(k+1) = x_i(k), \forall k \notin \mathcal{K}^i.$$

Consider the following assumption.

Assumption 5 *There is a sequence of nonempty sets $\{X(k)\}$ with*

$$\cdots \subset X(k+1) \subset X(k) \subset \cdots \subset X,$$

satisfying the following two conditions:

1. Synchronous Convergence Condition (SCC): *We have*

$$f(x) \in X(k+1), \forall k \text{ and } x \in X(k).$$

Furthermore, if $\{y_k\}$ is a sequence such that $y_k \in X(k)$ for every k, then every limit point of $\{y_k\}$ is a fixed point of f.

2. Box Condition (BC): *For every k, there exist sets $X_i(k) \subset X_i$ such that*

$$X(k) = X_1(k) \times X_2(k) \times \ldots X_n(k).$$

Then we have the following result.

Theorem 7 Asynchronous Convergence Theorem [7]: *If the synchronous convergence condition and box condition of Assumption 5 hold, and the initial solution estimate $x(0) = [x_1(0), \ldots, x_n(0)]^\top$ belongs to the set $X(0)$, then every limit point of $\{x(k)\}$ is a fixed point of f.*

This is a powerful result that can be applied to many different problems. The main idea behind its proof is that if there is a time k_1 such that $x_j(\tau_j^i(k_1)) \in X_j(k)$ for all j and all i, then the SCC and the BC conditions above guarantee that $x(k_1+1) \in X(k+1)$. Then, $x(k) \in X(k+1)$ for all $k \geq k_1$ and due to the total asynchronism assumption there will be always another time $k_2 > k_1$ such that $x_j(\tau_j^i(k_2)) \in X_j(k+1)$ for all j and all i. Since initially we have $x_j(\tau_j^i(0)) = x_j(0) \in X_j(0)$, we can use the above arguments in an induction.

Now we state the main result of this chapter.

Theorem 8 *For the N-member swarm modeled in Eq. (6.2) with $g(\cdot)$ as given in Eq. (6.3), if Assumption (4) holds and $x_{i+1}(0) - x_i(0) > \epsilon, i = 1, \ldots, N-1$, then the swarm member positions will converge asymptotically to the comfortable position x^c.*

Proof: In order to prove this result we once again consider the synchronous case. Recall that for this case the system can be described by

$$e(k+1) = A(k)e(k).$$

In the previous section it was shown that for the synchronous case we have $\lambda(A(k)) \leq \bar{\rho} < 1$ for all k and that $e(k) \to 0$ as $k \to \infty$ (i.e., the position with comfortable intermember distance x^c). This implies that $A(k)$ is a maximum norm contraction mapping for all k. Define the sets

$$E(k) = \{e \in \mathbb{R}^{N-1} : \|e\|_\infty \leq \bar{\rho}^k \|e(0)\|_\infty\}.$$

Then, since $A(k)$ is a maximum norm contraction mapping for all k we have $e(k) \in E(k)$ for all k and

$$\ldots \subset E(k+1) \subset E(k) \subset \ldots \subset E = \mathbb{R}^{N-1}.$$

Moreover, each $E(k)$ can be expressed as

$$E(k) = E_2(k) \times E_3(k) \times \ldots E_N(k).$$

Since the position with comfortable intermember distance $e = 0$ (i.e., $x = x^c$) is the unique fixed point of the system and the synchronous swarm converges to it, it is implied that Assumption 5 above is satisfied. Applying the Asynchronous Convergence Theorem we obtain the result. ∎

This result is important because it says that the stability of the system will be preserved (i.e., the system will converge to the comfortable distance) even though we have totally asynchronous motions. Note that the fact that in the asynchronous case the min and max operations are preserved does not change the result since the stability properties of the synchronous system is preserved even with them present in the model. In fact, having them is, in a sense, beneficial because they also serve as another neighbor position sensing by the members that come to an ϵ distance from each other and this provides more accurate neighbor position information.

A direct consequence of Theorem 8 is the stability of swarm in which one member in the middle is stationary, whereas all the other middle members try to move as above and both of the edge members try to move to a distance d from their neighbors. In other words, suppose the swarm is described by

$$\begin{aligned}
x_1(k+1) &= \min\{x_1(k) - g(x_1(k) + d - x_2(\tau_2^1(k))), \\
&\qquad x_2(k) - \epsilon\} \forall k \in \mathcal{K}^1, \\
x_j(k+1) &= x_j(k), \forall k \text{ and for some } j, 1 \leq j \leq N \\
x_i(k+1) &= \max\{x_{i-1}(k) + \epsilon, \min\{x_i(k) - g(x_i(k) \\
&\qquad - \frac{x_{i-1}(\tau_{i-1}^i(k)) + x_{i+1}(\tau_{i+1}^i(k))}{2}),
\end{aligned}$$

$$
\begin{aligned}
& x_{i+1}(k) - \epsilon\}\}, \forall k \in \mathcal{K}^i, \\
& i = 2, \ldots, N-1, i \neq j, \\
x_N(k+1) &= \max\{x_{N-1}(k) + \epsilon, x_N(k) - g(x_N(k) \\
& -x_{N-1}(\tau_{N-1}^N(k)) - d)\}, \forall k \in \mathcal{K}^N. \qquad (6.6)
\end{aligned}
$$

In this case we have the following corollary as a direct consequence of Theorem 8.

Corollary 1 *For the N-member swarm modeled in Eq. (6.6) with $g(\cdot)$ as given in Eq. (6.3), if Assumption (4) holds and $x_{i+1}(0) - x_i(0) > \epsilon, i = 1, \ldots, N-1$, then the swarm member positions will converge asymptotically to x^c, where x^c is defined such that $x_j^c = x_j(0)$ and $x_i^c = x_j(0) + (i-j)d$, for all $i \neq j$.*

The importance of this result is for systems in which the "leader" of the swarm is not the first (or the last) member, but a member in the middle.

In this chapter we considered discrete time asynchronous swarms with time delays in one-dimensional space. Extension of these results to higher dimensions is not straightforward and needs further research.

CHAPTER 7

FORMATION CONTROL OF MOBILE ROBOTS

In the recent years there has been a significant interest in the control of multiple agents (i.e., a swarm of agents) moving in a formation or performing a coordinated task. This is because there are many potential applications of such systems including formation control of uninhabited autonomous vehicles (UAV's), coordination and control of teams of robots, control of satellite formations or clusters of telescopes, etc. In this chapter we consider the formation control problem of a system of M agents in the context of nonlinear output regulation (servomechanism) problem. As a difference from the work in the preceding chapters, the agents are assumed to have nonlinear dynamics and we are concerned with controller development. First, we consider a generic model for an agent with general nonlinear dynamics, and later we focus on a dynamic model of mobile robots.

7.1 The General Model

Consider a multi-agent system that consists of M agents (individuals) with motion dynamics given by

$$\begin{aligned} \dot{x}^i &= f_i(x^i, \mu^i, u^i), \\ y^i &= h_i(x^i, \mu^i), 1 \leq i \leq M, \end{aligned} \tag{7.1}$$

where $x^i \in \mathbb{R}^{n_i}$ represent the local state of each agent, $u^i \in \mathbb{R}^{m_i}$ are the local control inputs, and $y^i \in \mathbb{R}^{m_i}$ are the local outputs which are geometric variables that are used to define the formation. These variables can either be just the state of the system or output projections onto some space on which one wants the formation to evolve. We assume that the functions f_i and $h_i, i = 1, \ldots, M$, are known and smooth.

The signals $\mu^i \in \mathbb{R}^{r_i}$ represent the local exogenous inputs (i.e., reference inputs and disturbances) which are assumed to be generated by the local neutrally stable systems

$$\dot{\mu}^i = g_{\mu^i}(\mu^i), i = 1, \ldots, M, \tag{7.2}$$

where g_{μ^i} are also known and smooth. Note that the assumption that we know the dynamics g_{μ^i} is not absolutely necessary. In fact, we only need to know the dynamics of an *internal model* which can generate the same output signals as the system in Eq. (7.2) (the output of that system will be defined later). For the full information case the internal model is the system itself. For the error feedback case, on the other hand, it is an immersion of the system.

Formation Constraints: We assume that there are a set of predefined constraints

$$\eta_{i,j}(y^i, y^j) = 0, 1 \leq i, j, \leq M, j \neq i, \tag{7.3}$$

which uniquely determine the formation.

Remark: Note that it is not necessary to have constraints for every pair of agents. It is enough to have only minimal number of constraints, which uniquely determine the desired formation. It is possible, for example, to obtain such a set of minimal number of constraints, by using the concepts of rigid and unfoldable graphs from graph theory. ■

Now, assume that there exists a *virtual leader* for the formation and the individuals (i.e., the formation) are required to follow (track) that leader. In other words, the objective is to design each of the local control inputs u^i such that the formation constraints in Eq. (7.3) are satisfied and the formation follows the trajectories of the virtual leader. We assume that the dynamics of the virtual leader are generated by the neutrally stable system

$$\begin{aligned} \dot{s} &= g_s(s), \\ y^l &= q_s(s), \end{aligned} \tag{7.4}$$

where $s \in \mathbb{R}^r$ and g_s is known and smooth.

The assumption that the system in Eq. (7.4) is neutrally stable is a little bit restrictive. However, note that it still covers a large class of reference trajectories including constant and periodic (e.g., sinusoidal) trajectories. Such reference trajectories can be found in many practical applications such as orbiting satellites around the earth or agents guarding an object etc. Moreover, it is possible to generate more complicated trajectories by switching between a sequence of stable exosystems. In particular, note that the output of a system which is a chain of d integrators is a *spline* of degree d [63]. Therefore, given any smooth trajectory, it is possible to approximate it using splines [115] and for that reason find a sequence of exosystems that generate these splines (and therefore the desired trajectory). The only problem for this case is that we need the switching to be slow enough (implying that the reference trajectory is smooth enough) so that tracking can be achieved.

Tracking Constraints: We assume that there are a set of predefined constraints

$$\eta_{i,l}(y^i, y^l) = 0, 1 \leq i \leq M, \tag{7.5}$$

which need to be satisfied by the agents during motion.

Note that the formation and tracking constraints cannot be just arbitrary. In other words, in order for the problem to be solvable the formation constraints and the tracking constraints need to be nonconflicting, i.e., simultaneous satisfaction of both of the constraints should be feasible.

Now, since the (requred) dynamics of the agents are tied to the dynamics of the virtual leader through the tracking constraints, it is possible to view the dynamics of the virtual leader as external inputs to the individual agent dynamics. With this in mind, for each i we define $s^i = [s^\top, \mu^{i\top}]^\top$ and each of the local exosystems becomes

$$\dot{s}^i = g_i(s^i) = \begin{bmatrix} g_s(s) \\ g_{\mu^i}(\mu^i) \end{bmatrix}, \tag{7.6}$$

which are neutrally stable and the $g_i(s^i)$ are known and smooth.

Note that we can view the constraints $\eta_{i,j}$ and $\eta_{i,l}$ as the new outputs of the system and develop the local controllers u^i to regulate these outputs to zero. However, here we will not consider this case. Instead, we have the following simplifying assumption.

Assumption 6 *There exist known smooth mappings $q_i(s^i), i = 1, \ldots, M$ such that*

$$\begin{aligned} \eta_{i,j}(q_i(s^i), q_j(s^j)) &= 0, 1 \leq i, j \leq M, j \neq i, \\ \eta_{i,l}(q_i(s^i), q_s(s)) &= 0, 1 \leq i \leq M. \end{aligned}$$

Remark: Assumption 6 constitutes, in a sense, a "feasibility assumption." In other words, if the formation constraints and the tracking constraints are nonconflicting (implying that the desired formation is feasible), then this assumption is always satisfied. Therefore, such $q_i(s^i), i = 1, \ldots, M$ always exist. However, in general, we

may not always know these mappings, which makes the assumption a bit restrictive.

■

7.2 The Nonlinear Servomechanism Based Controller

Now, note that if we can force the output of each system to satisfy $y^i = q_i(s^i)$, then we will guarantee that both the formation constraints and the tracking constraints are satisfied. With this objective in mind we can redefine the new (error) output of each agent as $e^i = \bar{h}_i(x_i, s^i) = y^i - q_i(s^i) = h_i(x_i, \mu^i) - q_i(s^i)$ and rewrite the system to obtain

$$\begin{aligned} \dot{x}^i &= \bar{f}_i(x^i, s^i, u^i), \\ e^i &= \bar{h}_i(x_i, s^i), 1 \leq i \leq M, \end{aligned} \tag{7.7}$$

where we used the notation $\bar{f}_i$ since we used s^i instead of μ^i in f_i. Note that with this formulation the problem of formation control and trajectory following (i.e., both the formation constraints and the tracking constraints satisfied) in the presence of disturbances is equivalent to the problem of decentralized nonlinear output regulation (servomechanism) of the class of systems described in Eq. (7.7).

In Appendix A we analyze the decentralized output regulation problem for a class of nonlinear system including interconnected systems in the framework of [54]. Note that the system here is a special case of the systems considered there. (Actually, the problem is even simpler since the agent dynamics are decoupled.) Therefore, we can directly apply the results obtained there. Now, we briefly describe the conditions for the solvability of the problem (for more information see Appendix A or [54]).

Let $A_i = \frac{\partial f_i}{\partial x_i}(0,0,0)$, $B_i = \frac{\partial f_i}{\partial u_i},(0,0,0)$, and $C_i = \frac{\partial h_i}{\partial x}(0,0)$. Then, necessary conditions for the solvability of the problem are that

1. Each of the pairs (A_i, B_i) is controllable and

2. There exist mappings $x^i = \pi^i(s^i)$ and $u^i = c^i(s^i), 1 \leq i \leq M$, with $\pi^i(0) = 0$ and $c^i(0) = 0, 1 \leq i \leq M$, defined in a neighborhood S_i^o of the origin of $\mathbb{R}^{r_i+r}$, respectively, such that

$$\begin{aligned} \frac{\partial \pi^i(s^i)}{\partial s^i} g_i(s^i) &= f_i(\pi^i(s^i), c^i(s^i)), \\ 0 &= h_i(\pi^i(s^i)) - q_i(s^i), 1 \leq i \leq M, \end{aligned} \tag{7.8}$$

   for all $s^i \in S_i^o$, respectively.

Full Information Controller

For some systems the states s^i of the exosystems may be known and it may be possible to solve the nonlinear partial differential equations in Eq. (7.8) for the mappings $\pi^i(s^i)$ and $c^i(s^i)$. In that case the above two conditions are also sufficient for the solvability of the problem. In fact, one controller that achieves the (local) formation control and collective trajectory tracking is given by

$$u^i = c^i(s^i) + K_i(x^i - \pi^i(s^i)),$$

where each of the matrices K_i is chosen such that for all i the matrices $(A_i - B_i K_i)$ are Hurwitz. This controller is a direct consequence of the results in [54] (since the system is decoupled).

Error Feedback Controller

In general, it may not be possible to know s^i or to solve Eq. (7.8) for the mappings $\pi^i(s^i)$ and $c^i(s^i)$. Therefore, it may be desirable to develop a decentralized dynamic error feedback controller (i.e., a controller that uses only the local output information e^i) which still achieves the objective.

In order for the error feedback nonlinear servomechanism problem to be solvable we need a few more necessary (and sufficient) conditions to be satisfied in addition to above mentioned two conditions (needed for the full information case). These conditions are the following:

1. The autonomous systems with outputs

$$\begin{aligned} \dot{s}^i &= g_i(s^i), \\ u^i &= c^i(s^i), 1 \leq i \leq M \end{aligned}$$

are immersed into

$$\begin{aligned} \dot{\xi}^i &= \varphi_i(\xi^i), \\ u^i &= \gamma_i(\xi^i), 1 \leq i \leq M, \end{aligned} \tag{7.9}$$

defined on neighborhoods $\Omega_i, 1 \leq i \leq M$, of the origins of $\mathbb{R}^{p_i}$, respectively, in which $\varphi_i(0) = 0$ and $\gamma_i(0) = 0, 1 \leq i \leq M$.

2. The matrices

$$\Phi_i = \left[\frac{\partial \varphi_i}{\partial \xi^i}\right]_{\xi^i=0} \quad \text{and} \quad \Gamma_i = \left[\frac{\partial \gamma_i}{\partial \xi^i}\right]_{\xi^i=0}$$

for $1 \leq i \leq M$ are such that each of the pairs

$$\left[\begin{array}{cc} A_i & 0 \\ N_i C_i & \Phi_i \end{array}\right], \quad \left[\begin{array}{c} B_i \\ 0 \end{array}\right], \quad 1 \leq i \leq M, \tag{7.10}$$

is stabilizable for some $N_i, 1 \leq i \leq M$, and each of the pairs

$$\left[\begin{array}{cc} C_i & 0 \end{array}\right], \quad \left[\begin{array}{cc} A_i & B_i\Gamma_i \\ 0 & \Phi_i \end{array}\right], \quad 1 \leq i \leq M, \tag{7.11}$$

is detectable.

If these conditions are satisfied, the decentralized error feedback nonlinear servomechanism problem is solvable and the local controllers which solve the problem are given by

$$\begin{aligned} \dot{\xi}^i &= \varphi_i(\xi^i) + N_i e^i, \\ \dot{\chi}^i &= \Psi_i \chi^i + L_i e^i, \\ u^i &= \gamma_i(\xi^i) + G_i \chi^i, 1 \leq i \leq M, \end{aligned} \tag{7.12}$$

where the matrices Ψ_i, L_i, and G_i are chosen such that the matrices

$$\tilde{A}_i = \begin{bmatrix} \bar{A}_i & \bar{B}_i G_i \\ L_i \bar{C}_i & \Psi_i \end{bmatrix},$$

where

$$\bar{A}_i = \begin{bmatrix} A_i & B_i \Gamma_i \\ N_i C_i & \Phi_i \end{bmatrix}, \bar{B}_i = \begin{bmatrix} B_i \\ 0 \end{bmatrix}, \text{ and } \bar{C}_i = \begin{bmatrix} C_i & 0 \end{bmatrix},$$

are Hurwitz. Note that such a triple of matrices always exists. In other words, the above conditions guarantee the existence of such a stabilizing controller. For example, one possible choice is an observer based controller given by [59]

$$\Psi_i = \bar{A}_i - \bar{B}_i K_i - H_i \bar{C}_i, G_i = K_i, L_i = -H_i,$$

where K_i and H_i are such that the matrices $(\bar{A}_i - \bar{B}_i K_i)$ and $(\bar{A}_i - H_i \bar{C}_i)$ are Hurwitz.

Remark: Note that the results described above are local results for the general nonlinear vehicle dynamics. In other words, they do not hold for all possible initial conditions. If, however, the vehicle dynamics for the agents were linear, then the results would hold globally. It is possible to obtain global or semiglobal results also for a class of nonlinear dynamics. This could be done by considering vehicle dynamics of the form of the systems described in [98, 96, 97, 60] and adapting their procedures to the framework considered here. ■

7.3 Formation Control of Mobile Robots

In this section we consider the dynamics of mobile robots and apply the controller discussed in the preceding section for formation control.

7.3.1 The Robot Dynamic Model

Consider a system of M mobile robots in $\mathbb{R}^2$ with motion equations given by

$$\begin{aligned}
\dot{x}^i &= v^i \cos(\theta^i), \\
\dot{y}^i &= v^i \sin(\theta^i), \\
\dot{\theta}^i &= w^i \\
\dot{v}^i &= \frac{1}{m_i} F^i, \\
\dot{w}^i &= \frac{1}{J_i} \tau^i, 1 \leq i \leq M,
\end{aligned}$$

where x^i and y^i are the Cartesian coordinates, θ^i is the steering angle, v^i is the linear speed, and w^i is the angular speed of each agent. The quantities m_i and J_i are positive constants and represent the mass and the moment of inertia of each agent, respectively. The control inputs to the system are the force input F^i and the torque input τ^i. Note that this model includes both kinematic and dynamic equations for the system. In other words, it is obtained by adding the velocity (linear and angular) dynamics to the system (which are neglected in the kinematic only model). This is equivalent to adding two integrators to the kinematic system. Note that the system is in an affine form.

7.3.2 Problem Definition

In this section we assume that the point of interest of each robot is a point in front of the robot at a distance d_i from the center of the robot. In other words, we

are interested in the point z^i with coordinates given by

$$z^i = \begin{bmatrix} x^i + d_i \cos(\theta^i) \\ y^i + d_i \sin(\theta^i) \end{bmatrix}.$$

This point may represent a gripper at the end of a hand of length d_i or a sensor position in front of the robot. We will treat z^i as the output of the system. (The gripper may be holding something or performing some cooperative task and therefore may be the point of interest. Similarly, if it were a sensor, there may be a requirement for the sensor to be positioned in a particular way.)

Now, assume that the formation constrains are described in terms of the relative distances of the outputs (points of interest) of the subsystems (agents) and are given by

$$\|z^i - z^j\| = d_{i,j}, 1 \leq i, j \leq M, j \neq i.$$

Similarly, assume that the tracking constraints are also described as relative distances of the outputs of the agents with respect to the output position of the virtual leader and are given by

$$\|z^i - z^l\| = d_{i,l}, 1 \leq i \leq M,$$

where z^l is the output of the virtual leader. Note that, as was mentioned before, it is not required to have constraints for every pair of individuals and every individual and the virtual leader. We need to have only a sufficient number of constraints which uniquely determine the formation.

We assume that the reference trajectories to be tracked by the formation are generated by the linear neutrally stable exosystem

$$\begin{aligned} \dot{s} &= G_s s, \\ y^l &= C_s s, \end{aligned} \tag{7.13}$$

and that we do not have any local exogenous inputs to the system.

Now, note that Assumption 6 is easily satisfied (provided that the constraints are feasible). In other words, there exist vectors r^i such that $\|r^i - r^j\| = d_{i,j}$ and $\|r^i\| = d_{i,l}$. We can choose any set of r^i which satisfy these conditions. Then, for each agent i the trajectory to be tracked can be defined as

$$q_i(s) = C_s s + r^i.$$

This $q_i(s^i)$ implies that the relative position of the output of each robot with respect to the output position of the virtual leader is given by the corresponding constant vector r^i.

7.3.3 Controller Development

In Appendix B it was shown that with appropriate change of coordinates and choice of control input the input-output dynamics with respect to the above defined z^i can be linearized. The dynamics of the robot in the new coordinates are given by (see Appendix B)

$$\begin{aligned} \dot{z}^i &= \zeta^i \\ \dot{\zeta}^i &= u^i \\ \dot{\theta}^i &= -\frac{1}{d_i}\zeta_1^i \sin(\theta^i) + \frac{1}{d_i}\zeta_2^i \cos(\theta^i). \end{aligned}$$

Note that the state θ^i represent the unobservable states and that the zero dynamics of the system are marginally stable since when $\zeta^i = 0$ we have $\dot{\theta}^i = 0$.

Since the input-output map of the system is linear, one can analytically solve for the manifold equations using

$$\pi_1^i(s) = q_i(s), \quad \pi_2^i(s) = \tfrac{\partial q_i(s)}{\partial s} G_s s, \quad c^i(s) = \tfrac{\partial \pi_2^i(s)}{\partial s} G_s s.$$

Note, however, that these are only a part of the manifold corresponding to the linear part of the dynamics. For the part corresponding to the unobservable dynamics we have the following assumption.

Assumption 7 *There exists a mappings* $\lambda^i(s)$ *with* $\lambda(0) = 0$ *such that*

$$\frac{\partial \lambda^i(s)}{\partial s} G_s s = -\frac{1}{l_i}\pi^i_{2,1}(s)\sin(\lambda^i(s)) + \frac{1}{l_i}\pi^i_{2,2}(s)\cos(\lambda^i(s)).$$

We do not need to know $\lambda^i(s)$ in order to be able to implement the controller.

Full Information Controller

Now, define $\tilde{x}^i_1 = z^i - \pi^i_1(s)$, $\tilde{x}^i_2 = \zeta^i - \pi^i_2(s)$, and $\tilde{u}^i = u^i - c^i(s)$. Then, the system becomes

$$\begin{aligned} \dot{\tilde{x}}^i_1 &= \tilde{x}^i_2 \\ \dot{\tilde{x}}^i_2 &= \tilde{u}^i \end{aligned}$$

and the problem is reduced to the problem of stabilization of the above system. By choosing the stabilizing controller as

$$\tilde{u}^i = -\alpha_1 \tilde{x}^i_1 - \alpha_2 \tilde{x}^i_2$$

with α_1 and α_2 such that the matrix

$$\begin{bmatrix} 0 & 1 \\ -\alpha_1 & -\alpha_2 \end{bmatrix}$$

is Hurwitz we know that we will achieve exponential stability of the system (i.e., exponentially fast convergence to the zero error manifold). For example, the choice of $\alpha_1 = 2$ and $\alpha_2 = 3$ will render the poles of the system at -1 and -2. From here

the (full information) controller that achieves both formation control and trajectory tracking for the system is given by

$$u^i = c^i(s) - \alpha_1 \left(z^i - \pi_1^i(s)\right) - \alpha_2 \left(\zeta^i - \pi_2^i(s)\right),$$

and the final control input to the robot $[F^{i\top}, \tau^{i\top}]^\top$ is obtained by inserting u^i in the linearizing control in Eq. (B.1) in Appendix B.

Here the first term in the control input guarantees that the agent tracks the trajectory generated by the virtual leader (once it is on the trajectory), whereas the second term moves it towards that trajectory if initially it is not on the trajectory. Note that the individuals do not need to have information about the other agents in the system. They only need to know the information about the virtual leader and their relative desired positions r^i. Note, however, that inherently there is a drawback in this since it cannot guarantee avoidance of collisions between the robots. In order to avoid collisions it may be possible to augment (redesign) the stabilizing controller with a collision avoidance term (e.g., a term based on on artificial social potential fields or attraction/repulsion between the agents, similar to the swarms considered earlier). However, this is a topic of further research and will not be considered here.

Another observation we need to mention here is that since the zero dynamics of the equations are not asymptotically stable (recall that they are only neutrally stable), during a transient they may grow large. However, note that the state of the zero dynamics (unobservable dynamics) θ^i corresponds to the orientation angle of the robot, and is 2π periodic. Therefore, the temporary instability (possible during a transient) in θ^i does not constitute any real danger. Physically it means that during transient, while the robot is trying to reach the zero error manifold, it may rotate around itself several times.

Error Feedback Controller

Now, we will consider the case in which the exogenous signals are not known. Instead, we have only the measurement of the output error e^i. To this end, first note that since the exosystem that we consider is linear there exist always a mapping $\tau^i(s^i)$ such that it is immersed into a linear observable system. In fact, one such mapping is given by

$$\tau^i(s) = \begin{bmatrix} c^i(s) \\ \frac{\partial c^i(s)}{\partial s} G_s s \end{bmatrix}.$$

With the above transformation this system is immersed into the linear system

$$\begin{aligned} \dot{\tau}^i(s) &= \Phi_i \tau^i(s), \\ c^i(s) &= \Gamma_i \tau^i(s), \end{aligned}$$

which is in observable canonical form and has eigenvalues on the imaginary axis. By choosing the matrices N_i such that the pairs (Φ_i, N_i) are controllable (e.g., choose N_i such that the pair is in controllable canonical form), the pair in Eq. (7.10) stabilizable and the pair in Eq. (7.11) is already detectable for the above internal model. Then, the interconnection of the internal model and system is stabilizable. This implies that we can easily choose the dynamic controller (Ψ_i, G_i, L_i) as described in the previous section (or any other means as long as it stabilizes the closed loop system) and complete the design of the controller.

7.3.4 Other Possible Designs

One of the drawbacks of the of the partially feedback linearizing controller, based on which the results in the previous section were developed, is that the zero dynamics

of the system are not asymptotically stable, which may degrade the transient performance. Another possible drawback could be the fact that each of the agents must know its global coordinates (i.e., coordinates with respect to some global coordinate system) x, y, and θ. In some applications, this may not be the case. Instead, there may be a leader (virtual or not) which knows its global coordinates, whereas, the other robots know (can measure) only their relative coordinates with respect to the preceding agents. Moreover, the transformation there holds only for a particular point on a distance d from the center of the robot and does not hold for the center itself. Therefore, it may not be possible to use the partially feedback linearizing controller if the point of interest is the center of the robot.

In cases such as the ones above there may be a need for development of a different type of controller. One alternative would be to fully linearize the system by usin dynamic feedback. In fact, it can be shown that by adding an integrator to one of the inputs of the system and appropriate change of coordinates, the system dynamics with respect to the output

$$z^i = \begin{bmatrix} x^i \\ y^i \end{bmatrix},$$

can be fully linearized (see Eq. (B.2 in Appendix B) with the condition that $v^i \neq 0$. Then, one can design the controller using (possibly) output regulation framework for the linearized system such that the control objectives (the formation and tracking constraints) are satisfied. Note, however, that special care must be taken in order to ensure that $v^i \neq 0$.

As an alternative for the case in which the agents know (or can measure) only their relative coordinates (i.e., relative position and orientation), then the local model derived in Appendix B can be used. As was shown in Appendix B, for this case also

the system dynamics can be fully linearized with respect to the output

$$z^j = \begin{bmatrix} l_{ij} \\ \psi_{ij} \end{bmatrix},$$

which is the vector of the relative distance l_{ij} and relative orientation ψ_{ij} of the follower agent j with respect to leading agent i. This transformation also is possible with condition that $v^i \neq 0$. Note also that there is also a drawback, which is the fact that the linearizing transformation for the relative dynamics of the follwer agent j depends also on the state of the leading agent i. Therefore, developing a controller that achieves satisfactory formation control needs careful consideration and additional research. Nevertheless, following this approach can lead to potentially useful result.

7.3.5 Simulation Examples

In this section we will provide an example problem, show the controller development and provide simulation examples. Assume that we have a system consisting of three agents, which are required to move in an equilateral triangle formation along a circle. This implies that the trajectories of the virtual leader are generated by the linear given in Eq. (7.13) with

$$G_s = \begin{bmatrix} 0 & -\beta & 0 & 0 \\ \beta & 0 & 0 & 0 \\ 0 & 0 & 0 & -\beta \\ 0 & 0 & \beta & 0 \end{bmatrix}, \quad C_s = \begin{bmatrix} 1 & 0 & 0 & 0 \\ 0 & 0 & 1 & 0 \end{bmatrix}.$$

Assume that the parameter $\beta = 1$ and initial conditions are $s(0) = [10, 0, 10, 10]^\top$. Assume that the virtual leader is located at the center of the triangle and the relative position vectors for the agents are given by

$$r^1 = \begin{bmatrix} 0 \\ 1 \end{bmatrix}, r^2 = \begin{bmatrix} \frac{\sqrt{3}}{2} \\ -\frac{1}{2} \end{bmatrix}, \text{ and } r^3 = \begin{bmatrix} -\frac{\sqrt{3}}{2} \\ -\frac{1}{2} \end{bmatrix}.$$

Then, the desired position of agent i is given by

$$q_i(s) = \begin{bmatrix} s_1 \\ s_3 \end{bmatrix} + r^i.$$

Using the above $q_i(s)$ we can solve for the manifold equations to obtain

$$\pi_1^i(s) = \begin{bmatrix} s_1 \\ s_3 \end{bmatrix} + r^i, \quad \pi_2^i(s) = \beta \begin{bmatrix} s_2 \\ s_4 \end{bmatrix}, \quad c^i(s) = -\beta^2 \begin{bmatrix} s_1 \\ s_3 \end{bmatrix},$$

using which the full information controller is given by

$$u^i = -\beta^2 \begin{bmatrix} s_1 \\ s_3 \end{bmatrix} - \alpha_1 \left(z^i - r^i - \begin{bmatrix} s_1 \\ s_3 \end{bmatrix} \right) - \alpha_2 \left(\zeta^i - \beta \begin{bmatrix} s_2 \\ s_4 \end{bmatrix} \right).$$

For the stabilizing controller we choose the parameters as $\alpha_1 = 2$ and $\alpha_2 = 3$, which lead to the poles at -1 and -2. Figure 7.1 shows the response of the system for about 15 seconds. As you can see, initially the individuals are not in the required formation; however, they form the formation very fast (exponentially fast) and follow the required trajectory in a formation.

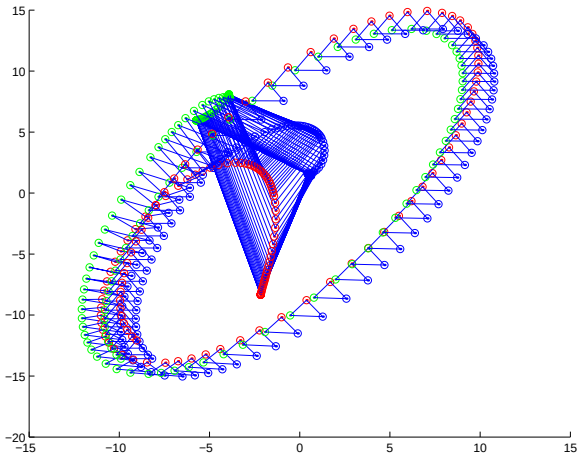

Figure 7.1: The response for the full information controller with $\alpha_1 = 2$ and $\alpha_2 = 3$.

Before developing the error feedback controller note that for this problem the dynamics of the system are decoupled for the two dimensions (of the state space). Therefore, we will also decouple the problem of the servocontroller design. In other words, we will consider each dimension as a separate single-input-single-output system and design the controller for that dimension. (Actually, we will design a controller for one dimension only and use the same structure for the other dimension too, since the dynamics in both dimensions is the same.)

Considering only the single dimensional subsystem generating the controller we have

$$\begin{aligned} \dot{s} &= \begin{bmatrix} 0 & -\beta \\ \beta & 0 \end{bmatrix} s \\ c^i(s) &= -\beta^2 s_1, \end{aligned}$$

and the transformation $\tau^i(s)$ is given by

$$\tau^i(s) = \begin{bmatrix} -\beta^2 s_1 \\ \beta^3 s_2 \end{bmatrix}.$$

Using that transformation the system is immersed into

$$\begin{aligned} \dot{\tau}^i(s) &= \begin{bmatrix} 0 & 1 \\ -\beta^2 & 0 \end{bmatrix} \tau^i(s), \\ c^i(s) &= \begin{bmatrix} 1 & 0 \end{bmatrix} \tau^i(s). \end{aligned}$$

Note that for this system we have

$$A_i = \begin{bmatrix} 0 & 1 \\ 0 & 0 \end{bmatrix}, B_i = \begin{bmatrix} 0 \\ 1 \end{bmatrix}, C_i = \begin{bmatrix} 1 & 0 \end{bmatrix}, \Phi_i = \begin{bmatrix} 0 & 1 \\ -\beta^2 & 0 \end{bmatrix}, \text{ and } \Gamma_i = \begin{bmatrix} 1 & 0 \end{bmatrix}.$$

By choosing

$$N_i = \begin{bmatrix} 0 \\ 1 \end{bmatrix},$$

the interconnection of the internal model and system is stabilizable for any constant β.

Now, choose the desired pole locations for the closed loop system and the observer as $[-1, -2, -3, -4]$ and find the stabilizing controller by using the Matlab command `place` as

$$\begin{aligned} L_i &= place(\bar{A}_i, \bar{C}_i^\top, [-1, -2, -3, -4])^\top, \\ G_i &= place(\bar{A}_i, \bar{B}_i, [-1, -2, -3, -4]), \\ \Psi_i &= \bar{A}_i - \bar{B}_i G_i - L_i \bar{C}_i, \end{aligned}$$

which are given by

$$\Psi_i = \begin{bmatrix} -10 & 1 & 0 & 0 \\ -59 & -10 & 10 & -40 \\ -40 & 0 & 0 & 1 \\ -33 & 0 & -1 & 0 \end{bmatrix}, G_i = \begin{bmatrix} 34 \\ 10 \\ -9 \\ 40 \end{bmatrix}, \text{ and } L_i = \begin{bmatrix} -10 & -25 & -40 & -34 \end{bmatrix}.$$

The plot on the left in Figure 7.2 shows the motion of the system for about 20 seconds. Note that it takes more time for the system (compared to the full

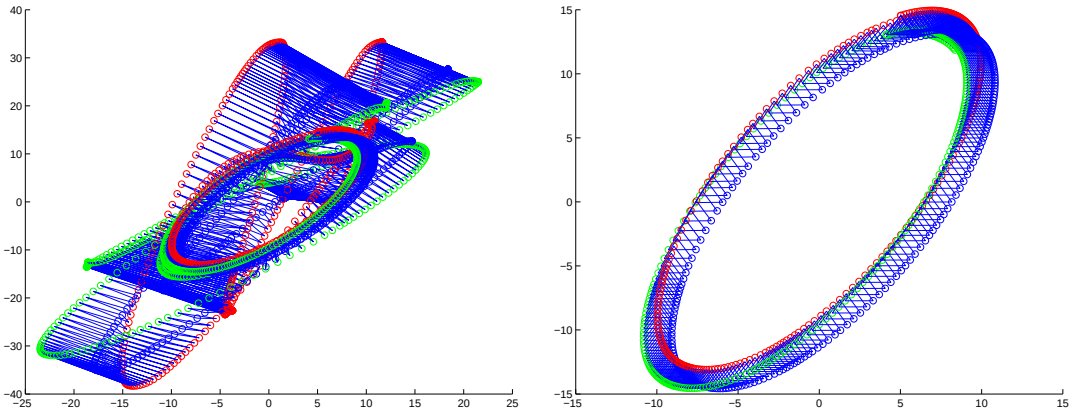

For about 20 seconds. After 15 seconds.

Figure 7.2: The response for the error feedback controller.

information case) to converge to the desired formation and to follow the trajectory of the virtual leader. This is due to the fact that it takes some time for the observer states to converge and therefore to generate the appropriate control input. Nevertheless, it still converges in a short period of time. The plot on the right in Figure 7.2 shows the trajectories of the three agents for the last 5 seconds of the above case. As you can see, they have converged to the desired formation and follow the desired trajectory.

Figure 7.3 shows another simulation (for which we do not show the controller development), in which we used a set of three neutrally stable exosystems and a (circular) sequence of switching between them. This was done in order to simu-

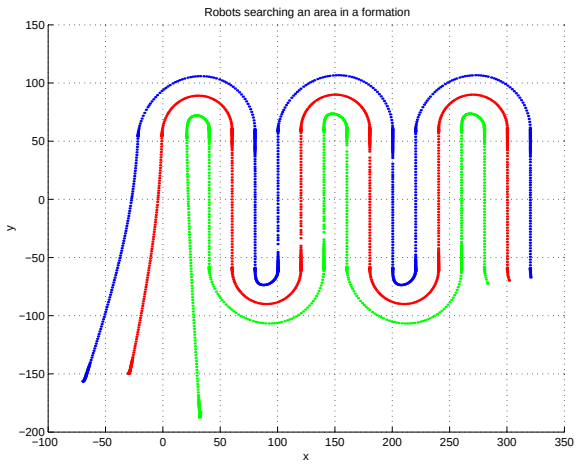

Figure 7.3: Three robots searching an area.

late a searching behavior of three robots which needed to move aligned though a predefined rectangular region and it was not possible to generate their path using single neutrally stable exosystem. The plot shown in the figure is for the case using the full information controller. As expected, the robots move to the area, align with

each other (as required by the formation constraints), and perform the search keeping the needed distance. As was mentioned before, by appropriately switching between the exosystems, it is possible to generate (and therefore track) even more complex trajectories.

CHAPTER 8

CONCLUSIONS

In this chapter we will summarize the work done in this dissertation and also will point out some potentially fruitful future research directions.

8.1 Summary and Contributions

In this dissertation we considered the problem of mathematically modeling and performing stability analysis of swarms. First, we considered stationary aggregating swarms in Chapter 2 and showed that for the given model cohesiveness of the swarm is achieved in a finite time. We also derived explicit bounds on the swarm size and the time of convergence. The results derived are global and hold for any dimension n of the state space. Following that, in Chapter 3 we extended the results in Chapter 2 to incorporate different types of attraction/repulsion functions in the model. In particular, we allowed for unbounded repulsions, therefore guaranteeing avoidance of collisions. We also showed that the model can easily be modified to describe uniform swarm density as in real biological swarms or to achieve formation stabilization for any desired formation. In Chapter 4 we considered social foraging swarms (i.e., swarms moving in a profile of nutrients or toxic substances) and showed collective

convergence to more favorable (nutrient rich) regions and divergence from unfavorable (toxic) regions of the profile. All these results are based on the use of artificial potential functions and are unique results on swarm cohesiveness establishing bounds on swarm size. Note also that the results in these chapters are very much related to optimization theory. In fact, one may view the social foraging swarm as a distributed minimization of the profile function using a distributed gradient method.

The biological literature [9, 114, 47, 80] provided the main inspiration for these results. However, as a difference from the work in biology, we were able to perform rigorous stability analysis. Other work with immediate relevance to the work in these chapters includes the literature on multi-agent control using artificial potential functions [88, 64]. Our swarm model can be viewed as a type of social potential fields method described in [88]. However, note that no stability analysis was performed in [88]. The recent results in [64] consider a very similar model to ours and also use Lyapunov stability theory for analysis. Note, however, that they are not concerned with cohesiveness of the swarm as we are and also their results are local. To best of our knowledge, our results are the first that view cohesiveness as a stability property and simultaneously establish bounds on the swarm size.

In Chapter 5 we considered the problem of modeling and analysis of the aggregation and cohesiveness of honey bee clusters and in-transit swarms. In the honey bee literature there are many experimental results published [101, 76, 10, 11, 77, 73, 3, 1, 95, 91]; however, there have not been any mathematical models developed. Even though the analysis in the chapter is not very rigorous, it is (to best of our knowledge) the first attempt to create a mathematical model for the clustering or swarming

behavior of honey bees. Therefore, it has the potential of triggering further research and (possibly) experimental studies in the area.

In Chapter 6 we diverged from the work in the previous chapters by considering a discrete time one-dimensional asynchronous swarm model with time delays. Note that the problem of performing stability analysis of swarms under asynchronism and time delays is, in general, not an easy problem. We were able to obtain stability by making use of some earlier results from parallel and distributed computation literature. Note that one dimensional swarms are very similar to the platooning in automated highway system, which is an area which has been studied extensively (see for example [5, 105, 104, 23]). The closest results to our work in this chapter is the work by Liu and Passino in [68, 67, 69, 70]. In fact, in our work in this chapter we used the single swarm member model from [68]. However, we used different model for interindividual attractions and repulsions and also different mathematical tools for stability analysis.

In Chapter 7 we considered the formation control problem for a multi-agent system. We showed that the problem can be approached in the framework of decentralized nonlinear output regulation (servomechanism) problem and explicitly specified the controller which achieves formation stabilization as well as trajectory tracking. We also showed how the controller can be used for formation control of mobile robots. To best of our knowledge, this is the first attempt to consider the formation control problem in the context of output regulation. It differs from the other work on formation control [28, 29, 32, 79] not only because we use output regulation theory, but also because we consider a general nonlinear dynamic model and then apply it to formation control of robots. The algorithm has some drawbacks (e.g., we cannot guarantee collision avoidance). However, it is an initial step for developing rigorous

multi-agent coordination and control strategies based on nonlinear output regulation theory.

In Appendix A decentralized output regulation of a class of nonlinear systems was considered. It basically constitutes an extension of the results on linear output regulation in [26] to the nonlinear case in the framework of [54]. Therefore, Appendix A is not directly an integral part of this work. However, the results developed there provided a basis for the results in Chapter 7. Moreover, they are a small contribution to the nonlinear output regulation literature on their own.

Appendix B discusses three useful transformations (representations) of the dynamics of a mobile robot. One of these transformations is used in Chapter 7 to partially linearize the system dynamics before developing the nonlinear servomechanism based controller.

8.2 Future Research Directions

There are several possible potentially fruitful research directions which can be pursued starting with this work as a base. First, note that in the swarm models considered in Chapters 2, 3, and 4 all the individuals were assumed to know the exact (relative) position of all the other individuals. Therefore, a good contribution would be to consider the case in which there is some kind of communication topology between the agents, i.e., the swarm members can communicate or sense only a subset of the other agents and the swarming behavior is based only on these sensed individuals. The communication topology can be considered to be fixed (i.e., the individuals can see only a predefined fixed set of other individuals) or dynamic (i.e., the set of individuals which can be seen by a given swarm member can vary). For example, consider the

case in which the agents are able to sense (see) only their nearest neighbors and the neighbors can change with time. Proving stability under such conditions is an open problem that needs to be analyzed.

As another extension we can consider stability of the system under uncertainties such as measurement errors or communication delays. In other words, assume that the agents measure the relative position of their neighbors using sensors and there are imperfections in the sensors. Can we still guarantee similar swarming behavior? Or, assume that the swarm members communicate their position to their neighbors and there are communication delays. Therefore, since the agents are moving, at the time when individual i receives the position information of individual j, individual j has already moved to another position. Can we still guarantee stability?

Note that the model of social foraging swarm in Chapter 4 can be considered as a model of a multi-agent system moving in a environment. In that case, the profile represents the environment, and nutrients are analogous to targets (to which the agents are required to move) and toxic substances are analogous to threats (which the agents need to avoid). Note, however, that the profile that we considered is a static profile, i.e., it does not change with time. It is an open problem to analyze the stability characteristics of the emergent behavior for dynamically varying profiles. This will allow us to handle cases of moving or "pop-up" targets and/or threats.

The swarm model that we consider constitutes essentially a kinematic model for swarming behavior. In this context, the swarm members of our model can be viewed as virtual agents that generate the trajectories tracked by real agents with their own dynamics. If we have a group (a swarm) of vehicles with their own dynamics with the requirement of some kind of swarming behavior (e.g., formation keeping).

Then, we can use the above approach, or, in contrast, we can consider developing a control strategy that will directly achieve the swarming behavior. Therefore, given known, general fixed vehicle (agent) dynamics, there is a need for a general controller controller development for swarming behavior.

Analyzing the stability of asynchronous swarms with time delays is important since many biological or engineering systems may have these characteristics. In Chapter 6 we considered the problem in one dimension. However, developing a general n-dimensional swarm model and performing rigorous stability analysis of the emergent behavior is an important open problem.

In Chapter 7 we considered the formation control problem for a general multi-agent system and in particular for mobile robots. One issue that we did not directly address is the collision avoidance problem. Therefore, during steady state the system may perform well. However, we cannot guarantee that collisions will not occur during the transient. Therefore, the stabilizing controller may need to be augmented or redesigned in order to address this issue. One possible approach could be to approach the problem using artificial social potential fields (with possible unbounded repulsion). Another issue is that in the developments in Chapter 7 we had the implicit assumption that all of the agents (robots) know their coordinates with respect to a global coordinate system. In some engineering applications this may not be the case. Instead, there may only be a leader which knows its global coordinates and the rest of the agents may only know their position relative to the preceding neighbors. Can we develop a decentralized nonlinear output regulation based controller for the system of this form? Developing of such a controller would constitute an important contribution to the formation control literature.

Swarming of honey bees is a spectacular phenomena that occurs when the hive gets crowded and the queen leaves the hive together with few thousand worker bees and few drones. So far there has not been a mathematical model generated for this behavior. In Chapter 5 we tried to create a simple model, which can be viewed as a preliminary work in this area. It may serve as a starting point for development of general, complex, and realistic model for honey bee swarming behavior. We believe that this not only will help better understand the behavior of the honey bees but also will trigger more experimental results in the area and can eventually lead to development of swarm prevention techniques, therefore having important impact on the honey bee agriculture.

Finally, we as engineers usually would like to implement the techniques that we develop. Sometimes implementation of seemingly easy methods is not that straightforward, because of neglected dynamics or some other implementation issues. Therefore, in order to verify the operation of the developed theory, there is a need for comprehensive experimental (implementation) studies. Such studies may also provide us with more insights for a better understanding the behavior of real biological swarms.

APPENDIX A

DECENTRALIZED REGULATION OF A CLASS OF NONLINEAR SYSTEMS

In this appendix we investigate the decentralized output regulation problem of a class of nonlinear systems. We show that the results of decentralized output regulation of linear systems can easily be adapted to nonlinear systems within the Isidori-Byrnes framework. The resulting decentralized controller consists of local controllers, each of which is a parallel connection of a stabilizer and a (partial) internal model. In the next section we start by providing some background on the literature on nonlinear output regulation.

A.1 Introduction

The output regulation problem, or the so called servomechanism problem, has been studied extensively in the past few decades. For the class of linear systems, the problem was studied and solved in the 70's. See for example [26, 24, 34, 33]. The output regulation of nonlinear systems was first pursued by Huang and Rugh [51] for systems with constant exogenous signals and by Isidori and Byrnes [55] for more general class of exosystems (see also [54]). In [53] the servomechanism problem for systems with slowly varying but not necessarily bounded exogenous signals was

addressed, and a solution method based on the series expansion of the system functions and the solution of the regulator equations was presented. It was also shown that the solution of the problem depends also on the higher order harmonics of the system. Later in [52] the results were extended to present an approximate method for calculating the solution of the regulator equations and was shown that under the developed strategy a "guaranteed" bounded tracking is achieved where the bound on the tracking error depends on the quality of the approximation. Similarly, in [16, 112] neural networks were used to approximate the solutions of the regulator equations. Recent research in this area has been focusing on robust regional, semiglobal, or global regulation of nonlinear systems. See for example [60, 98, 96, 97, 99]. In [97, 99] the authors use adaptive internal model for semiglobal output regulation in presence of unknown (but parametrized) linear exosystem. This result is important since it puts the output regulation problem in the framework of adaptive control.

The decentralized servomechanism problem for linear systems was considered by Davison in [25], where he provides necessary and sufficient conditions for the solvability of the problem. Here we extend his results for the regulation of nonlinear systems in the framework of [55] (see also [54]).

A.2 The Decentralized Regulation Problem

In this section we consider the problem of finding a decentralized controller for the output regulation of a class of nonlinear systems described by

$$\begin{aligned} \dot{x} &= \sum_{i=1}^{\nu} f_i(x, w, u_i), \\ e_i &= h_i(x, w), 1 \leq i \leq \nu, \end{aligned} \tag{A.1}$$

where $x \in \mathbb{R}^n$ is the state, $u_i \in \mathbb{R}^{m_i}$ and $e_i \in \mathbb{R}^{m_i}, 1 \leq i \leq \nu$, $(m = \sum_{i=1}^{\nu} m_i)$ are the control inputs and outputs at each local station, respectively. The functions f_i and $h_i, i = 1, \ldots, \nu$, are known and smooth, and $m_i, i = 1, \ldots, \nu$, and ν are known. (We consider a square system for ease of analysis; however, note that it is not essential for the results to hold.) The signal $w \in \mathbb{R}^r$ represents the exogenous inputs, that are the reference inputs, that need to be tracked, and the disturbances, that need to be rejected. It is assumed that all the exogenous signals are generated by a neutrally stable exosystem

$$\dot{w} = s(w), \tag{A.2}$$

where s is known and smooth.

The problem is to regulate each of the outputs $e_i, i = 1 \ldots \nu$, to zero using only local (decentralized) controls $u_i, i = 1 \ldots \nu$, that use only the (local) information from the corresponding output e_i. We define the problem as follows.

Decentralized Output Regulation Problem (DORP): Given a nonlinear system of the form of Eq. (A.1) and a neutrally stable exosystem in the form of Eq. (A.2), find, if possible ν integers $p_1, p_2 \ldots, p_\nu$, and mappings $\eta_i(\xi_i, e_i)$ and $\theta_i(\xi_i), 1 \leq i \leq \nu$, where $\xi_i \in \mathbb{R}^{p_i}$, such that the following conditions are satisfied:

(S) The equilibrium $(x, \xi_1, \ldots, \xi_\nu) = (0, 0, \ldots, 0)$ of

$$\begin{aligned} \dot{x} &= \sum_{i=1}^{\nu} f_i(x, 0, \theta_i(\xi_i)), \\ \dot{\xi}_i &= \eta_i(\xi_i, h_i(x, 0)), 1 \leq i \leq \nu, \end{aligned} \tag{A.3}$$

is locally exponentially stable.

(R) There exists a neighborhood V of the origin of $X \times \Omega \times W$, where $\Omega = \Omega_1 \times \ldots \times \Omega_\nu$,

with $\Omega_i \subset \mathbb{R}^{p_i}$, such that, for each initial condition $(x(0), \xi(0), w(0)) \in V$ (where $\xi(0) = [\xi_1^\top(0), \ldots, \xi_\nu^\top(0)]^\top$), the solution of the system

$$\begin{aligned} \dot{x} &= \sum_{i=1}^{\nu} f_i(x, w, \theta_i(\xi_i)), \\ \dot{\xi}_i &= \eta_i(\xi_i, h_i(x, w)), 1 \leq i \leq \nu, \\ \dot{w} &= s(w) \end{aligned} \tag{A.4}$$

satisfies the condition

$$\lim_{t \to \infty} h_i(x(t), w(t)) = 0, 1 \leq i \leq \nu. \tag{A.5}$$

Before proceeding we will make the following definitions. Let $A_i = \frac{\partial f_i}{\partial x}(0,0,0)$, $B_i = \frac{\partial f_i}{\partial u_i}(0,0,0)$, $C_i = \frac{\partial h_i}{\partial x}(0,0)$, $S = \frac{\partial s}{\partial w}(0)$, $F_i = \frac{\partial \eta_i}{\partial \xi_i}(0,0)$, $G_i = \frac{\partial \eta_i}{\partial e_i}, (0,0)$, and $H_i = \frac{\partial \theta_i}{\partial \xi_i}(0)$. Then, using these define $A = \sum_{i=1}^{\nu} A_i$, $B = [B_1, \ldots, B_\nu]$, $C = [C_1^\top, \ldots, C_\nu^\top]^\top$, $F = bd[F_1, \ldots, F_\nu]$, $G = bd[G_1, \ldots, G_\nu]$, and $H = bd[H_1, \ldots, H_\nu]$, where *bd* stands for *block diagonal*. Now, we have the following result, which is a decentralized version of those in [55].

Lemma 12 *Assume that for some $\eta_i(\xi_i, e_i)$ and $\theta_i(\xi_i), 1 \leq i \leq \nu$, the condition* **(S)** *is satisfied. Then, the condition* **(R)** *is also satisfied if, and only if, there exist mappings $x = \pi(w)$ and $\xi_i = \sigma_i(w), 1 \leq i \leq \nu$, with $\pi(0) = 0$ and $\sigma_i(0) = 0, 1 \leq i \leq \nu$, defined in a neighborhood W^o of the origin of $\mathbb{R}^r$ satisfying the conditions*

$$\begin{aligned} \frac{\partial \pi}{\partial w} s(w) &= \sum_{i=1}^{\nu} f_i(\pi(w), w, \theta_i(\sigma_i(w))), \\ \frac{\partial \sigma_i}{\partial w} s(w) &= \eta_i(\sigma_i(w), 0), 1 \leq i \leq \nu, \\ 0 &= h_i(\pi(w), w), 1 \leq i \leq \nu, \end{aligned} \tag{A.6}$$

for all $w \in W^o$.

Proof: Necessity: Since the systems satisfies condition **(S)** with the above controller we have that the eigenvalues of the matrix (that is the linearization of the closed loop system around the origin)

$$\begin{bmatrix} A & BH \\ GC & F \end{bmatrix}$$

are located on the open left half complex plane, whereas, the eigenvalues of S (the linearization of the exosystem) are all on the imaginary axis (because of its neutral stability). From the center manifold theory [13] we know that there exists a center manifold $x = \pi(w)$ and $\xi_i = \sigma_i(w), 1 \leq i \leq \nu$, such that the following equations are satisfied

$$\begin{aligned} \frac{\partial \pi}{\partial w} s(w) &= \sum_{i=1}^{\nu} f_i(\pi(w), w, \theta_i(\sigma_i(w))), \\ \frac{\partial \sigma_i}{\partial w} s(w) &= \eta_i(\sigma_i(w), h_i(\pi(w), w)), 1 \leq i \leq \nu. \end{aligned} \tag{A.7}$$

Now, assume that the condition **(R)** is satisfied but the last equalities in Eq. (A.6) do not hold. Then, there is an output i, $1 \leq i \leq \nu$, such that for some w^o and $\pi(w^o)$ we have

$$\|h_i(\pi(w^o), w^o))\| = M_i > 0$$

and there exists a neighborhood U of $(\pi(w^o), w^o)$ such that

$$\|h_i(\pi(w), w))\| > M_i/2$$

for all $(\pi(w), w) \in U$. On the other hand, since condition **(R)** holds there exists a time $T > 0$ such that for all $t > T$

$$\|h_i(\pi(w(t)), w(t)))\| < M_i/2.$$

However, since the exosystem is neutrally stable, always there is some time $t_1 > T$ such that $(\pi(w(t_1)), w(t_1)) \in U$ which leads to a contradiction. Therefore, the last

equalities in Eq. (A.6) hold. Substituting their values in the other two equations implies that all the equalities in Eq. (A.6) hold.

Sufficiency: Assume that Eq. (A.6) are satisfied. Then, by construction $x = \pi(w)$ and $\xi_i = \sigma_i(w), 1 \leq i \leq \nu$, constitute a center manifold for the system. From the properties of the center manifolds we know that for some $M > 0$ and $a > 0$ we have

$$\|\bar{x}(t) - \bar{\pi}(w(t))\| \leq Me^{-at}\|\bar{x}(0) - \bar{\pi}(w(0))\|, \forall t \geq 0,$$

where $\bar{x} = [x, \xi_1, \ldots, \xi_\nu]^\top$ and $\bar{\pi} = [\pi, \sigma_1, \ldots, \sigma_\nu]^\top$. Define $\tilde{x} = x(t) - \pi(w(t))$. Then, we have

$$\lim_{t\to\infty} e_i(t) = \lim_{t\to\infty} h_i(\pi(w(t)) + \tilde{x}(t), w(t)) = h_i(\pi(w(t)), w(t)) = 0,$$

for all $1 \leq i \leq \nu$. Therefore, the condition **(R)** is satisfied. ∎

Before proceeding further, we have to introduce the notion of *fixed modes* [25, 113].

Definition 2 *Consider a linear time invariant system described by the triple* $(C, A, B) \in \mathbb{R}^{m\times n} \times \mathbb{R}^{n\times n} \times \mathbb{R}^{n\times m}$. *Let* $\mathbf{K}$ *be a set of matrices in* $\mathbb{R}^{m\times m}$. *Then, the set of fixed modes of* (C, A, B) *with respect to* $\mathbf{K}$ *is defined as follows:*

$$\Lambda(C, A, B, \mathbf{K}) = \bigcap_{K\in\mathbf{K}} \lambda(A + BKC),$$

where $\lambda(A + BKC)$ *is the set of eigenvalues of* $(A + BKC)$.

In other words, the set of fixed modes with respect to a given set of matrices are the set of eigenvalues that cannot be changed by an output feedback with a gain matrix within this set. Note that $\Lambda(C, A, B, \mathbb{R}^{m\times m})$ is the set of the modes of A that are either uncontrollable or unobservable. We will consider only the set of block diagonal gain matrices

$$\mathbf{K_{bd}} = \{K : K = bd[K_1, \ldots, K_\nu], K_i \in \mathbb{R}^{m_i\times m_i}, i = 1, \ldots, \nu\}.$$

Below, we will use the notation $\{\Omega^o, \varphi, \gamma\}$ to denote a system

$$\begin{aligned} \dot{\xi} &= \varphi(\xi), \\ u &= \gamma(\xi), \end{aligned}$$

defined for $\xi \in \Omega^o$. Now, we have the following result.

Theorem 9 *The DORP is solvable if, and only if, there exist mappings $x = \pi(w)$ and $u_i = c_i(w), 1 \leq i \leq \nu$, with $\pi(0) = 0$ and $c_i(0) = 0, 1 \leq i \leq \nu$, all defined in a neighborhood W^o of the origin of $\mathbb{R}^r$ and satisfying the conditions*

$$\begin{aligned} \frac{\partial \pi}{\partial w} s(w) &= \sum_{i=1}^{\nu} f_i(\pi(w), w, c_i(w)), \\ 0 &= h_i(\pi(w), w), 1 \leq i \leq \nu, \end{aligned} \tag{A.8}$$

for all $w \in W^o$, and such that the autonomous systems with outputs $\{W^o, s, c_i\}, 1 \leq i \leq \nu$, are immersed into

$$\begin{aligned} \dot{\xi}_i &= \varphi_i(\xi_i), \\ u_i &= \gamma_i(\xi_i), 1 \leq i \leq \nu, \end{aligned} \tag{A.9}$$

defined on neighborhoods $\Omega_i, 1 \leq i \leq \nu$, of the origins of $\mathbb{R}^{p_i}$, respectively, in which $\varphi_i(0) = 0$ and $\gamma_i(0) = 0, 1 \leq i \leq \nu$, and the matrices

$$\Phi_i = \left[\frac{\partial \varphi_i}{\partial \xi_i}\right]_{\xi_i = 0} \quad \textit{and} \quad \Gamma_i = \left[\frac{\partial \gamma_i}{\partial \xi_i}\right]_{\xi_i = 0}$$

for $1 \leq i \leq \nu$ are such that all the fixed modes with respect to $\mathbf{K_{bd}}$ of the triple

$$\left[\begin{array}{cc} C & 0 \end{array}\right], \quad \left[\begin{array}{cc} A & B\Gamma \\ NC & \Phi \end{array}\right], \quad \left[\begin{array}{c} B \\ 0 \end{array}\right], \tag{A.10}$$

where $\Phi = bd[\Phi_1, \ldots, \Phi_\nu]$ and $\Gamma = bd[\Gamma_1, \ldots, \Gamma_\nu]$, have negative real parts, for some choice of $N = bd[N_1, \ldots, N_\nu]$.

Proof: Necessity: Suppose that the local controllers

$$u_i \;=\; \theta_i(\xi_i), \;\; \dot{\xi}_i \;=\; \eta_i(\xi_i, e_i), \;\; 1 \leq i \leq \nu, \tag{A.11}$$

solve the decentralized regulation problem. Then, by Lemma 12 there exist mappings $x = \pi(w)$ and $\xi_i = \sigma_i(w), 1 \leq i \leq \nu$, with $\pi(0) = 0$ and $\sigma_i(0) = 0, 1 \leq i \leq \nu$, such that Eq. (A.6) are satisfied. Set $c_i(w) = \theta_i(\sigma_i(w))$, $\gamma_i(\xi_i) = \theta_i(\xi_i)$, $\varphi_i(\xi_i) = \eta(\xi_i, 0)$, $1 \leq i \leq \nu$. Now, note that these satisfy Eq. (A.8). Moreover, we have $\frac{\partial \sigma_i}{\partial w} s(w) = \varphi_i(\sigma_i(w))$ and $c_i(w) = \gamma_i(\sigma_i(w))$, $1 \leq i \leq \nu$, implying that $\{W^o, s, c_i\}$ are immersed into $\{\Omega_i^o, \varphi_i, \gamma_i\}$, for all $1 \leq i \leq \nu$. Moreover, since the given local controllers solve the regulation problem, the eigenvalues of the matrix

$$\begin{bmatrix} A & B\Gamma \\ GC & \Phi \end{bmatrix}$$

are all located in the open left half plane. This, on the other hand, implies that all the fixed modes of the triple in (A.10) have negative real parts for $N = G$, i.e., $N_i = G_i, 1 \leq i \leq \nu$.

Sufficiency: Choose $N_i, 1 \leq i \leq \nu$, such that the triple in (A.10) has all of its fixed modes with negative real parts. Then from Theorem 1 in [113] we know that the decentralized stabilization problem of the system described by the above triple is solvable using dynamic output feedback. In other words, there exist integers $q_1, \ldots, q_\nu$, all greater than or equal to zero, and a real constant matrices of the form $M = bd[M_1, \ldots, M_\nu], L = bd[L_1, \ldots, L_\nu]$, and $\Psi = bd[\Psi_1, \ldots, \Psi_\nu]$, where $L_i \in \mathbb{R}^{q_i \times m_i}, M_i \in \mathbb{R}^{m_i \times q_i}$, and $\Psi_i \in \mathbb{R}^{q_i \times q_i}$, such that the roots of the polynomial $\det(\lambda I - A_e - B_e K_e C_e)$ have negative real parts. Above the matrices K_e, A_e, B_e, and C_e are

$$\begin{bmatrix} 0 & M \\ L & \Psi \end{bmatrix} \;\; \begin{bmatrix} \bar{A} & 0 \\ 0 & 0 \end{bmatrix} \;\; \begin{bmatrix} \bar{B} & 0 \\ 0 & I \end{bmatrix} \;\; \begin{bmatrix} \bar{C} & 0 \\ 0 & I \end{bmatrix},$$

respectively, and $\bar{C}, \bar{A}$, and $\bar{B}$ represent the matrices in (A.10).

Then choose each of the stabilizing local compensators as

$$\dot{\chi}_i = \Psi_i \chi_i + L_i e_i, 1 \leq i \leq \nu, \tag{A.12}$$

and the overall control input as

$$u_i = \gamma_i(\xi_i) + M_i \chi_i, \tag{A.13}$$

which render the matrix $(A_e + B_e K_e C_e) =$

$$\begin{bmatrix} A & B_1\Gamma_1 & B_2\Gamma_2 & \dots & B_\nu\Gamma_\nu & B_1M_1 & \dots & B_\nu M_\nu \\ N_1C_1 & \Phi_1 & 0 & \dots & 0 & 0 & \dots & 0 \\ N_2C_2 & 0 & \Phi_2 & \ddots & \vdots & \vdots & & \vdots \\ \vdots & \vdots & \ddots & \ddots & 0 & \vdots & & \vdots \\ N_\nu C_\nu & 0 & \dots & 0 & \Phi_\nu & 0 & & \vdots \\ L_1C_1 & 0 & \dots & \dots & 0 & \Psi_1 & \ddots & \vdots \\ \vdots & \vdots & & & & \ddots & \ddots & 0 \\ L_\nu C_\nu & 0 & \dots & \dots & \dots & \dots & 0 & \Psi\nu \end{bmatrix}$$

Hurwitz. In other words, the system is rendered exponentially stable in the first approximation. Moreover, by hypothesis there exist mappings $x = \pi(w)$ and $\xi_i = \sigma_i(w), 1 \leq i \leq \nu$, with $\pi(0) = 0$, $\sigma_i(0) = 0, 1 \leq i \leq \nu$, and $\xi_i = \tau_i(w)$ such that Eq. (A.8) hold together with (because of the immersion) $\frac{\partial \tau_i}{\partial w} s(w) = \varphi_i(\tau_i(w))$ and $c_i(w) = \gamma_i(\tau_i(w))$, $1 \leq i \leq \nu$. Then Eq. (A.8) together with $\xi_i = \tau_i(w), \chi_i = 0$, $1 \leq i \leq \nu$, satisfy Eq. (A.6). This, on the other hand, implies that the sufficient conditions of Lemma 12 are satisfied (i.e., we have local controller that satisfies conditions **(S)** and Eq. (A.6) are satisfied), and therefore, regulation is achieved. ∎

From this formulation, we have that each of our local controllers have the following form

$$\dot{\xi}_i \;\; = \;\; \varphi_i(\xi_i) + N_i e_i,$$

$$\begin{aligned} \dot{\chi}_i &= \Psi_i \chi_i + L_i e_i, \\ u_i &= \gamma_i(\xi_i) + M_i \chi_i, 1 \leq i \leq \nu. \end{aligned} \tag{A.14}$$

In other words, each of the local controllers consists of a parallel connection of a dynamic compensator and a servocompensator.

Note that with appropriate definitions, this system can be converted to the general form discussed in [54]. In other words, define $u = [u_1, \ldots, u_\nu]^\top$, $e = [e_1, \ldots, e_\nu]^\top$, $\xi = [\xi_1, \ldots, \xi_\nu]^\top$, $\chi = [\chi_1, \ldots, \chi_\nu]^\top$, $c(w) = [c_1(w), \ldots, c_\nu(w)]^\top$, $\gamma(\xi) = [\gamma_1(\xi_1), \ldots, \gamma_\nu(\xi_\nu)]^\top$, $\varphi(\xi) = [\varphi_1(\xi_1), \ldots, \varphi_\nu(\xi_\nu)]^\top$. Then, the controller in compact form becomes

$$\begin{aligned} \dot{\xi} &= \varphi(\xi) + Ne, \\ \dot{\chi} &= \Psi\chi + Le, \\ u &= \gamma(\xi) + M\chi, \end{aligned} \tag{A.15}$$

which is exactly the form of the centralized controller discussed in [54]. Note that the overall controller consists of a decentralized stabilizer and a decentralized internal model or servocompensator. The job of the servocompensator is to generate the control input that will render the zero error manifold invariant. On the other hand, the dynamic compensator acts as stabilizer that yields this manifold locally attractive.

The analysis here can be viewed, in a sense, as a special case of the more general framework developed in [54], with the restriction that the controller matrices have the block diagonal form as above. Natural consequence of this requirement is the extra condition that the three matrices in (A.10) do not have unstable fixed modes with respect to $\mathbf{K_{bd}}$. On the other hand, it is possible to present the results here in a more general framework so that the results in [54] are viewed as a special case of

the ones here. To see this, note that the conditions on controllability of

$$\left[\begin{array}{cc} A & 0 \\ NC & \Phi \end{array}\right], \quad \left[\begin{array}{c} B \\ 0 \end{array}\right],$$

and detectability of

$$\left[\begin{array}{cc} C & 0 \end{array}\right], \quad \left[\begin{array}{cc} A & B\Gamma \\ 0 & \Phi \end{array}\right],$$

are equivalent to that the triple

$$\left[\begin{array}{cc} C & 0 \end{array}\right], \quad \left[\begin{array}{cc} A & B\Gamma \\ NC & \Phi \end{array}\right], \quad \left[\begin{array}{c} B \\ 0 \end{array}\right],$$

has no unstable fixed modes with respect to the set of $m \times m$ real matrices $\mathbf{K}$. In other words, the results here can be stated with respect to any general set of given matrices (of appropriate dimensions), say $\bar{\mathbf{K}}$, that will include as special case the analysis in [54] when $\bar{\mathbf{K}} = \mathbf{K}$ and the decentralized control mechanism presented here when $\bar{\mathbf{K}} = \mathbf{K_{bd}}$.

Since the above result is stated in terms of the fixed modes of the cascade connection of the plant and the servocompensator, one issue to be addressed here is the characterization of the fixed modes. In other words, how do we determine the existence of fixed modes. A nice and simple characterization of the fixed modes of decentralized systems was provided in [2]. Consider the linear decentralized system

$$\begin{aligned} \dot{x} &= \bar{A}x + \sum_{i=1}^{\nu} \bar{B}_i u_i, \\ y_i &= \bar{C}_i x, 1 \leq i \leq \nu. \end{aligned} \tag{A.16}$$

Then, for any index set $\mathcal{I} = \{i_1, \ldots, i_j\} \subset \{1, 2, \ldots, \nu\}$ and its complement $\mathcal{I}^c = \{i_k, \ldots, i_l\}$ (i.e., $\mathcal{I} \cup \mathcal{I}^c = \{1, 2, \ldots, \nu\}$ and $\mathcal{I} \cap \mathcal{I}^c = \emptyset$) denote by $\tilde{B}_{\mathcal{I}} = [\bar{B}_{i_1}, \ldots, \bar{B}_{i_j}]$ and $\tilde{C}_{\mathcal{I}^c} = [\bar{C}_{i_k}^\top, \ldots, \bar{C}_{i_l}^\top]^\top$. Then, a complex number $\lambda \in \mathbb{C}$ is a decentralized fixed

mode of $(\bar{C}, \bar{A}, \bar{B})$ if, and only if,

$$\det \begin{bmatrix} \bar{A} - \lambda I & \tilde{B}_{\mathcal{I}} \\ \tilde{C}_{\mathcal{I}^c} & 0 \end{bmatrix} = 0$$

for some $\mathcal{I} \subset \{1, 2, \ldots, \nu\}$.

Note that the above equation does not hold for λ that are not eigenvalues of $\bar{A}$. Therefore, one needs to check it for only those λ that are eigenvalues of $\bar{A}$. In the view of this, for our system for each N one can find the eigenvalues of

$$\bar{A} = \begin{bmatrix} A & B\Gamma \\ NC & \Phi \end{bmatrix}$$

and then check for the existence of fixed modes. Still, however, this condition is in terms of the cascade connection of the plant and the servocompensator (as in the above theorem). It is possible to show that sufficient condition for the triple in (A.10) not to have unstable fixed modes with respect to the set of block diagonal matrices $\mathbf{K_{bd}}$ is that

1. the triple (C, A, B) does not have any unstable fixed modes with respect $\mathbf{K_{bd}}$ and
2. $\det \begin{bmatrix} A - \lambda I & B \\ C & 0 \end{bmatrix} \neq 0$ for all λ that are unstable eigenvalues of Φ.

In the next section, we consider the class of interconnected systems that can be considered as a special case of the general class discussed so far.

A.3 Regulation of a Class of Interconnected Systems

In this section, we consider the output regulation problem of the class of interconnected systems described by

$$\begin{aligned} \dot{x}_i &= f_i(x_1, \ldots, x_\nu, w_i, u_i), \\ e_i &= h_i(x_i, w_i), 1 \leq i \leq \nu, \end{aligned} \tag{A.17}$$

where $x_i \in \mathbb{R}^{n_i}$ $(n = \sum_{i=1}^{\nu} n_i)$ represent the local state of each subsystem, $u_i \in \mathbb{R}^{m_i}$ and $e_i \in \mathbb{R}^{m_i}, 1 \leq i \leq \nu$, $(m = \sum_{i=1}^{\nu} m_i)$ are the local control inputs and outputs, respectively. The signal $w_i \in \mathbb{R}^{r_i}$ $(r = \sum_{i=1}^{\nu} r_i)$ are the local exogenous inputs to each subsystem and are generated by neutrally stable exosystems

$$\dot{w}_i = s_i(w_i), 1 \leq i \leq \nu. \tag{A.18}$$

We assume that all the above functions f_i, h_i, and s_i are known and smooth. As before, the objective is to design a regulator that uses only local controls that will provide asymptotic regulation of the output of each of the subsystems to zero.

From the earlier analysis we know that a necessary condition for the existence of a solution of this problem is the existence of mappings $x_i = \pi_i(w_i)$ and $u_i = c_i(w_i), 1 \leq i \leq \nu$, with $\pi_i(0) = 0$ and $c_i(0) = 0, 1 \leq i \leq \nu$, defined in a neighborhood W_i^o of the origin of $\mathbb{R}^{r_i}$, respectively, such that

$$\begin{aligned} \frac{\partial \pi_i}{\partial w_i} s_i(w_i) &= f_i(\pi_1(w_1), \ldots, \pi_\nu(w_\nu), w_i, c_i(w_i)), \\ 0 &= h_i(\pi_i(w_i), w_i), 1 \leq i \leq \nu, \end{aligned} \tag{A.19}$$

for all $w_i \in W_i^o$, respectively.

Once again let $A_i = \frac{\partial f_i}{\partial x_i}(0, \ldots, 0, 0, 0)$, $E_{i,j} = \frac{\partial f_i}{\partial x_j}(0, \ldots, 0, 0, 0)$, $B_i = \frac{\partial f_i}{\partial u_i}, (0, \ldots, 0, 0, 0)$, and $C_i = \frac{\partial h_i}{\partial x}(0, 0)$. Then, define

$$A = \begin{bmatrix} A_1 & E_{1,2} & \ldots & E_{1,\nu} \\ E_{2,1} & \ddots & \ddots & \vdots \\ \vdots & \ddots & \ddots & E_{\nu-1,\nu} \\ E_{\nu,1} & \ldots & E_{\nu,\nu-1} & A_\nu \end{bmatrix} \begin{array}{l} B = bd[B_1, \ldots, B_\nu], \\ \mathcal{C} = bd[C_1, \ldots, C_\nu]. \end{array} \tag{A.20}$$

Then, the linearization of the system in (A.17) around the origin can be represented as

$$\dot{x}_i = A_i x_i + \sum_{j=1, j \neq i}^{\nu} E_{i,j} x_j + B_i u_i$$

$$y_i \;=\; C_i x_i, 1 \leq i \leq \nu, \tag{A.21}$$

where we assumed $w = 0$ and ignored the higher order terms.

One can easily see that it is possible to establish a counterpart of Lemma 12 also for this case. Therefore, we will not present such a result here. However, to establish the main result of this section we will need the following lemma that is taken from [25].

Lemma 13 *Consider the interconnected composite system in (A.21) and assume that each of the subsystems $(C_i, A_i, B_i), i = 1, \ldots, \nu$, are all stabilizable and detectable. Then, there exists a scalar $E > 0$, such that for the class of nonzero interconnection gains $E_{i,j}$ satisfying $\|E_{i,j}\| < E, i = 1, \ldots, \nu, j = 1, \ldots, \nu, i \neq j$, the system is stabilizable via decentralized control.*

The rationale behind the proof of this lemma is as follows. Assume that $E_{i,j} = 0$ for all $1 \leq i \leq \nu, 1 \leq j \leq \nu, i \neq j$, then since each of the subsystems is stabilizable and detectable and the system is decoupled, we can find an appropriate local output feedback such that all the eigenvalues of the closed loop system would have negative real parts. Therefore, if the interconnections are sufficiently weak, then the stability properties of the closed loop system matrix are preserved.

Let $\bar{E} = \sup\{E\}$, where E is as defined in the above lemma. Now, we state the main result of this section.

Theorem 10 *The DORP for the interconnected system in (A.17) is solvable if*

1. *There exist mappings $x_i = \pi_i(w_i)$ and $u_i = c_i(w_i), 1 \leq i \leq \nu$, with $\pi_i(0) = 0$ and $c_i(0) = 0, 1 \leq i \leq \nu$, defined in a neighborhood W_i^o of the origin of $\mathbb{R}^{r_i}$, respectively, such that Eq. (A.19) are satisfied for all $w_i \in W_i^o$, respectively.*

2. *The autonomous systems with outputs* $\{W_i^o, s_i, c_i\}, 1 \leq i \leq \nu$, *are immersed into*

$$\begin{aligned} \dot{\xi}_i &= \varphi(\xi_i), \\ u_i &= \gamma_i(\xi_i), 1 \leq i \leq \nu, \end{aligned} \tag{A.22}$$

defined on neighborhoods $\Omega_i, 1 \leq i \leq \nu$, *of the origins of* $\mathbb{R}^{p_i}$, *respectively, in which* $\varphi_i(0) = 0$ *and* $\gamma_i(0) = 0, 1 \leq i \leq \nu$.

3. *The matrices*

$$\Phi_i = \left[\frac{\partial \varphi_i}{\partial \xi_i}\right]_{\xi_i=0} \quad \textit{and} \quad \Gamma_i = \left[\frac{\partial \gamma_i}{\partial \xi_i}\right]_{\xi_i=0}$$

for $1 \leq i \leq \nu$ *are such that each of the pairs*

$$\left[\begin{array}{cc} A_i & 0 \\ N_i C_i & \Phi_i \end{array} \right], \quad \left[\begin{array}{c} B_i \\ 0 \end{array} \right], \quad 1 \leq i \leq \nu, \tag{A.23}$$

is stabilizable for some $N_i, 1 \leq i \leq \nu$, *and each of the pairs*

$$\left[\begin{array}{cc} C_i & 0 \end{array} \right], \quad \left[\begin{array}{cc} A_i & B_i\Gamma_i \\ 0 & \Phi_i \end{array} \right], \quad 1 \leq i \leq \nu, \tag{A.24}$$

is detectable.

4. *The interconnections satisfy* $\|E_{i,j}\| \leq \bar{E}$.

Proof: We will show that the conditions above satisfy the sufficient conditions of Lemma 12. To this end, choose the matrices $N_i, 1 \leq i \leq \nu$, such that the pairs in (A.23) are stabilizable. Now, note that each of the triples

$$\left[\begin{array}{cc} C_i & 0 \end{array} \right], \quad \left[\begin{array}{cc} A_i & B_i\Gamma_i \\ N_i C_i & \Phi_i \end{array} \right], \quad \left[\begin{array}{c} B_i \\ 0 \end{array} \right],$$

is stabilizable and detectable. Therefore, there exist matrices Ψ_i, L_i, and $M_i, i \leq i \leq \nu$, such that the matrices

$$\bar{A}_i = \begin{bmatrix} \begin{bmatrix} A_i & B_i\Gamma_i \\ N_iC_i & \Phi_i \end{bmatrix} & \begin{bmatrix} B_i \\ 0 \end{bmatrix} M_i \\ L_i \begin{bmatrix} C_i & 0 \end{bmatrix} & \Psi_i \end{bmatrix}$$

have their eigenvalues in the open left half plane. Define

$$\bar{E}_{i,j} = \begin{bmatrix} E_{i,j} & 0 & 0 \\ 0 & 0 & 0 \\ 0 & 0 & 0 \end{bmatrix}.$$

Then, the linearization of the closed loop system equations become

$$\begin{bmatrix} \bar{A}_1 & \bar{E}_{1,2} & \dots & \bar{E}_{1,\nu} \\ \bar{E}_{2,1} & \ddots & \ddots & \vdots \\ \vdots & \ddots & \ddots & \bar{E}_{\nu-1,\nu} \\ \bar{E}_{\nu,1} & \dots & \bar{E}_{\nu,\nu-1} & \bar{A}_\nu \end{bmatrix}.$$

Since the interconnections satisfy $\|E_{i,j}\| \leq \bar{E}$, from Lemma 13 we know that there exists a decentralized controller that stabilizes the system. In other words, above we can choose the matrices L_i, M_i, and Ψ_i such that the closed loop system is stable. This proves that the condition **(S)** is satisfied. This together with the other hypotheses of the theorem satisfy the sufficiency conditions of Lemma 12 (or an equivalent modified version of Lemma 12 for interconnected systems), and this completes the proof. ∎

A sufficient condition of the pairs in (A.23) and (A.24) to be stabilizable and detectable, respectively, is that no unstable transmission zero of (C_i, A_i, B_i) is a pole of Φ_i, or in other words,

$$\operatorname{rank} \begin{bmatrix} A_i - \lambda I & B_i \\ C_i & 0 \end{bmatrix} = n_i + m_i$$

for all unstable eigenvalues λ of Φ_i.

A.4 Extensions

A.4.1 Decentralized Structurally Stable Regulation

It is not difficult to see that the analysis presented so far can easily be extended to the problem of robust regulation of systems with unknown parameters, i.e., structurally stable regulation. In other words, consider the system

$$\begin{aligned} \dot{x} &= \sum_{i=1}^{\nu} f_i(x, w, u_i, \mu), \\ e_i &= h_i(x, w, \mu), 1 \leq i \leq \nu, \end{aligned} \tag{A.25}$$

where $\mu \in \mathbb{R}^s$ is a vector of unknown parameters. The analysis easily follows in the line presented so far after redefining the exogenous signal and the exosystem as $w_a = [w^\top, \mu^\top]^\top$ and

$$\dot{w^a} = s^a(w^a) = \begin{bmatrix} s(w) \\ 0 \end{bmatrix}.$$

Similarly, we can redefine the equations of the system as

$$\begin{aligned} \dot{x} &= \sum_{i=1}^{\nu} f_i^a(x, w^a, u_i), \\ e_i &= h_i^a(x, w^a), 1 \leq i \leq \nu, \end{aligned} \tag{A.26}$$

which is exactly in the form of Eq. (A.1). Therefore, all the earlier results follow with w replaced with w^a and the linearization of the system evaluated at the nominal value $\bar{\mu}$ of μ. Then, the results hold for any μ that is in a sufficiently small neighborhood of $\bar{\mu}$.

A.4.2 Discrete Time Systems

After the results in [55] on the nonlinear regulation problem for continuous time systems, several authors considered discrete time systems and obtained parallel results. See for example [14, 50, 15]. From these articles, one easily notices that the

discrete time results follow the continuous time ones with only minor differences. One difference that arises between the two cases is that the center manifold theory for maps is used in the discrete time case. Therefore, the regulator equations in (A.8) become

$$\begin{aligned} \pi(s(w)) &= \sum_{i=1}^{\nu} f_i(\pi(w), w, c_i(w)), \\ 0 &= h_i(\pi(w), w), 1 \leq i \leq \nu. \end{aligned} \tag{A.27}$$

In other words, the partial derivatives in the continuous time regulator equations are replaced with composition of functions in the discrete time ones. The rest of the analysis follows in the lines parallel to the continuous time case. Therefore, the development in the earlier sections can without any difficulty be extended to the discrete time systems.

A.5 Final Remarks

The problem of output regulation in presence of uncertainties and disturbances is an important problem in control theory. It has been extensively studied and solved for linear systems, and locally for nonlinear systems, and globally or semiglobally for some classes of nonlinear systems. Efforts to develop conditions for the solvability of the problem in a semiglobal or global sense as well as developing effective controllers for these still continue. In this appendix, we presented conditions for the solution of the local problem using decentralized controllers. Some of the ideas and results developed here were used for developing decentralized nonlinear servomechanism based controllers of r formation control of multi-agent systems in Chapter 7.

APPENDIX B

ROBOT DYNAMICS

In this appendix we consider the dynamics of a mobile robot and show that with appropriate change of coordinates they can be either partially or fully linearized. In particlar, we show the dynamics of a point which is on a distance d in front of the robot can be partially linearized with a static controller, whereas the dynamics of the actual pision of the robot can be fully linearized with a static controller. Then, we derive a model of the (local) relative dynamics of a robot following another robot.

B.1 The Robot Dynamic Model

Consider a mobile robot whose equations of motion are given by

$$\begin{aligned}
\dot{x} &= v\cos(\theta), \\
\dot{y} &= v\sin(\theta), \\
\dot{\theta} &= w \\
\dot{v} &= \frac{1}{m}F, \\
\dot{w} &= \frac{1}{J}\tau,
\end{aligned}$$

where x and y are the Cartesian coordinates with respect to some global coordante system, θ is the steering angle, v is the linear speed, and w is the angular speed of

the robot. The quantities m and J are positive constants and represent the mass and the moment of inertia of the robot, respectively. The control inputs to the system are the force input F and the torque input τ.

B.2 Partial Feedback Linearization

Consider a point z in front of the robot at a distance d from its center, whose coordinates are given by

$$z = \begin{bmatrix} x + d\cos(\theta) \\ y + d\sin(\theta) \end{bmatrix}.$$

Define z as the ouput of the system and note that with respect that output the system is input-output feedback linearizable with a constant relative degree. To see this differentiate the output z and obtain

$$\begin{aligned} \dot{z} &= \begin{bmatrix} v\cos(\theta) - dw\sin(\theta) \\ v\sin(\theta) + dw\cos(\theta) \end{bmatrix} \\ &= \begin{bmatrix} \cos(\theta) & -d\sin(\theta) \\ \sin(\theta) & d\cos(\theta) \end{bmatrix} \begin{bmatrix} v \\ w \end{bmatrix}. \end{aligned}$$

Similarly, the second derivative of the output is given by

$$\begin{aligned} \ddot{z} &= \begin{bmatrix} -vw\sin(\theta^i) - dw^2\cos(\theta) + \frac{1}{m}F\cos(\theta) - \frac{d}{J}\tau\sin(\theta) \\ vw\cos(\theta) - dw^2\sin(\theta) + \frac{1}{m}F\sin(\theta) + \frac{d}{J}\tau\cos(\theta) \end{bmatrix} \\ &= \begin{bmatrix} -vw\sin(\theta) - dw^2\cos(\theta) \\ vw\cos(\theta) - dw^2\sin(\theta) \end{bmatrix} + \begin{bmatrix} \frac{1}{m}\cos(\theta) & -\frac{d}{J}\sin(\theta) \\ \frac{1}{m}\sin(\theta) & \frac{d}{J}\cos(\theta) \end{bmatrix} \begin{bmatrix} F \\ \tau \end{bmatrix}. \end{aligned}$$

By choosing

$$\begin{bmatrix} F \\ \tau \end{bmatrix} = \begin{bmatrix} \frac{1}{m}\cos(\theta) & -\frac{d}{J}\sin(\theta) \\ \frac{1}{m}\sin(\theta) & \frac{d}{J}\cos(\theta) \end{bmatrix}^{-1} \left[u - \begin{bmatrix} -vw\sin(\theta) - dw^2\cos(\theta) \\ vw\cos(\theta) - dw^2\sin(\theta) \end{bmatrix} \right], \tag{B.1}$$

where $u = [u_1, u_2]^\top$, we obtain

$$\ddot{z} = u.$$

Note that the matrix

$$\begin{bmatrix} \frac{1}{m}\cos(\theta) & -\frac{d}{J}\sin(\theta) \\ \frac{1}{m}\sin(\theta) & \frac{d}{J}\cos(\theta) \end{bmatrix}$$

is always invertible, since its determinant is given by $\frac{d}{mJ}$ (implying that the linearizing controller always exists).

Let $\zeta = \dot{z}$ to obtain

$$\begin{aligned}
\dot{z} &= \zeta \\
\dot{\zeta} &= u \\
\dot{\theta} &= -\frac{1}{d}\zeta_1 \sin(\theta) + \frac{1}{d}\zeta_2 \cos(\theta),
\end{aligned}$$

where the last equation is obtained by inverting the $\dot{z}$ equation. The state θ represent the unobservable states (which is rendered unobservable because of our particular choice of control) that do not appear at the output. Note that the zero dynamics of the system are marginally stable since when $\zeta = 0$ we have $\dot{\theta} = 0$.

B.3 Full Linearization Using Dynamic Feedback

Consider dynamic equations of a mobile robot given in Eq. (B.1). The reason why it is not possible to fully linearize that system is that one of inputs (the force input) appears too early at the output. Therefore, by delaying that input it might be possibel to fully linearize that syste. To thi end, add an integrator at that input in order to delay it. Then, the motion equation of the robot becomes

$$\begin{aligned}
\dot{x} &= v \cos(\theta), \\
\dot{y} &= v \sin(\theta), \\
\dot{v} &= \frac{1}{m}\xi, \\
\dot{\xi} &= u_1, \\
\dot{\theta} &= w \\
\dot{w} &= \frac{1}{J}u_2,
\end{aligned}$$

where we denoted the (new) control inputs to the system with u_1 (the derivative of the force) and u_2 (the torque). (Note that these are not the same inputs considered in the previous section.) Now, define the position of the robot as the output (the point of interest) of the robot. In other words, let

$$z = \begin{bmatrix} x \\ y \end{bmatrix}.$$

Then, we have the first derivative

$$\dot{z} = \begin{bmatrix} v\cos(\theta) \\ v\sin(\theta) \end{bmatrix},$$

the second derivative

$$\ddot{z} = \begin{bmatrix} \frac{1}{m}\xi\cos(\theta) - vw\sin(\theta) \\ \frac{1}{m}\xi\sin(\theta) + vw\cos(\theta) \end{bmatrix},$$

and the third derivative

$$z^{(3)} = \begin{bmatrix} -\frac{2}{m}\xi w\sin(\theta) - v(w)^2\cos(\theta) \\ \frac{2}{m}\xi w\cos(\theta) - v(w)^2\sin(\theta) \end{bmatrix} + \begin{bmatrix} \frac{1}{m}\cos(\theta) & -\frac{v}{J}\sin(\theta) \\ \frac{1}{m}\sin(\theta) & \frac{v}{J}\cos(\theta) \end{bmatrix} \begin{bmatrix} u_1 \\ u_2 \end{bmatrix}.$$

Then, similar to above, with the choice of the linearizing control

$$\begin{bmatrix} u_1 \\ u_2 \end{bmatrix} = \begin{bmatrix} \frac{1}{m}\cos(\theta) & -\frac{v}{J}\sin(\theta) \\ \frac{1}{m}\sin(\theta) & \frac{v}{J}\cos(\theta) \end{bmatrix}^{-1} \left[\nu - \begin{bmatrix} -\frac{2}{m}\xi w\sin(\theta) - v(w)^2\cos(\theta) \\ \frac{2}{m}\xi w\cos(\theta) - v(w)^2\sin(\theta) \end{bmatrix}\right],$$

we obtain

$$z^{(3)} = \nu, \tag{B.2}$$

where $\nu = [\nu_1, \nu_2]^\top$.

Note that the determinant of the square matrix in front of the control vector is given by $\frac{v}{mJ}$, implying that it is invertible provided that $v \neq 0$, i.e., the velocity of the robot is nonzero. Therefore, provided that $v \neq 0$, we can use the above feedback linearizing controller to fully linearize the system dynamics. Note, however, that special care must be taken in order to guarantee that the velocity of the robot is always nonzero (especially during the transient).

B.4 Local Model for a Group of Robots

In this section we will derive local (relative) coordinates of a robot following another robot. Let l_{ij} denote the relative distance between robots (agents) i and j. Assume that agent i is leading and agent j is following. Assume that the angle between the direction of motion of agent i and the line connecting the positions of agent i and j is denoted by ψ_{ij}. (See Figure B.1.) From the figure one can see that

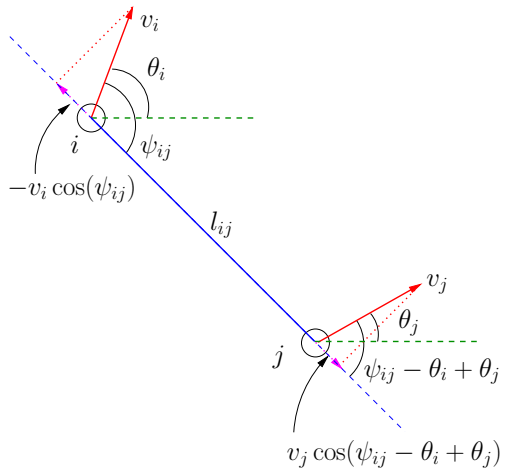

Figure B.1: The kinematics of the inter-agent distance.

the kinematics of the distance between the agents i and j can be written as

$$\dot{l}_{ij} = -v_i\cos(\psi_{ij}) + v_j\cos(\psi_{ij} - \theta_i + \theta_j). \tag{B.3}$$

In a similar manner to above we can write the kinematics of the relative angle ψ_{ij}. In particular, by noting that the change in the angle is affected only by the components of the agent velocities which are perpendicular to l_{ij} and using the fact that the arc

length in a circle is given by

$$arch\ length = angle \times radius$$

one can show that the kinematics of the angle ψ_{ij} are given by (see Figure B.2)

$$\dot{\psi}_{ij} = w_i + \frac{1}{l_{ij}} v_i \sin(\psi_{ij}) - \frac{1}{l_{ij}} v_j \sin(\psi_{ij} - \theta_i + \theta_j). \tag{B.4}$$

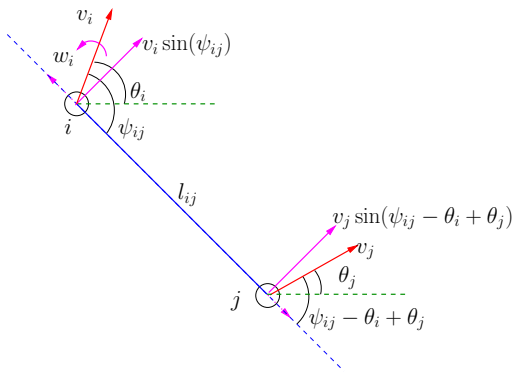

Figure B.2: The kinematics of the relative angle.

Note that given agent i the two variables l_{ij} and ψ_{ij} *uniquely determine* the exact position of agent j in two dimensional space. Similarly, given two agents i and j one can use the relative distances l_{ik} and l_{jk} to *uniquely determine* the position of a third agent k.

Using the above kinematic variables for the relative position and the orientation of the following robot j with respect to the leading robot i together with the dynamics of the robot we obtain

$$\dot{l}_{ij} \quad = \quad -v_i \cos(\psi_{ij}) + v_j \cos(\psi_{ij} - \theta_{ij})$$

$$
\begin{aligned}
\dot{\psi}_{ij} &= w_i + \frac{1}{l_{ij}} v_i \sin(\psi_{ij}) + \frac{1}{l_{ij}} v_j \sin(\psi_{ij} - \theta_{ij}) \\
\dot{v}_j &= \frac{1}{m_j} \xi_j, \\
\dot{\xi}_j &= u_1^j, \\
\dot{\theta}_{ij} &= w_i - w_j \\
\dot{w}_j &= \frac{1}{J_j} u_2^j.
\end{aligned} \tag{B.5}
$$

For this system, by defining the output of the system as

$$
z^j = \begin{bmatrix} l_{ij} \\ \psi_{ij} \end{bmatrix},
$$

one can actually show that the dynamics are full feedback linearizable under the same condition $v_j \neq 0$. Note, however, that the linearizing transformation depends also on the state of the leading agent i. Therefore, the control input to agent j , will need information about the state (and possibly the inputs) of agent i.

BIBLIOGRAPHY

[1] J. T. Ambrose. Swarms in transit. *Bee World*, 57:101–109, 1976.

[2] B. D. O. Anderson and D. J. Clements. Algebraic characterization of fixed modes in decentralized control. *Automatica*, 17(5):703–712, 1981.

[3] A. Avitabile, R. A. Morse, and R. Boch. Swarming honey bees guded by pheromones. *Annuals of the Entomological Society of America*, 68(6):1079–1082, 1975.

[4] T. Balch and R. C. Arkin. Behavior-based formation control for multirobot teams. *IEEE Trans. on Robotics and Automation*, 14(6):926–939, December 1998.

[5] J. Bender and R. Fenton. On the flow capacity of automated highways. *Transport. Sci.*, 4:52–63, February 1970.

[6] G. Beni and P. Liang. Pattern reconfiguration in swarms—convergence of a distributed asynchronous and bounded iterative algorithm. *IEEE Trans. on Robotics and Automation*, 12(3):485–490, June 1996.

[7] Dimitri P. Bertsekas and John N. Tsitsiklis. *Parallel and Distributed Computation: Numerical Methods*. Athena Scientific, Belmont, MA, 1997.

[8] E. Bonabeau, M. Dorigo, and G. Theraulaz. *Swarm Intelligence: From Natural to Artificial Systems*. Oxford Univ. Press, NY, 1999.

[9] C. M. Breder. Equations descriptive of fish schools and other animal aggregations. *Ecology*, 35(3):361–370, 1954.

[10] C. G. Butler and R. K. Callow anf J. R. Chapman. 9-hydroxydec-trans-2-enoic acid, a pheromone stabilizing honeybee swarms. *Nature*, 201:733, 1964.

[11] C. G. Butler and J. Simpson. Pheromones of the honeybee (*apis mellifera* l.) which enable her workers to follow her when swarming. *Proceedings of the Royal Entomological Society of London*, 42:149–154, 1967.

[12] S. Camazine, P. K. Visscher, J. Finley, and R. S. Vetter. House-hunting by honey bee swarms: collective decisions and individual behaviors. *Insectes soc.*, 46:348–360, 1999.

[13] J. Carr. *Applications of the Centre Manifold Theory.* Springer Verlag, New York, 1981.

[14] B. Castillo and S. Di Gennaro. Asymptotic output traking for siso nonlinear discrete time systems. In *Proc. of Conf. Decision Contr.*, pages 1802–1806, Brighton, England, December 1991.

[15] B. Castillo, S. Di Gennaro, S. Monaco, and D. Normand-Cyrot. Nonlinear regulation for a class of discrete-time systems. *Systems and Control Letters*, 20:57–65, 1993.

[16] Y.-C. Chu and J. Huang. A neural-network method for the nonlinear servomechanism problem. *IEEE Trans. on Neural Networks*, 10(6):1412–1423, November 1999.

[17] M. Clerc and J. Kennedy. The particle swarm—explosion, stability, and convergence in a multidimensional complex space. *IEEE Trans. on Evolutionary Computation*, 6(1):58–73, February 2002.

[18] Z. Csahok and T. Vicsek. Lattice-gas model for collective bilogical motion. *Physical Review E*, 52(5):5297–5303, November 1995.

[19] A. Czirok, A.-L. Barabasi, and T. Vicsek. Collective motion of self-propelled particles: Kinetic phase transition in one dimension. *Physical Review Letters*, 82(1):209–212, January 1999.

[20] A. Czirok, E. Ben-Jacob, I. Cohen, and T. Vicsek. Formation of complex bacterial colonies via self-generated vortices. *Physical Review E*, 54(2):1791–1801, August 1996.

[21] A. Czirok, H. E. Stanley, and T. Vicsek. Spontaneously ordered motion of self-propelled partciles. *Journal of Physics A: Mathematical, Nuclear and General*, 30:1375–1385, 1997.

[22] A. Czirok and T. Vicsek. Collective behavior of interacting self-propelled particles. *Physica A*, 281:17–29, 2000.

[23] S. Darbha and K. R. Rajagopal. Intelligent cruise control systems and traffic flow stability. *Transportation Research Part C*, 7:329–352, 1999.

[24] E. J. Davison. The robust control of a servomechanism problem for linear time-invariant multivariable systems. *IEEE Trans. on Automatic Control*, AC-21(1):25–34, February 1976.

[25] E. J. Davison. The robust decentralized control of a general servomechanism problem. *IEEE Trans. on Automatic Control*, AC-21(1):14–24, February 1976.

[26] E. J. Davison and A. Goldenberg. Robust decentralized control of a general servomechanism problem: The servocompensator. *Automatica*, 11:461–471, 1975.

[27] D. C. Dennett. *Darwin's Dangerous Idea*. Simon and Schuster, 1996.

[28] J. P. Desai, J. Ostrowski, and V. Kumar. Controlling formations of multiple mobile robots. In *Proc. of IEEE International Conference on Robotics and Automation*, pages 2864–2869, Leuven, Belgium, May 1998.

[29] J. P. Desai, J. Ostrowski, and V. Kumar. Modeling and control of formations of nonholonomic mobile robots. *IEEE Trans. on Robotics and Automation*, 17(6):905–908, December 2001.

[30] R. Durrett and S. Levin. The importance of being discrete (and spatial). *Theoretical Population Biology*, 46:363–394, 1994.

[31] L. Edelstein-Keshet. *Mathematical Models in Biology*. Brikhäuser Mathematics Series. The Random House, New Yourk, 1989.

[32] M. Egerstedt and X. Hu. Formation constrained multi-agent control. *IEEE Trans. on Robotics and Automation*, 17(6):947–951, December 2001.

[33] B. A. Francis. The linear multivariable regulator problem. *SIAM Journal on Control and Optimization*, 15(3):486–505, 1977.

[34] B. A. Francis and W. M. Wonham. The internal model principle of control theory. *Automatica*, 12:457–465, 1976.

[35] A. Fujimori, M. Teramoto, P. N. Nikiforuk, and M. M. Gupta. Cooperative collision avoidance between multiple mobile robots. *Journal of Robotic Systems*, 17(7):347–363, 2000.

[36] V. Gazi and K. M. Passino. Decentralized regulation of a class of nonlinear systems. In *Proc. of Conf. Decision Contr.*, pages 3014–3019, Orlando, FL, December 2001.

[37] V. Gazi and K. M. Passino. Stability of a one-dimensional discrete-time asynchronous swarm. In *Proc. of the joint IEEE Int. Symp. on Intelligent Control/IEEE Conf. on Control Applications*, pages 19–24, Mexico City, Mexico, September 2001.

[38] V. Gazi and K. M. Passino. A class of attraction/repulsion functions for stable swarm aggregations. In *Proc. of Conf. Decision Contr.*, Las Vegas, Nevada, December 2002.

[39] V. Gazi and K. M. Passino. Stability analysis of social foraging swarms: Combined effects of attractant/repellent profiles. In *Proc. of Conf. Decision Contr.*, Las Vegas, Nevada, December 2002.

[40] V. Gazi and K. M. Passino. Stability analysis of swarms. In *Proc. American Control Conf.*, pages 1813–1818, Anchorage, Alaska, May 2002.

[41] V. Gazi and K. M. Passino. Stability analysis of swarms in an environment with an attractant/repellent profile. In *Proc. American Control Conf.*, pages 1819–1824, Anchorage, Alaska, May 2002.

[42] E. Gelenbe, N. Schmajuk, J. Staddon, and J. Reif. Autonomous search by robots and animals: A survey. *Robotics and Autonomous Systems*, 22:23–34, 1997.

[43] F. Giulietti, L. Pollini, and M. Innocenti. Autonomous formation flight. *IEEE Control Systems Magazine*, 20(6):34–44, December 2000.

[44] P. Grindrod. Models of individual aggregation or clustering in single and multi-species communities. *Journal of Mathematical Biology*, 26:651–660, 1988.

[45] D. Grünbaum. Schooling as a strategy for taxis in a noisy environment. In J. K. Parrish and W. M. Hamner, editors, *Animal Groups in Three Dimensions*, pages 257–281. Cambridge Iniversity Press, 1997.

[46] D. Grünbaum. Schooling as a strategy for taxis in a noisy environment. *Evolutionary Ecology*, 12:503–522, 1998.

[47] D. Grünbaum and A. Okubo. Modeling social animal aggregations. In *Frontiers in Theoretical Biology*, volume 100 of *Lecture Notes in Biomathematics*, pages 296–325. Springer-Verlag, New York, 1994.

[48] S. Gueron and S. A. Levin. The dynamics of group formation. *Mathematical Biosciences*, 128:243–264, 1995.

[49] S. Gueron, S. A. Levin, and D. I. Rubenstein. The dynamics of herds: From individuals to aggregations. *Journal of Theoretical Biology*, 182:85–98, 1996.

[50] J. Huang and C. F. Lin. On the discrete-time nonlinear servomechanism problem. In *Proc. American Control Conf.*, pages 844–848, San Fracisco, California, June 1993.

[51] J. Huang and W. J. Rugh. On a nonlinear multivariable servomechanism problem. *Automatica*, 26:963–972, 1990.

[52] J. Huang and W. J. Rugh. An approximate method for the nonlinear servomechanism problem. *IEEE Trans. on Automatic Control*, 37(9):1395–1398, September 1992.

[53] J. Huang and W. J. Rugh. Stabilization on zero-error manifolds and the nonlinear servomechanism problem. *IEEE Trans. on Automatic Control*, 37(7):1009–1013, July 1992.

[54] A. Isidori. *Nonlinear Control Systems*. Springer-Verlag, third edition, 1995.

[55] A. Isidori and C. I. Byrnes. Output regulation of nonlinear systems. *IEEE Trans. on Automatic Control*, 35(2):131–140, February 1990.

[56] K. Jin, P. Liang, and G. Beni. Stability of synchronized distributed control of discrete swarm structures. In *Proc. of IEEE International Conference on Robotics and Automation*, pages 1033–1038, San Diego, California, May 1994.

[57] W. Kang, N. Xi, and A. Sparks. Formation control of autonomous agents in $3d$ space. In *IEEEICRA*, pages 1755–1760, San Francisco, CA, April 2000.

[58] J. Kennedy and R. C. Eberhart. *Swarm Intelligence*. Morgan Kaufmann Publisher, 2001.

[59] H. K. Khalil. *Nonlinear Systems*. Prentice Hall, Upper Saddle River, NJ, second edition, 1996.

[60] H. K. Khalil. On the design of robust servomechanisms for minimum phase nonlinear systems. *Int. J. Robust Nonlinear Control*, 10:339–361, 2000.

[61] O. Khatib. Real-time obstacle avoidance for manipulators and mobile robots. *The International Journal of Robotics Research*, 5(1):90–98, 1986.

[62] D. E. Koditschek. An approach to autonomous robot assembly. *Robotica*, 12:137–155, 1994.

[63] A. J. Krener. The construction of optimal linear and nonlinear regulators. In A. Isidori and T. J. Tarn, editors, *Systems, Models, and Feedback: Theory and Applications*, pages 301–322. Birkhäuser, 1992.

[64] N. E. Leonard and E. Fiorelli. Virtual leaders, artificial potentials and coordinated control of groups. In *Proc. of Conf. Decision Contr.*, pages 2968–2973, Orlando, FL, December 2001.

[65] H. Levine and W.-J. Rappel. Self-organization in systems of self-propelled particles. *Physical Review E*, 63(1):017101–1–017101–4, January 2001.

[66] L. A. Lewis and S. S. Schneider. The modulation of worker behavior by a vibration signal during house hunting in swarms of the honeybee, *apis mellifera*. *Behavioral Ecology and Sociobiology*, 48:154–164, 2000.

[67] Y. Liu, K. M. Passino, and M. Polycarpou. Stability analysis of one-dimensional asynchronous mobile swarms. In *Proc. of Conf. Decision Contr.*, pages 1077–1082, Orlando, FL, December 2001.

[68] Y. Liu, K. M. Passino, and M. Polycarpou. Stability analysis of one-dimensional asynchronous swarms. In *Proc. American Control Conf.*, pages 716–721, Arlington, VA, June 2001.

[69] Y. Liu, K. M. Passino, and M. M. Polycarpou. Stability analysis of one-dimensional asynchronous swarms. submitted for publication to IEEE Transactions on Automatic Control, April 2001.

[70] Y. Liu, K. M. Passino, and M. M. Polycarpou. Stability analysis of m-dimensional asynchronous swarms with a fixed communication topology. In *Proc. American Control Conf.*, pages 1278–1283, Anchorage, Alaska, May 2002.

[71] M. Lizana and V. Padron. A specially discrete model for aggregating populations. *Journal of Mathematical Biology*, 38:79–102, 1999.

[72] M.T. Madigan, J.M. Martinko, and J. Parker. *Biology of Microorganisms*. Prentice Hall, NJ, 8 edition, 1997.

[73] D. Mautz, R. Boch, and R. A. Morse. Queen finding by swarming honey bees. *Annuals of the Entomological Society of America*, 65(2):440–443, 1972.

[74] A. S. Mikhailov and D. H. Zanette. Noise-induced breakdown of coherent collective motion in swarms. *Physical Review E*, 60(4):4571–4575, October 1999.

[75] A. Modilner and L. Edelstein-Keshet. A non-local model for a swarm. *Journal of Mathematical Biology*, 38:534–570, 1999.

[76] R. A. Morse. Swarm orientation in honeybees. *Science*, 141:357–358, July 1963.

[77] R. A. Morse and R. Boch. Pheromone concert in swarming honey bees (hymenoptera: Apidae). *Annuals of the Entomological Society of America*, 64(6):1414–1417, 1971.

[78] J. D. Murray. *Mathematical Biology*. Springer-Verlag, New Yourk, 1989.

[79] P. Ögren, M. Egerstedt, and X. Hu. A control Lyapunov function approach to multi-agent coordination. In *Proc. of Conf. Decision Contr.*, pages 1150–1155, Orlando, FL, December 2001.

[80] A. Okubo. Dynamical aspects of animal grouping: swarms, schools, flocks, and herds. *Advances in Biophysics*, 22:1–94, 1986.

[81] A. Pand, P. Seiler, and K. Hedrick. Mesh stability of look-ahead interconnected systems. *IEEE Trans. on Automatic Control*, 47(2):403–407, February 2002.

[82] J. K. Parrish and L. Edelstein-Keshet. Complexity, pattern, and evolutionary trade-offs in animal aggregations. *Science*, 284:99–101, April 1999.

[83] J. K. Parrish and W. M. Hamner, editors. *Animal Groups in Three Dimensions*. Cambridge University Press, 1997.

[84] B. L. Partridge. The structure and function of fish schools. *Scientific American*, 245:114–123, 1982.

[85] K.M. Passino. Biomimicry of bacterial foraging for distributed optimization and control. *IEEE Control Systems Magazine*, 22(3):52–67, June 2002.

[86] M. M. Polycarpou, Y. Yang, and K. M. Passino. Cooperative control of distributed multi-agent systems. submitted for publication to IEEE Control Systems Magazine, June 2001.

[87] E. M. Rauch, M. M. Millonas, and D. R. Chialvo. Pattern formation and functionality in swarm models. *Physics Letters A*, 207:185–193, October 1995.

[88] J. H. Reif and H. Wang. Social potential fields: A distributed behavioral control for autonomous robots. *Robotics and Autonomous Systems*, 27:171–194, 1999.

[89] C. W. Reynolds. Flocks, herds, and schools: A distributed behavioral model. *Comp. Graph.*, 21(4):25–34, 1987.

[90] E. Rimon and D. E. Koditschek. Exact robot navigation using artificial potential functions. *IEEE Trans. on Robotics and Automation*, 8(5):501–518, October 1992.

[91] J. O. Schmidt, K. N. Slessor, and M. L. Winson. Roles of nasonov and queen pheromones in attraction of honeybee swarms. *Naturwissenschaften*, 80:573–575, 1993.

[92] T. D. Seeley. *Honeybee ecology*. Princeton University Press, Princeton, NJ, 1985.

[93] T. D. Seeley. *The Wisdom of the Hive: The Social Physiology of Honey Bee Colonies*. Harward University Press, Cambridge, Mass, 1995.

[94] T. D. Seeley and S. C. Buhrman. Group decision making in swarms of honey bees. *Behavioral Ecology and Sociobiology*, 45:19–31, 1999.

[95] T. D. Seeley, R. A. Morse, and P. K. Visscher. The natural history of the flight of honey bee swarms. *Psyche*, 86(2-3):103–113, June-September 1979.

[96] A. Serrani and A. Isidori. Global robust output regulation for a class of nonlinear systems. *Systems and Control Letters*, 39(2):133–139, February 2000.

[97] A. Serrani and A. Isidori. Semiglobal nonlinear output regulation with adaptive internal model. In *Proc. of Conf. Decision Contr.*, pages 1649–1654, Sydney, Australia, December 2000.

[98] A. Serrani, A. Isidori, and L. Marconi. Semiglobal robust output regulation of minimum-phase nonlinear systems. *Int. J. Robust Nonlinear Control*, 10:379–396, 2000.

[99] A. Serrani, A. Isidori, and L. Marconi. Semiglobal nonlinear output regulation with adaptive internal model. *IEEE Trans. on Automatic Control*, 46(8):1178–1194, August 2001.

[100] N. Shimoyama, K. Sugawa, T. Mizuguchi, Y. Hayakawa, and M. Sano. Collective motion in a system of motile elements. *Physical Review Letters*, 76(20):3870–3873, May 1996.

[101] J. Simpson and I. B. M. Riedel. The factor that causes swarming by honeybee colonies in small hives. *Journal of Apicultural Research*, 2:50–54, 1963.

[102] D.W. Stephens and J.R. Krebs. *Foraging Theory*. Princeton Univ. Press, Princeton, NJ, 1986.

[103] I. Suzuki and M. Yamashita. Distributed anonymous mobile robots: Formation of geometric patterns. *SIAM Journal on Computing*, 28(4):1347–1363, 1999.

[104] D. Swaroop. *String Stability of Interconnected systems: An Application to Platooning in Automated Highway Systems*. PhD thesis, Departnent of Mechanical Engineering, University of California, Berkeley 1995.

[105] D. Swaroop, J. K. Hedrick, C. C. Chien, and P. Ioannou. A comparison of spacing and headway control laws for automatically controlled vehicles. *Vehicle System Dynamics*, 23:597–625, 1994.

[106] P. Tabuada, G. J. Pappas, and P. Lima. Feasable formations of multi-agent systems. In *Proc. American Control Conf.*, pages 56–61, Arlington, VA, June 2001.

[107] J. Toner and Y. Tu. Long-range order in a two-dimensional dynamical xy model: How birds fly together. *Physical Review Letters*, 75(23):4326–4329, December 1995.

[108] J. Toner and Y. Tu. Flocks, herds, and schools: A quantitative theory of flocking. *Physical Review E*, 58(4):4828–4858, October 1998.

[109] R. Vaughan, N. Sumpter, J. Henderson, A. Frost, and S. Cameron. Experiments in automatic flock control. *Robotics and Autonomous Systems*, 31:109–117, 2000.

[110] T. Vicsek, A. Czirok, E. Ben-Jacob, I. Cohen, and O. Shochet. Novel type of phase transition in a system of self-driven particles. *Physical Review Letters*, 75(6):1226–1229, August 1995.

[111] T. Vicsek, A. Czirok, I. J. Farkas, and D. Helbing. Application of statistical mechanics to collective motion in biology. *Physica A*, 274:182–189, 1999.

[112] J. Wang, J. Huang, and S. T. Yau. Approximate nonlinear output regulation based on the universal approximation theorem. *Int. J. Robust Nonlinear Control*, 10:439–456, 2000.

[113] S.-H. Wang and E. J. Davison. On the stabilization of decentralized control systems. *IEEE Trans. on Automatic Control*, AC-18(5):473–478, October 1973.

[114] K. Warburton and J. Lazarus. Tendency-distance models of social cohesion in animal groups. *Journal of Theoretical Biology*, 150:473–488, 1991.

[115] G. A. Watson. *Approximation theory and numerical methods*. John Wiley, New York, 1980.

[116] M. L. Winston. *The Biology of the Honey Bee*. Harvard University Press, Cambridge, Massachusets, 1987.